Research Paper Series

No. 121

Asymptotic Expansion Formula of Option Price under Multifactor Heston Model

Kazuki Nagashima† Tsz-Kin Chung‡ Keiichi Tanaka§

March, 2013

†Daiwa SB Investments Ltd.,

‡Graduate School of Social Sciences, Tokyo Metropolitan University

§Graduate School of Social Sciences, Tokyo Metropolitan University

Asymptotic Expansion Formula of Option Price under Multifactor Heston Model

Kazuki Nagashima* Tsz-Kin Chung† Keiichi Tanaka‡§

March 18, 2013

Abstract

The stochastic volatility model of Heston (1993) has found difficulty in describing some of the important features of implied volatility dynamics, leading to a quest for multifactor extensions as well as the incoporation of time-dependent model parameters. In this paper, we develop an asymptotic expansion approach to multifactor Heston model with time-dependent parameter. We extend the result in Benhamou, Gobet and Miri (2010) and show that the extension to multifactor model involves an extra expansion term that captures the interaction between variance factors. The expansion formula under constant parameter can be explicitly computed, while the incorporation of time-dependent parameters is straight-forward under the framework. We show that the error bound of the approximation formula for the multifactor case can be formulated as the sum of error in the one-factor case. The approximation formula allows one to study the effect of multifactor extension and time-dependent parameters in a simple and unified framework. Moreover, the fast and efficient approximation formula is useful when one has to compute a large number of option prices, such as econometrics estimation using option data and evaluation of large-scale portfolio risk. As illustration, we calibrate a two-factor model to index option and variance swap data and find that it is possible to distinguish a short-term and long-term variance factors from the implied volatility surface and variance swap rates. Moreover, the two-factor model is able to reproduce the shapes of the implied volatility surface during various market scenarios.

1 Introduction

1.1 Background

For the last two decades, the stochastic volatility model of Heston (1993) has been one of the most popular choices in the modeling of price dynamics of various asset classes, including equity price, foreign exchange rate and interest rate. In the Heston model, one assumes the asset price to follow a lognormal process, with the stochastic variance driven by a Cox-Ingersoll-Ross (CIR) process which can be correlated with the asset price itself. The Heston model provides a succinct description to a number of important empirical features in the dynamics of asset price, such as the leverage effect, the mean-reversion nature and the clustering of volatility. In terms of derivatives pricing, the model has gained popularity on trading desks given its ability to manage the implied volatility smile along with its nice analytical tractability in the pricing of standard European-type options. Nevertheless, the one-factor dynamics and solution approach in Heston (1993) have a number of drawbacks. Firstly, it does not provide enough flexibility to model simultaneously the short-term and long-term implied volatility smile, given the fact that the level and slope of the smile generated by the model cannot be independently determined. This often forces analysts to adapt two different sets of model parameters to price and risk-manage short-term and long-term options separately. Such remedy, however, could misprice exotic derivatives that are sensitive to the realized path of volatility. On the other hand, the assumption of constant model parameters implies certain restrictions on the shape of the model-implied volatility surface. For example, when the correlation between the asset price and stochastic volatility is constant, the term structure of the volatility skew is governed by the speed of mean-reversion of the volatility process. Such restriction implies that the implied volatility surface has to be flattened-out in the long-run, making it difficult to capture the market scenario in which the long-term skewness is persistent. Some hedge funds have reportedly taken

*Daiwa SB Investments Ltd. E-mail: kazuki@gate01.com

†Graduate School of Social Sciences, Tokyo Metropolitan University. E-mail: chung-tszkin@ed.tmu.ac.jp

‡Graduate School of Social Sciences, Tokyo Metropolitan University. E-mail: tanaka-keiichi@tmu.ac.jp

§The third author acknowledges financial support by Ishii Memorial Securities Research Promotion Foundation and MEXT Grand-in-Aid .

advantage of such mispricing in long-term options and generated significant alpha during the recent financial crisis. These shortcomings of the Heston model have raise the questions on whether increasing the number of factors of the variance process, or relaxing the assumption of constant model parameters, would yield a more realistic description of the volatility dynamics.

It is well-known that the Heston model fall within the general affine diffusion (AD) framework in Duffie et al. (2000), in which the characteristic function can be obtained in closed-form when model parameters are constant. In order to price European-type options, one then has to numerically invert a Fourier transform with respect to the characteristic function. As discussed in a number of studies, one often encounters the following numerical challenges when implementing the Heston model: i.) the choice of the integration region and grid size (Carr and Madan, 1999), ii.) the contour of inverting the Fourier transform (Lee, 2004, Lord and Kahl, 2007), and iii.) the choice of the branch cut on the complex plane for the logarithm function (Kahl and Lord, 2010). This requires analysts to make judious choices for these numerical parameters in the model implementation. Furthermore, the extension to time-dependent model parameters is not straight-forward using the characteristic function approach. In particular, the nice analytical tractability of the characteristic function for Heston model will be destroyed when model parameter are time-dependent. While it is still feasible to derive a recursive closed-form formula when model parameters are piecewise-constant, for general time-dependent parameters, one has to solve numerically a system of ordinary differential equation (known as the Riccati equation). In this case, although the computation time for a single option price is still within a second, the numerical burden becomes significant when one attempts to use the option pricing formula for the purpose of calibration or statistical inference. Indeed, the lack of an accurate and easy-to-use approximation formula for the Heston model has somewhat hindered its popularity in the financial market, in comparison to some other stochastic volatility models such as the one proposed by Hagan et al. (2002), which has a simple and intuitive approximation formula. In reality, a closed-form approximation formula brings the necessary transparency of a derivative pricing model for market participants to use it for trading and risk management purpose.

In this paper, we develop an asymptotic expansion approach to multifactor Heston model with time-dependent parameter. Asymptotic expansion has been found to be very efficient in various area of derivatives pricing. For stochastic volatility models, a number of papers have developed the asymptotic formula of the implied volatility smile near expiry under various dynamical assumptions. For example, see Hagan et al. (2002), Labordere (2005), Alos et al. (2007), Osajima (2007), Antonelli and Scarlatti (2009), Fukasawa (2011) and Takahashi and Yamada (2012). Nevertheless, the extension to time-dependent parameters are not trivial in some of these approaches. For long-term maturity, Fouque et al. (2000) suggest the asymptotic expansion of the mean reversion parameter based on singular perturbation. Fouque et al. (2004) further extend the approach to general stochastic volatility models with homogeneous parameters when the variance follows an Ornstein-Uhlenbeck process. Apart from option pricings, Tanaka et al. (2010) use the Gram-Charlier expansion to derives asymptotic approximation for interest rate derivatives, Papageorgiou and Sircar (2009) use singular perturbation technique to price single-name and multi-name credit derivatives under stochastic volatility, and Bayraktar and Yang (2011) use similar technique for equity-credit hybrid modeling.

Using Malliavin calculus, Benhamou et al. (2010) develop a fast and accurate approximation formula of option prices under the Heston model with time dependent parameters. By the asymptotic expansion with respect to the volatility of volatility, they show that the put option price can be approximated by the Black-Scholes formula, with a number of correction terms related to the Greeks of the option. In this paper, we extend their results and develop the approximation formula under the general multifactor Heston model with time-dependent parameters. We find that the expansion terms can be expressed as a sum of the expansion terms as obtained in Benhamou et al. (2010), plus a new term that captures the interaction between different variance factors. We show that the error bound of the approximation formula for the multifactor case can be formulated as the sum of error in the one-factor case. We perform numerical analysis and study the accuracy of the formula under different parameter settings.

1.2 Literature Review

Recently, there is a growing number of papers that consider the multifactor extension of the Heston model in derivatives pricing. Fonseca et al. (2008) propose a multifactor Heston model based on the Wishart process and consider the option pricing in the foreign exchange market. Christoffersen et al. (2009) shows that a two-factor Heston model performs much better than a one-factor model in capturing the dynamics of the implied volatility of the S&P 500 index options. The two-factor model allows a flexible modeling of the volatility surface such that the level and slope of the volatility smile can be independently determined given the additional degree of freedom. Moreover, they find that the estimated variance factors can be identified as a strongly mean-reverting short-term variance factor, and a long-term factor that is slowly mean-reverting. Zhang and Chu (2010) use a non-parametric approach to analysis the index option dataset and verify the conclusion in Christoffersen et al. (2009). They find that one needs to use at least two factors in order to sufficiently capture the dynamics of implied volatility in both the time-series and cross-sectional dimensions. These observations are consistent with the series of works by Froque et al. (2000, 2003 and 2004) that conjecture the multiscale nature of stochastic volatility. Froque and Lorig (2011) propose an extension to the one-factor Heston model by adding an extra fast mean-reverting component and find that such extension allows a significant improvement in the fitting of volatility smile for index options.

Besides the application in European option pricing, multifactor stochastic volatility models have also been used heavily in the pricing of exotic derivatives that are sensitive to volatility, such as various forward-starting options and variance swap. Variance swap is a financial instrument actively traded in the over-the-counter market since last decade. At maturity, the buyer of a variance swap receives the difference between the realized variance over the contractual period and a fixed strike rate, which is known as the variance swap rate. Heston-type stochastic volatility model is popular in the modeling of volatility derivatives given its closed-form solution in pricing continuously-monitored variance swap. Nevertheless, Bengomi (2009) highlights that the one-factor Heston model could lead to the mispricing of pricing of exotic derivatives, such as forward-starting options, cliquets and variance swaps. He suggests that a properly designed volatility smile model for the pricing and risk management of exotic derivatives should have the separate controls on i.) the term structure of volatility, ii.) short-term volatility skew, and iii.) the correlation between the spot price and volatility. This indicates the need to pursue a multifactor stochastic volatility model. For the pricing of variance swaps, Bushler (2006) proposes a class of no-arbitrage variance curve models with multiple stochastic volatility factors, in which the Heston model is a special case. He mentions that it is common in the market place to use a two-factor model in order to capture the term structure of variance swaps written on major stock market indices. In short, one needs a multifactor stochastic volatility model in order to consistently price standard European options and volatility derivatives.

In parallel to the literature of derivatives pricing, there are a number of recent papers in financial economics that estimate stochastic volatility models using the time-series of spot price and cross-sectional option prices. Ait-Sahalia and Kimmel (2007) use Edgeworth expansion to derive an approximate closed-form likelihood function for the one-factor Heston model, and estimate the model jointly with the time-series of spot price and cross-sectional option prices using the maximum-likelihood method. In a similar fashion, Yu et al. (2010) adopt a Bayesian econometrics approach and use Monte-Carlo Markov Chain (MCMC) to estimate stochastic volatility model. In these econometrics estimation, one has to compute the model-implied option prices during each iteration in optimizing the likelihood function, or when generating the sampling draw for the MCMC estimation. When the characteristic function approach is employed to compute the option prices, one has to perform a very large number of numerical Fourier inversion during the estimation process, which could be extremely time-consuming. In view of this, we need a fast and accurate approximation formula for the pricing of standard European options.

1.3 Outline

The outline of the paper is as follows. In Section 2, we present the mathematical formulation of the multifactor Heston model and highlight its property in derivatives pricing. In Section 3, we develop the asymptotic expansion formula under the multifactor Heston model and presents the error estimate of the approximation. Section 4 contains the numerical illustration and study the accuracy of the approximation formula under various parameter setting. Section 5 discusses the calibration procedure to index option and variance swap data for a two-factor model using the approximation formula. Section 6 concludes.

2 Multifactor Heston Model

2.1 Mathematical Formulation

We fix a filtered probability space $(\Omega, \mathcal{F}, (\mathcal{F}_t)_{0\leq t\leq T}, \mathbb{P})$, where $\mathbb{P}$ denotes the forward measure, X_t is the log-forward price and the variance factors υ_{it}, $i = 1, 2, ..., n$, satisfy the following system of stochastic differential equations

$$X_t = x_0 + \sum_{i=1}^{n} \left[\int_0^t \sqrt{\upsilon_{is}} dW_s^i - \frac{1}{2} \int_0^t \upsilon_{is} ds \right],$$

$$\upsilon_{it} = \upsilon_{i0} + \int_0^t \kappa_i(\theta_{is} - \upsilon_{is}) ds + \int_0^t \xi_{is} \sqrt{\upsilon_{is}} dB_s^i, \tag{1}$$

where κ_i is the mean-reversion speed, θ_{is} is the mean-reversion level and ξ_{is} is the volatility-of-volatility (Vol-of-Vol) for the i^{th} variance factor. The correlation structure for the variance factors υ_{it} is given by

$$\begin{aligned} d\langle W^i, W^j\rangle &= d\langle B^i, B^j\rangle = 0, \\ d\langle W^i, B^j\rangle_t &= \delta_{ij}\rho_{it}dt, \qquad i,j \in \{1,2,...,n\}, \end{aligned}$$

such that there are n-pairs of correlated Brownian motions $\left\{\left(W_t^1, B_t^1\right), \left(W_t^2, B_t^2\right), ..., \left(W_t^n, B_t^n\right)\right\}$, and δ_{ij} is the Kronecker delta. For each variance factor υ_{it}, we assume the parameters $(\kappa_i, \upsilon_{i0})$ are positive constants, while we allow the parameters $(\theta_{it}, \xi_{it}, \rho_{it})$ to be time-dependent (deterministic). In order to guarantee the positivity of the variance factors and the nondegeneracy of X_t, we set out the following assumptions that are made on the model parameters throughout the derivation in Section 2 and 3.

Assumption I

$$\inf_{t\in[0,T]} \xi_{it} > 0, \qquad \sup_{t\in[0,T]} |\rho_{it}| < 1, \qquad \inf_{t\in[0,T]} \left(\frac{2\kappa_i\theta_{it}}{\xi_{it}^2}\right) \geq 1,$$

for all $i = 1, 2, ..., n$. In particular, the last assumption can be considered as the generalization of the Feller condition in the case of time-dependent parameters.

Christoffersen et al. (2009) consider a two-factor Heston model in (1) with $n = 2$ and constant model parameters. As noted by Christoffersen et al. (2009), the multifactor Heston model describes an independence between the level and the slope of volatility smile curves (moneyness effect) and stochastic correlation (term structure effect), by regarding a first factor υ_{1t} as a short-term variance factor and the second factor υ_{2t} as the long term one. As the result, the model is able to provide a rich structure of volatility surfaces that can be observed in the index option market. We then present some basic property of the model below.

2.2 Stochastic Correlation and the Term Structure of Volatility

In the multifactor Heston model, the instantaneous variance of dX_t and the instantaneous covariance between dX_t and $d\upsilon_t$ are given by

$$Var[dX_t] = \sum_{i=1}^{n} \upsilon_{it}dt \triangleq \upsilon_t dt, \qquad Cov[dX_t, d\upsilon_t] = \sum_{i=1}^{n} \left[\xi_i\rho_i\upsilon_{it}\right] dt. \tag{2}$$

Consider a fixed maturity, it is not difficult to observe that the level of implied volatility is primarily determined by $Var[dX_t]$, while the volatility skew (i.e., the slope of the implied volatility smile) is determined by $Cov[dX_t, d\upsilon_t]$. On the other hand, the time-variation of the implied volatility skew can be generated by the stochastic correlation

$$Corr[dX_t, d\upsilon_t] = \frac{Cov[dX_t, d\upsilon_t]}{\sqrt{Var[dX_t]}\sqrt{Var[d\upsilon_t]}} = \frac{\sum\limits_{i=1}^{n} \xi_i\rho_i\upsilon_{it}}{\sqrt{\sum\limits_{i=1}^{n} \upsilon_{it}}\sqrt{\sum\limits_{i=1}^{n} \xi_i^2\upsilon_{it}}}. \tag{3}$$

Under the multifactor Heston model, it is also straight-foward to compute the expected variance in the case of constant model parameter:

$$\mathbb{E}\left[\upsilon_s|\, \mathcal{F}_t\right] = \sum_{i=1}^{n} \left[\theta_i\left(1 - e^{-\kappa_i(T-t)}\right) + \upsilon_{i,0}e^{-\kappa_i(T-t)}\right]. \tag{4}$$

Hence, the fair strike of a continuously-monitoring variance swap for the contractural period $[t, T]$ can be readily obtained as

$$VS\left(t,T\right) = \mathbb{E}\left[\frac{1}{T-t}\int_t^T \upsilon_s ds \middle| \mathcal{F}_t\right] = \sum_{i=1}^{n} \left[\theta_i + \left(\upsilon_{i,0} - \theta_i\right)\frac{\left(1 - e^{-\kappa_i(T-t)}\right)}{\kappa_i\left(T-t\right)}\right]. \tag{5}$$

For the pricing of variance swap under discrete monitoring, we refer to readers to Zhang and Kwok (2013) and the references therein. As shown in Christoffersen et al. (2009), the multifactor Heston model can generate a rich flexibility for the term stucture of implied volatility. Similar multifactor volatility models have been considered in the pricing of volatility derivatives, see for example, Bengomi (2009) and Bushler (2006). It is worth to note that given the model parameters (θ_i, κ_i) for $i = 1, 2, ..., n$, one can explicitly back out the instantaneous variance $\upsilon_{i,0}$ for $i = 1, 2, ..., n$ from n observed market quotes of variance swaps.

2.3 Option Pricing under Multifactor Heston Model

It is well-known that the multifactor Heston model falls within the class of affine diffusion (AD) model in Duffie et al. (2000). In particular, given the independence of the variance factors, it is straight-forward to derive the characteristic function for X_t (in closed-form) as

$$\phi(X_t, \upsilon_{it}; t, T; i_0\omega) \triangleq \mathbb{E}\left[\exp\left(i_0\omega X_T\right)\middle|\,\mathcal{F}_t\right] = \exp\left[i_0\omega X_t + A\left(T-t\right) + \sum_{i=1}^{n} D_i\left(T-t,\omega\right)\upsilon_{it}\right], \tag{6}$$

where we denote $i_0 = \sqrt{-1}$ to be the imaginery number, and

$$A\left(\tau\right) = \sum_{i=1}^{n} \kappa_i\theta_i \left\{r_{i,-}\tau - \frac{2}{\xi_i^2}\ln\left[\frac{1-g_i\exp\left[-d_i\tau\right]}{1-g_i}\right]\right\}, \qquad D_i\left(\tau\right) = r_{i,-}\frac{1-\exp\left[-d_i\tau\right]}{1-g_i\exp\left[-d_i\tau\right]},$$

with $\tau = T - t$ and

$$\begin{aligned} r_{i,\pm} &= \frac{1}{2c_{i,2}}\left[-c_{i,1} \pm d_i\right], \quad g = \frac{r_{i,-}}{r_{i,+}}, \ \ d_i = \sqrt{c_{i,1}^2 - 4c_{i,0}c_{i,2}}, \\ c_{i,0} &= \frac{1}{2}i_0\omega\left(i_0\omega - 1\right), \quad c_{i,1} = \rho_i\xi_i\left(i_0\omega\right) - \kappa_i, \quad c_{i,2} = \frac{1}{2}\xi_i^2. \end{aligned}$$

See Appendix A for the derivation.

In what follows, we consider a put option with strike price K, time-to-maturity T, and denote $B\left(t,T\right)$ to be the risk-free discount factor. It is then possible to derive an integral representation of the put option price as

$$\begin{aligned} P\left(X_t, t\right) &= \frac{B\left(t,T\right)}{2\pi}\int_{i_0\varepsilon-\infty}^{i_0\varepsilon+\infty} \phi\left(-\omega\right)\left[-\frac{Ke^{i_0\omega\ln K}}{\omega^2 - i\omega}\right]d\omega \\ &= \frac{KB\left(t,T\right)}{\pi}\int_0^{\infty} \Re\left\{\frac{e^{i_0(\zeta+i_0\varepsilon)\ln K}\phi\left(-\left(\zeta+i_0\varepsilon\right)\right)}{i_0\left(\zeta+i_0\varepsilon\right) - \left(\zeta+i_0\varepsilon\right)^2}\right\}d\zeta. \end{aligned} \tag{7}$$

where we have made use of the generalized Fourier transform of the payoff function $\left(K - e^x\right)^+$ as

$$\widetilde{P}\left(\omega, T\right) = \int_{-\infty}^{\infty} e^{i_0\omega x}\left(K - e^x\right)_+ dx = -\frac{Ke^{i_0\omega\ln K}}{\omega^2 - i_0\omega},$$

for $\varepsilon = \Im\left(\omega\right) \in \left(-\varepsilon_{\max}, 0\right)$ which denotes the contour on the complex plane. As discussed in Chung and Kwok (2012), it is straight-forward to compute the put option price of a particular strike price using standard numerical quadrature to invert the integral; alternatively, one may adopt the Fast Fourier transformation (FFT) technique in Carr and Madan (1999) to obtain option prices across a number of strikes.

3 Asymptotic Expansion with Malliavin Calculus

3.1 The Perturbed Multifactor Heston Model

In this section, we develop an asymptotic expansion for the put option price under the multifactor Heston model. We consider the following perturbed processes $X_t^{\epsilon}, \upsilon_{it}^{\epsilon_i}$ of (1) as parametrized by $\epsilon = \{\epsilon_i : epsilon_i \in [0,1],\ i = 1, 2, ..., n\}$ as

$$\begin{aligned} X_t^{\epsilon} &= x_0 + \sum_{i=1}^{n}\left[\int_0^t \sqrt{\upsilon_{is}^{\epsilon_i}}dW_s^i - \frac{1}{2}\int_0^t \upsilon_{is}^{\epsilon_i}ds\right], \\ \upsilon_{it}^{\epsilon_i} &= \upsilon_{i0} + \int_0^t \kappa_i(\theta_{is} - \upsilon_{is}^{\epsilon_i})ds + \epsilon_i\int_0^t \xi_{is}\sqrt{\upsilon_{is}^{\epsilon_i}}dB_t^i. \end{aligned} \tag{8}$$

It is not difficult to show that when $\epsilon_i = 0$, the variance process is deterministic and we have

$$\upsilon_{i0,t} \triangleq \upsilon_{it}^0 = e^{-\kappa_i t}\left(\upsilon_{i0} + \int_0^t e^{\kappa_i s}\kappa_i\theta_{is}ds\right); \tag{9}$$

On the other hand, when $\epsilon_i = 1$, $\upsilon_{it}^{\epsilon_i}$ coincides with υ_{it}, the original variance process. It is noted that under Assumption I, each variance factor $\upsilon_{it}^{\epsilon_i}$ is guaranteed to be positive. Our aim is to obtain an asymptotic expansion of the discounted expectation $g(\epsilon)$ related to the put option pricing formula:

$$g(\epsilon) = e^{-\int_0^T r_t dt}\mathbb{E}\left[\left(K - e^{\int_0^T (r_t - q_t)dt + X_T^\epsilon}\right)_+\right], \tag{10}$$

where K is the strike price, T is the time-to-maturity, r_t is the risk-free rate and q_t is the dividend yield. When we set $\epsilon = 1_n$, i.e., $\epsilon_i = 1$ for all $i = 1, 2, ..., n$, the discounted expectation gives the put option pricing formula under the multifactor Heston model.

As the Brownian motions B_t^i are independent to each other, i.e., $d\left\langle B_t^i, B_t^j\right\rangle = \delta_{ij}dt$, we can rewrite (8) as

$$X_T^\epsilon = x_0 + \sum_{i=1}^n\left[\int_0^T \sqrt{\upsilon_{it}^{\epsilon_i}}\rho_{it}dB_t^i + \int_0^T \sqrt{\upsilon_{it}^{\epsilon_i}}\sqrt{1-\rho_{it}^2}dZ_t^i\right] - \frac{1}{2}\sum_{i=1}^n\int_0^T \upsilon_{it}^{\epsilon_i}dt,$$

where Z_t^i are independent Brownian motions such that $d\left\langle B_t^i, Z_t^j\right\rangle = 0$ for all i and j. Suppose we denote $\mathcal{F}_T^{B^i} = \sigma\left(B_t^i : 0 \le t \le T\right)$ to be the σ-algebra generated by the Brownian motion B_t^i up to time T, and $\mathcal{F}_T^B = \mathcal{F}_T^{B_1} \vee \mathcal{F}_T^{B_2} \vee \cdots \vee \mathcal{F}_T^{B_n}$ as the σ-algebra generated by $\left\{B_t^i : i = 1, 2, ..., n\right\}$ up to time T. It is easy to see that X_T^ϵ conditional on $\mathcal{F}_T^B$ is Gaussian distributed. Therefore, we can express the discounted expectation as

$$\begin{aligned} g(\epsilon) &= \mathbb{E}\left[e^{-\int_0^T r_t dt}\mathbb{E}\left[\left(K - e^{\int_0^T (r_t - q_t)dt + X_T^\epsilon}\right)_+\middle| \mathcal{F}_T^B\right]\right] \\ &= \mathbb{E}\left[P\left(x\left(\epsilon\right), y\left(\epsilon\right)\right)\right], \end{aligned} \tag{11}$$

where

$$x\left(\epsilon\right) \triangleq x_0 + \sum_{i=1}^n\left[\int_0^T \rho_{it}\sqrt{\upsilon_{it}^{\epsilon_i}}dB_t^i - \frac{1}{2}\rho_{it}^2\upsilon_{it}^{\epsilon_i}dt\right], \quad y\left(\epsilon\right) \triangleq \sum_{i=1}^n\int_0^T \left(1-\rho_{it}^2\right)\upsilon_{it}^{\epsilon_i}dt, \tag{12}$$

and $P(x, y)$ is the Black-Scholes formula for put option:

$$\begin{aligned} P(x,y) &\triangleq Ke^{-r_{eq}T}\mathcal{N}(d) - e^x e^{-q_{eq}T}\mathcal{N}(d - \sqrt{y}), \\ d &= \frac{1}{\sqrt{y}}\ln\left[\frac{Ke^{-r_{eq}T}}{e^x e^{-q_{eq}T}}\right] + \frac{1}{2}\sqrt{y}, \end{aligned} \tag{13}$$

where $r_{eq} = \frac{1}{T}\int_0^T r_t dt$ and $q_{eq} = \frac{1}{T}\int_0^T q_t dt$ are the equivalent interest rate and dividend rate when they are time-dependent, and $\mathcal{N}(\cdot)$ is the standard culmulative normal distribution.

3.2 Asymptotic Expansion for Multifactor Heston Model

To expand $g(\epsilon)$ around $\epsilon = 0_n$ asymptotically, let us rewrite (11) as

$$g(\epsilon) = \mathbb{E}[P(x' + \Delta x\left(\epsilon\right), y' + \Delta y\left(\epsilon\right))]$$

by decomposing (12) as $x\left(\epsilon\right) = x' + \Delta x\left(\epsilon\right)$ and $y\left(\epsilon\right) = y' + \Delta y\left(\epsilon\right)$, in which the two terms

$$\begin{aligned} x' &\triangleq x(0) = x_0 + \sum_{i=1}^n\left[\int_0^T \rho_{it}\sqrt{\upsilon_{i0,t}}dB_t^i - \frac{1}{2}\rho_{it}^2\upsilon_{i0,t}dt\right], \\ y' &\triangleq y(0) = \sum_{i=1}^n\int_0^T \left(1-\rho_{it}^2\right)\upsilon_{i0,t}dt \end{aligned}$$

correspond to the values of X_T and $Var(X_T)$, respectively, at the origin of the expansion, $\epsilon = 0_n$, and the rests

$$\begin{aligned} \Delta x\left(\epsilon\right) &= \sum_{i=1}^n \Gamma_{iT}^{\epsilon_i}, \text{ with } \Gamma_{iT}^{\epsilon_i} \triangleq \int_0^T \rho_{it}(\sqrt{\upsilon_{it}^{\epsilon_i}} - \sqrt{\upsilon_{i0,t}})dB_{it} - \int_0^T \frac{1}{2}\rho_{it}^2(\upsilon_{it}^{\epsilon_i} - \upsilon_{i0,t})dt, \\ \Delta y\left(\epsilon\right) &= \sum_{i=1}^n \Xi_{iT}^{\epsilon_i}, \text{ with } \Xi_{iT}^{\epsilon_i} \triangleq \int_0^T (1-\rho_{it}^2)(\upsilon_{it}^{\epsilon_i} - \upsilon_{i0,t})dt, \end{aligned}$$

capture the perturbed change of X_T and $Var(X_T)$, respectively, with respect to ϵ. To proceed, we introduce the multivariate Taylor expansion residual with respect to ϵ for a process Y_t^ϵ as

$$R_{\ell,t}^{Y^\epsilon} = R_{\ell,t}\left[Y^\epsilon\right] \triangleq Y_t^\epsilon - \sum_{m=0}^{\ell} \frac{1}{m!}\left(\sum_{i=1}^n h_i \frac{\partial}{\partial \epsilon_i}\right)^m Y_t^\epsilon \bigg|_{\epsilon=0_n,\{h_i\}=\{\epsilon_i\}}.$$

When ϵ is a single variate $\epsilon = \epsilon_i \mathbf{1}_i$, the above definition for a process $Y_t^{\epsilon_i}$ is equivalent to the case of one-factor in Benhamou et al. (2010)

$$R_{\ell,t}^{Y^{\epsilon_i}} = Y_t^{\epsilon_i} - \sum_{m=0}^{\ell} \frac{\epsilon_i^m}{m!} Y_{m,t}^{\epsilon_i} \quad , \quad Y_{m,t} \triangleq \frac{\partial^m Y_t^{\epsilon_i}}{\partial \epsilon_i^m}\bigg|_{\epsilon_i=0}.$$

First we see that the second-order expansion of the variance factors are given by

$$\begin{aligned}
\upsilon_{it}^{\epsilon_i} &= \upsilon_{i0,t} + \epsilon_i \upsilon_{i1,t} + \frac{1}{2!}\epsilon_i^2 \upsilon_{i2,t} + R_{2,T}^{\upsilon_i^{\epsilon_i}}, \\
\sqrt{\upsilon_{it}^{\epsilon_i}} &= \sqrt{\upsilon_{i0,t}} + \epsilon_i \frac{\upsilon_{i1,t}}{2(\upsilon_{i0,t})^{1/2}} + \frac{1}{2!}\epsilon_i^2\left(\frac{\upsilon_{i2,t}}{2(\upsilon_{i0,t})^{1/2}} - \frac{(\upsilon_{i1,t})^2}{4(\upsilon_{i0,t})^{3/2}}\right) + R_{2,T}^{\sqrt{\upsilon_i^{\epsilon_i}}},
\end{aligned}$$

with

$$\upsilon_{i0,t} = e^{-\kappa_i t}\left(\upsilon_{i0} + \int_0^t e^{\kappa_i s}\kappa_i \theta_{is} ds\right), \tag{14}$$

$$\upsilon_{i1,t} = e^{-\kappa_i t}\int_0^t e^{\kappa_i s}\xi_{is}\sqrt{\upsilon_{i0,s}}dB_s^i, \tag{15}$$

$$\upsilon_{i2,t} = e^{-\kappa_i t}\int_0^t e^{\kappa_i s}\xi_{is}\frac{\upsilon_{i1,s}}{(\upsilon_{i0,s})^{1/2}}dB_s^i. \tag{16}$$

As a result, the second order expansion for $\Gamma_{iT}^{\epsilon_i}$ and $\Xi_{iT}^{\epsilon_i}$ with respect to in ϵ_i are given by

$$\Gamma_{iT}^{\epsilon_i} = \Gamma_{i0,T} + \epsilon_i \Gamma_{i1,T} + \frac{1}{2}\epsilon_i^2 \Gamma_{i2,T} + R_{2,T}^{\Gamma_i^{\epsilon_i}}$$

with

$$\begin{aligned}
\Gamma_{i0,T} &= \Gamma_{iT}^0 = 0, \quad \Gamma_{i1,T} = \int_0^T \rho_{it}\frac{\upsilon_{i1,t}}{2(\upsilon_{i0,t})^{1/2}}dB_t^i - \int_0^T \frac{\rho_{it}^2}{2}\upsilon_{i1,t}dt, \\
\Gamma_{i2,T} &= \int_0^T \rho_{it}\left[\frac{\upsilon_{i2,t}}{2(\upsilon_{i0,t})^{1/2}} - \frac{(\upsilon_{i1,t})^2}{4(\upsilon_{i0,t})^{3/2}}\right]dB_t^i - \int_0^T \frac{\rho_{it}^2}{2}\upsilon_{i2,t}dt,
\end{aligned} \tag{17}$$

and

$$\Xi_{iT}^{\epsilon_i} = \Xi_{i0,T} + \epsilon_i \Xi_{i1,T} + \frac{1}{2}\epsilon_i^2 \Xi_{i2,T} + R_{2,T}^{\Xi_i^{\epsilon_i}}$$

with

$$\Xi_{i0,T} = \Xi_{iT}^0 = 0, \quad \Xi_{i1,T} = \int_0^T (1-\rho_{it}^2)\upsilon_{i1,t}dt, \quad \Xi_{i2,T} = \int_0^T (1-\rho_{it}^2)\upsilon_{i2,t}dt. \tag{18}$$

These expansion terms will be used in the following derivation.

As shown in the Appendix B, by the application of chain rules for the formal derivatives on $\epsilon = (\epsilon_i)_i$ to the parameterized stochastic processes $\Gamma_{iT}^{\epsilon_i}$ and $\Xi_{iT}^{\epsilon_i}$, up to the second order, we arrive the following expansion formula

$$\begin{aligned}
g(\epsilon) &= \mathbb{E}\left[P(x',y')\right] + \mathbb{E}\left[\frac{\partial P(x',y')}{\partial x}\sum_{i=1}^n \Delta\Gamma_i^1\right] + \mathbb{E}\left[\frac{\partial P(x',y')}{\partial y}\sum_{i=1}^n \Delta\Xi_i^1\right] \\
&\quad + \frac{1}{2}\mathbb{E}\left[\frac{\partial^2 P(x',y')}{\partial x^2}\left(\sum_{i=1}^n \Delta\Gamma_i^2\right)^2\right] + \frac{1}{2}\mathbb{E}\left[\frac{\partial^2 P(x',y')}{\partial y^2}\left(\sum_{i=1}^n \Delta\Xi_i^2\right)^2\right] \\
&\quad + \mathbb{E}\left[\frac{\partial^2 P(x',y')}{\partial x \partial y}\left(\sum_{i=1}^n \Delta\Xi_i^2\right)\left(\sum_{i=1}^n \Delta\Gamma_i^2\right)\right] + \widetilde{\varepsilon}_n,
\end{aligned} \tag{19}$$

where $\widetilde{\varepsilon}_n$ is the expansion error, and the expansion terms are explicitly given by

$$
\begin{aligned}
\Delta\Gamma_i^1 &\triangleq \epsilon_i\Gamma_{i1,T}+\frac{\epsilon_i^2}{2}\Gamma_{i2,T}=\int_0^T\rho_{it}\left[\epsilon_i\frac{\upsilon_{i1,t}}{2(\upsilon_{i0,t})^{1/2}}+\frac{1}{2!}\epsilon_i^2\left(\frac{\upsilon_{i2,t}}{2(\upsilon_{i0,t})^{1/2}}-\frac{(\upsilon_{i1,t})^2}{4(\upsilon_{i0,t})^{3/2}}\right)\right]dB_t^i\\
&\quad -\int_0^T\frac{1}{2}\rho_{it}^2\left(\epsilon_i\upsilon_{i1,t}+\frac{1}{2}\epsilon_i^2\upsilon_{i2,t}\right)dt,\\
\Delta\Gamma_i^2 &\triangleq \epsilon_i\Gamma_{i1,T}=\int_0^T\rho_{it}\epsilon_i\frac{\upsilon_{i1,t}}{2(\upsilon_{i0,t})^{1/2}}dB_t^i-\int_0^T\frac{1}{2}\rho_{it}^2\epsilon_i\upsilon_{i1,t}dt,\\
\Delta\Xi_i^1 &\triangleq \epsilon_i\Xi_{i1,T}+\frac{\epsilon_i^2}{2}\Xi_{i2,T}=\int_0^T\left(1-\rho_{it}^2\right)\left(\epsilon_i\upsilon_{i1,t}+\frac{1}{2}\epsilon_i^2\upsilon_{i2,t}\right)dt,\\
\Delta\Xi_i^2 &\triangleq \epsilon_i\Xi_{i1,T}=\int_0^T\left(1-\rho_{it}^2\right)\epsilon_i\upsilon_{i1,t}dt,
\end{aligned}
\tag{20}
$$

for $i=1,2,...,n$.

From the structure of the expansion formula in (19), we notice that there are cross terms of different indices for the expansion terms in the last three expectations involving the second order derivatives. Hence, by using the following identities:

$$
\begin{aligned}
\left(\sum_{i=1}^n\zeta_j\right)\left(\sum_{j=1}^n\widetilde{\zeta}_j\right) &= \sum_{i=1}^n\zeta_i\widetilde{\zeta}_i+\sum_{i=2}^n\sum_{j=1}^{i-1}\left(\zeta_i\widetilde{\zeta}_j+\zeta_j\widetilde{\zeta}_i\right),\\
\left(\sum_{i=1}^n\zeta_i\right)^2 &= \sum_{i=1}^n\zeta_i\zeta_i+\sum_{i=2}^n\sum_{j=1}^{i-1}2\zeta_i\zeta_j,
\end{aligned}
$$

(19) is rewritten as

$$
\begin{aligned}
g(\epsilon) &= \mathbb{E}\left[P\left(x',y'\right)\right]\\
&\quad+\sum_{i=1}^n\left\{\mathbb{E}\left[\frac{\partial P}{\partial x}\Delta\Gamma_i^1\right]+\mathbb{E}\left[\frac{\partial P}{\partial y}\Delta\Xi_i^1\right]+\frac{1}{2}\mathbb{E}\left[\frac{\partial^2 P}{\partial x^2}\left(\Delta\Gamma_i^2\right)^2\right]+\frac{1}{2}\mathbb{E}\left[\frac{\partial^2 P}{\partial y^2}\left(\Delta\Xi_i^2\right)^2\right]+\mathbb{E}\left[\frac{\partial^2 P}{\partial x\partial y}\Delta\Gamma_i^2\Delta\Xi_i^2\right]\right\}\\
&\quad+\sum_{i=2}^n\sum_{j=1}^{i-1}\left\{\mathbb{E}\left[\frac{\partial^2 P}{\partial x^2}\Delta\Gamma_i^2\Delta\Gamma_j^2\right]+\mathbb{E}\left[\frac{\partial^2 P}{\partial y^2}\Delta\Xi_i^2\Delta\Xi_j^2\right]+\mathbb{E}\left[\frac{\partial^2 P}{\partial x\partial y}\Delta\Gamma_i^2\Delta\Xi_j^2\right]+\mathbb{E}\left[\frac{\partial^2 P}{\partial x\partial y}\Delta\Gamma_j^2\Delta\Xi_i^2\right]\right\}\\
&\quad+\widetilde{\varepsilon}_n,
\end{aligned}
\tag{21}
$$

where the term $\partial^{k+l}P/\partial x^k\partial y^l$ in the expectation is evaluated at (x',y'). The expectations regarding to the cross terms $\Delta\Gamma_i^2\Delta\Gamma_j^2, \Delta\Xi_i^2\Delta\Xi_j^2$, $\Delta\Gamma_i^2\Delta\Xi_j^2$ and $\Delta\Gamma_j^2\Delta\Xi_i^2$ in (21) are new terms that appear in the case of multifactor Heston model. Before we explicitly compute these expansion terms, we first present the following Proposition that is a natural extension of Proposition 2.1 in Benhamou et al. (2010) to the case of multifactor model.

Proposition 1 *When $\epsilon=1_n$, the expansion in (21) can be formulated as*

$$
g(1_n) = \mathbb{E}\left[P(x',y')\right]+\mathbb{E}\left[\frac{\partial P}{\partial y}(x',y')\sum_{i=1}^n\int_0^T\left(\upsilon_{i1,t}+\upsilon_{i2,t}\right)dt\right]+\frac{1}{2}\mathbb{E}\left[\frac{\partial^2 P}{\partial y^2}(x',y')\left(\sum_{i=1}^n\int_0^T\upsilon_{i1,t}dt\right)^2\right]+\widetilde{\varepsilon}_n.
$$

Proof. As we show in the Appendix C.1, by making use of the Malliavin calculus and the properties of the Black-Scholes pricing formula, when $\epsilon=1_n$, the summation of the cross terms in the third line of (21)

$$
\Phi_T^{i,j}=\mathbb{E}\left[\frac{\partial^2 P}{\partial x^2}\Delta\Gamma_i^2\Delta\Gamma_j^2\right]+\mathbb{E}\left[\frac{\partial^2 P}{\partial y^2}\Delta\Xi_i^2\Delta\Xi_j^2\right]+\mathbb{E}\left[\frac{\partial^2 P}{\partial x\partial y}\Delta\Gamma_i^2\Delta\Xi_j^2\right]+\mathbb{E}\left[\frac{\partial^2 P}{\partial x\partial y}\Delta\Gamma_j^2\Delta\Xi_i^2\right]
$$

can be expressed as

$$
\Phi_T^{i,j}=\mathbb{E}\left[\frac{\partial^2 P}{\partial y^2}(x',y')\int_0^T\left[\int_0^t\upsilon_{i1,s}ds\right]\upsilon_{j1,t}dt\right]+\mathbb{E}\left[\frac{\partial^2 P}{\partial y^2}(x',y')\int_0^T\left[\int_0^t\upsilon_{j1,s}ds\right]\upsilon_{i1,t}dt\right]
\tag{22}
$$

when $\epsilon = 1_n$. Then, by applying the identity

$$\left(\int_0^T f(t)\,dt\right)\left(\int_0^T g(t)\,dt\right) = \int_0^T \left[\int_0^t f(s)\,ds\right] g(t)\,dt + \int_0^T \left[\int_0^t g(s)\,ds\right] f(t)\,dt,$$

we have

$$\Phi_T^{i,j} = \mathbb{E}\left[\frac{\partial^2 P}{\partial y^2}(x', y')\left(\int_0^T \upsilon_{i1,t}dt\right)\left(\int_0^T \upsilon_{j1,t}dt\right)\right]. \tag{23}$$

It follows that

$$\begin{aligned} g(1_n) \;=\; & \mathbb{E}\left[P(x', y')\right] + \sum_{i=1}^n \mathbb{E}\left[\frac{\partial P}{\partial y}(x', y')\int_0^T (\upsilon_{i1,t} + \upsilon_{i2,t})\,dt\right] + \sum_{i=1}^n \frac{1}{2}\mathbb{E}\left[\frac{\partial^2 P}{\partial y^2}(x', y')\left(\int_0^T \upsilon_{i1,t}dt\right)^2\right] \\ & + \sum_{i=2}^n \sum_{j=1}^{i-1} \mathbb{E}\left[\frac{\partial^2 P}{\partial y^2}(x', y')\left(\int_0^T \upsilon_{i1,t}dt\right)\left(\int_0^T \upsilon_{j1,t}dt\right)\right] + \widetilde{\varepsilon}_n \end{aligned} \tag{24}$$

which is equivalent to the desired expression. ■

In the following Lemma for the case of one factor model, we keep the index i for the formula P_1^i for later use in the case of multifactor Heston model.

Lemma 2 (The One-factor Model, Benhamou et al. (2010)) *Suppose Assumption I holds and take $n = 1$, $i = 1$, i.e., single-factor Heston model with time-dependent parameters, the put option pricing formula can be approximated by*

$$g(1) = P\left(x_0, var_T^i\right) + P_1^i\left(x_0, var_T^i\right) + \widetilde{\varepsilon}_1,$$

where

$$P_1^i\left(x_0, var_T^i\right) = \sum_{k=1}^2 a_{k,T}^i \frac{\partial^{k+1}}{\partial x^k \partial y} P\left(x_0, var_T^i\right) + \sum_{k=0}^1 b_{2k,T}^i \frac{\partial^{2k+2}}{\partial x^{2k}\partial y^2} P\left(x_0, var_T^i\right)$$

is the expansion term of the one-factor Heston model, with $var_T^i = \int_0^T \upsilon_{i0,s}dt$ is the total variance, and the expansion coefficients $a_{k,T}^i$ and $b_{2k,T}^i$ are given by

$$\begin{aligned} a_{1,T}^i &= \int_0^T \phi_{i0}(s)\,\phi_{i1}(s)\,ds \int_s^T \phi_{i0}^{-1}(u)\,du \\ a_{2,T}^i &= \int_0^T \phi_{i0}(s)\,\phi_{i1}(s)\,ds \int_s^T \phi_{i3}(t)\,dt \int_t^T \phi_{i0}^{-1}(u)\,du \\ b_{0,T}^i &= \int_0^T \phi_{i0}^2(s)\,\phi_{i2}(s)\,ds \int_s^T \phi_{i0}^{-1}(t)\,dt \int_t^T \phi_{i0}^{-1}(u)\,du \\ b_{2,T}^i &= \frac{1}{2}\left(a_{1,T}^i\right)^2 \end{aligned} \tag{25}$$

with

$$\phi_{i0}(s) = e^{\kappa_i s}, \quad \phi_{i1}(s) = \rho_{is}\xi_{is}\upsilon_{i0,s}, \quad \phi_{i2}(s) = \xi_{is}^2\upsilon_{i0,s}, \quad \phi_{i3}(s) = \rho_{is}\xi_{is}.$$

Proof. See Benhamou et al. (2010) . ■

Notice that in the above result

$$P\left(x_0, var_T^i\right) = \mathbb{E}\left[P(x', y')\right], \quad P_1^i\left(x_0, var_T^i\right) = \mathbb{E}\left[\frac{\partial P}{\partial y}(x', y')\int_0^T (\upsilon_{i1,t} + \upsilon_{i2,t})\,dt\right] + \frac{1}{2}\mathbb{E}\left[\frac{\partial^2 P}{\partial y^2}(x', y')\left(\int_0^T \upsilon_{i1,t}dt\right)^2\right].$$

In our multifactor setting, there are interacted terms between different variance factors in (24)

$$\sum_{i=2}^n \sum_{j=1}^{i-1} \mathbb{E}\left[\frac{\partial^2 P}{\partial y^2}(x', y')\left(\int_0^T \upsilon_{i1,t}dt\right)\left(\int_0^T \upsilon_{j1,t}dt\right)\right],$$

which leads to additional terms $P_2^{i,j}\left(x_0, var_T\right)$ in the approximation formula as indicated in the following Theorem.

Theorem 3 (The Multifactor Model) *Suppose Assumption I holds and the expansion in (19) is valid, the put option pricing formula under the multifactor Heston model can be approximated by*

$$g\left(1_n\right) = P\left(x_0, var_T\right) + \sum_{i=1}^{n} P_1^i\left(x_0, var_T\right) + \sum_{i=2}^{n}\sum_{j=1}^{i-1} P_2^{i,j}\left(x_0, var_T\right) + \widetilde{\varepsilon}_n,$$

where $var_T = \sum_{i=1}^{n} \int_0^T \upsilon_{i0,t} dt = \int_0^T \upsilon_s dt$ *is the total variance, and*

$$P_2^{i,j}\left(x_0, var_T\right) = c_T^{i,j} \frac{\partial^4 P}{\partial x^2 y^2}\left(x_0, var_T\right)$$

in which $c_T^{i,j}$ *is the expansion coefficient due to the cross terms, which is given by*

$$c_T^{i,j} = \mathcal{C}\left(i,j\right) + \mathcal{C}\left(j,i\right),$$

where

$$\begin{aligned} \mathcal{C}\left(i,j\right) &= \int_0^T \phi_{i0}(s)\phi_{i1}(s)ds \int_s^T \phi_{j0}(t)\phi_{j1}(t)dt \left[\int_t^T \phi_{i0}^{-1}(u)du \int_u^T \phi_{j0}^{-1}(w)dw + \int_t^T \phi_{j0}^{-1}(u)du \int_u^T \phi_{i0}^{-1}(w)dw\right] \\ &+ \int_0^T \phi_{i0}(s)\phi_{i1}(s)ds \int_s^T \phi_{i0}^{-1}(t)dt \int_t^T \phi_{j0}(u)\phi_{j1}(u)du \int_u^T \phi_{j0}^{-1}(w)dw, \end{aligned} \tag{26}$$

with

$$\phi_{i0}(s) = e^{\kappa_i s},\ \ \phi_{i1}(s) = \rho_{is}\xi_{is}\upsilon_{i0,s}.$$

Proof. It is straightforward to check that it holds that

$$\mathbb{E}\left[P(x',y')\right] = P\left(x_0, var_T\right), \quad \mathbb{E}\left[\frac{\partial P}{\partial y}(x',y') \int_0^T \left(\upsilon_{i1,t} + \upsilon_{i2,t}\right) dt\right] + \frac{1}{2}\mathbb{E}\left[\frac{\partial^2 P}{\partial y^2}(x',y') \left(\int_0^T \upsilon_{i1,t} dt\right)^2\right] = P_1^i\left(x_0, var_T\right),$$

which corresponds to the first line on the right-hand side of (24). Therefore, it remains to calculate the terms (23) or (22) when $\epsilon = 1_n$. Due to the functional form of the Black-Scholes formula $P\left(x,y\right)$, we observe that

$$\mathbb{E}\left[\frac{\partial^{\ell+m}}{\partial x^{\ell}\partial y^{m}} P\left(x',y'\right)\right] = \frac{\partial^{\ell+m}}{\partial x^{\ell}\partial y^{m}} P\left(x_0, \sum_{i=1}^{n}\int_0^T \upsilon_{i0,t} dt\right).$$

Then, as shown in Appendix C.2, by applying the Malliavin calculus and the Fubini Theorem, the stochastic integrals within the two expectations in (22) can be transformed as

$$\Phi_T^{i,j} = c_T^{i,j} \frac{\partial^4 P}{\partial x^2 \partial y^2}\left(x_0, var_T\right), \tag{27}$$

which is $P_2^{i,j}\left(x_0, var_T\right)$. ■

When W^i and B^i are independent, it is observed that $\rho_{it} \equiv 0$ yields $\varphi_{i1}(t) \equiv 0$ and $\mathcal{C}\left(i,j\right) = 0$. Furthermore, when $\mathcal{C}\left(i,j\right) = \mathcal{C}\left(j,i\right) = 0$, we see $P_2^{i,j}\left(x_0, var_T\right) = 0$.

Corollary 4 *When all the model parameters are constant, the expansion coefficients* $a_{k,T}^i$ *and* $b_{2k,T}^i$ *in Lemma 2 can be explicitly computed as*

$$\begin{aligned} var_T &= m_{i0}\upsilon_{i0} + m_1\theta_i, & a_{2,T}^i &= \left(\rho_i\xi_i\right)^2\left(q_{i0}\upsilon_{i0} + q_{i1}\theta_i\right), \\ a_{1,T}^i &= \rho_i\xi_i\left(p_{i0}\upsilon_{i0} + p_{i1}\theta_i\right), & b_{0,T}^i &= \xi^2\left(r_{i0}\upsilon_{i0} + r_{i1}\theta_i\right), \end{aligned}$$

with

$$\begin{aligned} m_{i0} &= z_{mi}\left(e^{\kappa_i T} - 1\right), & m_{i1} &= T - z_{mi}\left(e^{\kappa_i T} - 1\right), \\ p_{i0} &= z_{pi}\left(-\kappa_i T + e^{\kappa_i T} - 1\right), & p_{i1} &= z_{pi}\left(\kappa_i T + e^{\kappa_i T}\left(\kappa_i T - 2\right) + 2\right), \\ q_{i0} &= z_{qi}\left(-\kappa_i T\left(\kappa_i T + 2\right) + 2e^{\kappa_i T} - 2\right), & q_{i1} &= z_{qi}\left(2e^{\kappa_i T}\left(\kappa_i T - 3\right) + \kappa_i T\left(\kappa_i T + 4\right) + 6\right), \\ r_{i0} &= z_{ri}\left(-4e^{\kappa_i T}\kappa_i T + 2e^{2\kappa_i T} - 2\right), & r_{i1} &= z_{ri}\left(4e^{\kappa_i T}\left(\kappa_i T + 1\right) + e^{2\kappa_i T}\left(2\kappa_i T - 5\right) + 1\right), \end{aligned}$$

and

$$z_{mi} = \frac{e^{-\kappa_i T}}{\kappa_i}, \quad z_{pi} = \frac{e^{-\kappa_i T}}{\kappa_i^2}, \quad z_{qi} = \frac{e^{-\kappa_i T}}{2\kappa_i^3}, \quad z_{ri} = \frac{e^{-2\kappa_i T}}{4\kappa_i^3}.$$

Corollary 5 *When all the model parameters are constant, the expansion coefficients $c_T^{i,j}$ in Theorem 3 can be explicitly computed as*

$$c_T^{i,j} = \rho_i \rho_j \xi_i \xi_j \left(y_0 \upsilon_{i0} \upsilon_{j0} + y_1 \upsilon_{i0} \theta_j + y_2 \upsilon_{j0} \theta_i + y_3 \theta_i \theta_j \right),$$

where

$$\begin{aligned}
y_0 &= z_y \left[e^{(\kappa_i+\kappa_j)T} - e^{\kappa_i T} (\kappa_j T + 1) - e^{\kappa_j T} (\kappa_i T + 1) + (\kappa_i T + 1)(\kappa_j T + 1) \right], \\
y_1 &= z_y \left[e^{(\kappa_i+\kappa_j)T} (\kappa_j T - 2) + e^{\kappa_i T} (\kappa_j T + 2) - e^{\kappa_j T} (\kappa_j T - 2)(\kappa_i T + 1) - (\kappa_j T + 2)(\kappa_i T + 1) \right], \\
y_2 &= z_y \left[e^{(\kappa_i+\kappa_j)T} (\kappa_i T - 2) + e^{\kappa_j T} (\kappa_j T + 2) - e^{\kappa_i T} (\kappa_i T - 2)(\kappa_j T + 1) - (\kappa_i T + 2)(\kappa_j T + 1) \right], \\
y_3 &= z_y \left[e^{(\kappa_i+\kappa_j)T} (\kappa_i T - 2)(\kappa_j T - 2) + e^{\kappa_i T} (\kappa_i T - 2)(\kappa_j T + 2) + e^{\kappa_j T} (\kappa_i T + 2)(\kappa_j T - 2) + (\kappa_i T + 2)(\kappa_j T + 2) \right],
\end{aligned}$$

and

$$z_y = \frac{e^{-(\kappa_i+\kappa_j)T}}{(\kappa_i \kappa_j)^2}.$$

The expansion coefficients for $a_{k,T}^i$ and $b_{2k,T}^i$ are obtained in Corollary 4.

Remark 6 *As shown in Theorem 3, the new expansion terms capture the interaction between different variance factors when the driving Brownian motions W^i and B^i are uncorrelated. In the case of constant paramters, the interaction is related to the covariance as $\rho_i \rho_j \xi_i \xi_j$. In other words, the interaction between two variance factors i and j are induced from its correlation to the underlying process X_t, as given by ρ_i and ρ_j respectively. As the expansion term is linked to the $\partial^4 P(x_0, var_T) / \partial x^2 \partial y^2$ of the Black-Scholes formula, the interaction term is most important for at-the-money-option when the sensitivity in Delta and Vega are significant.*

Theorem 7 *The order of magnitude of approximation error for the multifactor expansion formula in Theorem 3 can be estimated as*

$$|\widetilde{\varepsilon}_n| = O\left(\sum_{i=1}^{n} (\xi_{iSup})^3 T^2 \right). \tag{28}$$

Hence, it can be expressed as the sum of approximation error in the one-factor case in Benhamou et al. (2010).
Proof. *The proof is presented in the Appendix D.* ■

Remark 8 *It is important to note the approximation formula is derived under the Assumption I. In particular, we impose the Feller condition to be held for all the variance factors. Nevertheless, in practice, when the Heston-type stochastic volatility model is calibrated to market option prices, it is usually found that the Feller condition does not hold - and the model could give poor fit to the market implied volatility surface when the Feller condition is imposed during the optimization procedure.*

When the Feller condition does not hold, we are not able to guarantee the approximation formula to produce option prices that are non-negative and satisfying the no-arbitrage bounds. Indeed, in our numerical experiment, when we set the correlation to be highly negative, the approximation formula could produce negative option price for short-term deep out-out-the-money call option (i.e., option price below the intrinsic value for the corresponding deep in-the-money put option). In this case, one need to pay extra cautions when employing the approximation formula for calibration purpose as the model-implied option price could bleach the no-arbitrage bounds. To resolve this issue, we set the option value to be its intrinsic value when the approximation formula bleach those bounds.

4 Numerical Illustration

In this Section, we study the accuracy of the approximation formula for the multifactor Heston model. For illustration purpose, we consider the case of $n = 2$, i.e., the case of two-factor Heston model as in Christoffersen et al. (2009). We consider the scenario when the model parameters are constant as well as the case when the correlation coefficients are allowed to be time-dependent.

4.1 Constant Model Parameters

In the multifactor Heston model, the parameter κ_i controls the mean-reversion speed of the i^{th} variance factor and governs its impact to the term structure of implied volatility. Considering the expected variance given by

$$\mathbb{E}\left[\int_t^T \upsilon_s^i ds \middle| \mathcal{F}_t\right] = \theta_i \left(1 - e^{-\kappa_i(T-t)}\right) + \upsilon_{i,0} e^{-\kappa_i(T-t)}, \tag{29}$$

it can be observed that the i^{th} variance factor decays to its long-run mean level θ_i at the mean-reversion speed of κ_i. This means the i^{th} variance factor could affect the term structure of implied volatility for the time-to-maturity range that is characterised by the half-life (which is approximately $1/\kappa_i$) of the mean-reversion process. The intuition is that variance factors with different κ_i correspond to different time-scales of the stochastic volatility process that drive the stock price process. In the following, we assume that $\kappa_2 > \kappa_1$, such that υ_{1t} can be regarded as a long-term variance factor with a slow mean-reversion, while υ_{2t} can be regarded short-term variance factor with a fast mean-reversion,.

4.1.1 Accuracy of the Approximation Formula

To study the accuracy of the approximation formula for two-factor Heston model, we compute the put option prices using i.) the approximation formula derived in Section 3, ii.) the characteristic function approach discussed in Section 2, and iii.) direct Monte-Carlo simulation. For the characteristic function approach, we employ the adaptive integration routines in Matlab (with relative tolerance of 1e-08) to numerically invert the Fourier integral. For the Monte Carlo simulation, we apply the Euler scheme on the simulation of the log-stock price and variance factors, and adopt the full truncation scheme when the simulated variance path approaches zero. To achieve high convergence, the simulation is repeated 1,000,000 times and the time-step is kept at 0.01. We take the spot price to be 100, i.e., $x_0 = \ln(100)$, and consider range of moneyness is from 80% to 120% with the time-to-maturity of options for 1-month, 3-month, 6-month, 1-year and 2-year. This covers the range of options that are liquid for index option market and are commonly used for model calibration in practice. For simplicity, we assume the interest rate and dividend yield to be zero.

Example 9 (Zero Correlation) *We assume the model parameters to be constant as follows:*

ρ_1	κ_1	θ_1	ξ_1	υ_{10}	ρ_2	κ_2	θ_2	ξ_2	υ_{20}
0.0	0.5	0.10	0.25	0.10	0.0	5.0	0.05	0.5	0.05

in which there are no correlations between the stock price and the variance factors. For the model parameters, the first variance factor has a half-life of around 2 years (i.e., $\kappa_1 = 0.5$*), while the second variance factor has a half-life of 0.2 year (i.e.,* $\kappa_2 = 5.0$*). We set the mean levels of the long-term and short-term variance factors to be* $\theta_1 = 0.10$ *and* $\theta_2 = 0.05$ *respectively (i.e., 32% and 22% in terms of volatility points, where 1 volatility point = 1%). For simplicity, we set the initial variance (*υ_{10} *and* υ_{20}*) of each factor to its corresponding mean level. The Vol-of-Vol for the two variance factors are* $\xi_1 = 0.25$ *and* $\xi_2 = 0.5$*. As such, the Feller conditions are given by* 1.6 *and* 2.0 *respectivetly for the two factors. The parameters setting here is considered to be a moderate market scenario.*

In Example 9, we assume there are no correlations between stock price process and the two variance factors. In this case, the approximation formula can be simplified given that $a^i_{1,T} = a^i_{2,T} = b^i_{2,T} = c^{i,j}_T = 0$, such that the approximation formula includes only two correction terms involving the second order derivative with respect to the total variance y. The estimation of the put option prices at various moneyness and time-to-maturity is shown in Table 3. We also report the approximation error which is computed as the approximation price minus the exact closed-form price, and apprehend the error estimate as obtained in Theorem 7. From Table 1, it is found that the approximation formula is very accurate for short-tern options such as 3-month and 6-month options, in which the approximation errors are between 0 to 13 bps (take 1 bp = 0.0001). Given that a typical over-the-counter option quotes 4-5 decimal places, the approximation formula for short-term options are considered to be extremely accurate. For 1-year and 2-year options, the approximation errors are in the order-of-magnitude of 100 bps, implying the percentage error is less than 1% for long-term options. Indeed, the actual approximation error falls well below the error estimate as given in Theorem 5.

Example 10 (Negative Correlation) *We assume constant model parameters and negative correlations between the stock price and the variance factors with* $\rho_2 > \rho_1$*.*

ρ_1	κ_1	θ_1	ξ_1	υ_{10}	ρ_2	κ_2	θ_2	ξ_2	υ_{20}
-0.25	0.5	0.10	0.25	0.10	-0.5	5.0	0.05	0.5	0.05

Table 1: Estimation of put option prices for two-factor Heston model in Example 9. The model parameters are: $\rho_1 = 0.0, \kappa_1 = 0.5, \theta_1 = 0.10, \xi_1 = 0.5, \upsilon_{10} = 0.10, \rho_2 = 0.0, \kappa_2 = 5.0, \theta_2 = 0.05, \xi_2 = 1.0, \upsilon_{20} = 0.05$.

Moneyness	80	90	100	110	120	80	90	100	110	120
			Time-to-Maturity = 3M					Time-to-Maturity = 1Y		
Exact Solution	1.0731	3.3592	7.6739	14.0291	21.9643	5.9343	9.9852	15.1998	21.4538	28.5809
Approximation	1.0731	3.3588	7.6735	14.0286	21.9640	5.9313	9.9822	15.1970	21.4506	28.5772
Approximation Error	0.0000	0.0004	0.0004	0.0005	0.0003	0.0030	0.0029	0.0028	0.0032	0.0037
Error Estimate	0.0195					0.3125				
Monte-Carlo	1.0687	3.3521	7.6645	14.0169	21.9482	5.9326	9.9795	15.1906	21.4413	28.5662
MC Error	0.0035	0.0066	0.0101	0.0133	0.0158	0.0108	0.0145	0.0181	0.0216	0.0246
			Time-to-Maturity =6M					Time-to-Maturity = 2Y		
Exact Solution	2.8353	6.0373	10.8106	17.0468	24.4779	10.7735	15.6212	21.3036	27.7153	34.7488
Approximation	2.8343	6.0363	10.8099	17.0458	24.4765	10.7629	15.6087	21.2901	27.7014	34.7352
Approximation Error	0.0010	0.0010	0.0007	0.0010	0.0013	0.0106	0.0125	0.0136	0.0139	0.0136
Error Estimate	0.0781					1.2500				
Monte-Carlo	2.8302	6.0330	10.8088	17.0506	24.4835	10.7688	15.6198	21.3016	27.7118	34.7427
MC Error	0.0066	0.0101	0.0137	0.0170	0.0199	0.0160	0.0197	0.0234	0.0269	0.0301

Table 2: Estimation of put option prices for two-factor Heston model in Example 10. The model parameters are: $\rho_1 = -0.25, \kappa_1 = 0.5, \theta_1 = 0.10, \xi_1 = 0.5, \upsilon_{10} = 0.10, \rho_2 = -0.5, \kappa_2 = 5.0, \theta_2 = 0.05, \xi_2 = 1.0, \upsilon_{20} = 0.05$.

Moneyness	80	90	100	110	120	80	90	100	110	120
			Time-to-Maturity = 3M					Time-to-Maturity = 1Y		
Exact Solution	1.1831	3.4418	7.6476	13.8943	21.7878	6.0998	10.0250	15.0789	21.1755	28.1762
Approximation	1.1863	3.4422	7.6466	13.8922	21.7836	6.0960	10.0191	15.0744	21.1722	28.1714
Approximation Error	0.0032	0.0004	0.0009	0.0021	0.0042	0.0039	0.0060	0.0045	0.0033	0.0048
Error Estimate	0.0195					0.3125				
Monte-Carlo	1.1778	3.4370	7.6449	13.8930	21.7864	6.0913	10.0142	15.0661	21.1626	28.1609
MC Error	0.0038	0.0069	0.0104	0.0136	0.0161	0.0114	0.0150	0.0187	0.0221	0.0252
			Time-to-Maturity =6M					Time-to-Maturity = 2Y		
Exact Solution	2.9959	6.1177	10.7520	16.8510	24.1929	10.8630	15.5548	21.0656	27.3107	34.1972
Approximation	2.9977	6.1159	10.7500	16.8487	24.1878	10.8501	15.5381	21.0479	27.2926	34.1776
Approximation Error	0.0018	0.0018	0.0020	0.0023	0.0051	0.0129	0.0167	0.0177	0.0181	0.0196
Error Estimate	0.0781					1.2500				
Monte-Carlo	2.9860	6.1086	10.7467	16.8493	24.1949	10.8464	15.5423	21.0567	27.3022	34.1877
MC Error	0.0071	0.0105	0.0141	0.0174	0.0203	0.0165	0.0203	0.0240	0.0275	0.0308

The negative correlation generates the implied volatility skew due to the leverage effect. Other model parameters are the same as in Example 9.

In Example 10, we allow the correlations between stock price process and the two variance factors. It is expected the approximation errors to be larger given that the underlying dynamics are more complex in the presence of the leverage effect. As shown in Table 2, the approximation errors generally increase the stock price and the variance factors are negatively correlated. Nevertheless, the approximation formula for 3-month and 6-month options remain very accurate with the error of 4 to 51 bps. In the case of longer-term options, the approximation errors remain well-control at the level of several hundred bps. This indicates the approximation formula is accurate up to the second decimal place.

Example 11 (Approximation Accuracy and Error Estimate) *We study the approximation errors at different levels of the mean-reversion speed (*$0.5, 1.0, 2.0$ *and* 5.0*) and Vol-of-Vol parameter (from* 0.1 *to* 1.0*) for the short-term variance factor* υ_{2t}*. All other parameters are the same as in Example 10.*

In Theorem 7, we show that the approximation error is proportional to the cubic of the Vol-of-Vol parameter and the square of the time-to-maturity. It is therefore expected that the approximation accuracy could deteriorate sharply in the case of high volatility and long time-to-maturity. To study the accuracy of the approximation

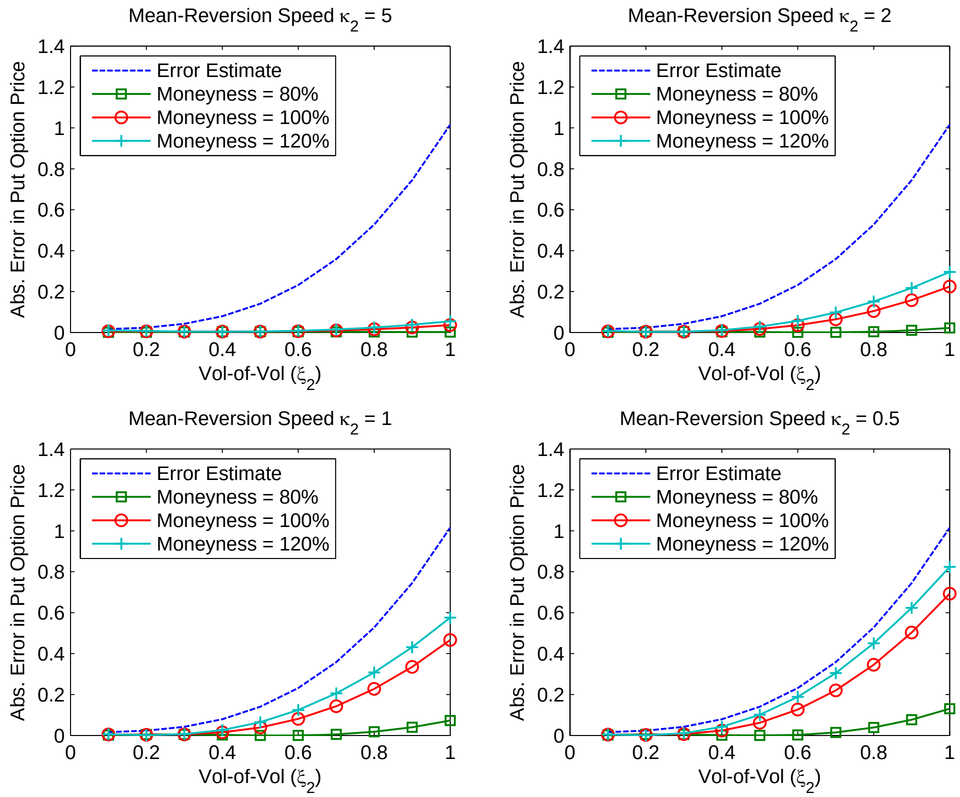

Figure 1: The plot of the absolute approximation error in put option price and the error estimate at different mean-reversion speed and Vol-of-Vol parameter for the short-term variance factor. Other parameters are the same as in Example 10.

formula, we focus on the 1-year time-horizon, then gradually increase the Vol-of-Vol parameter (ξ_2) for the short-term variance factor (υ_{2t}) at different mean-reversion speed (κ_2), while keeping other parameters the same as in Example 10. As a higher mean-reversion speed dampens the stochastic movements of the variance process, we would expect the approximation error to be smaller when the mean-reversion speed is high.

Figure 1 plots the approximation errors for different values of the mean-reversion speed and Vol-of-Vol parameter. We also plot the error estimate $e = \sum_{i=1}^{2} (\xi_{iSup})^3 T^2$ as a reference. It is worth to note that the error estimate e here only indicates the order of magnitude of the approximation error, instead of an upper bound. As can be seen, the error estimate e is a good measure for the accuracy for at-the-money options when the mean-reversion speed is slow, but it significantly overestimates the pricing errors for deep out-of-the-money put options. It is interesting to note that the actual approximation error falls within the error estimate e, unless the mean-reversion speed is small. Hence, the error estimate can be considered to be a conservative measure of the approximation error under realistic parameter setting. Moreover, this means the approximation accuracy appears to be better than a second order expansion in Vol-of-Vol when the mean-reversion parameter is not too small, and the Vol-of-Vol parameter is not too large.

4.1.2 Implied Volatility Surface

Example 12 *We show the implied volatility surfaces as generated by the following model parameter settings.*

	ρ_1	κ_1	θ_1	ξ_1	υ_{10}	ρ_2	κ_2	θ_2	ξ_2	υ_{20}
Scenario 1	-0.5	0.5	0.10	0.5	0.05	-0.8	5.0	0.04	1.0	0.02
Scenario 2	-0.5	0.5	0.10	0.5	0.05	-0.8	5.0	0.01	1.0	0.02
Scenario 3	0.0	0.5	0.10	0.5	0.05	-0.8	5.0	0.01	1.0	0.02
Scenario 4	0.5	0.5	0.10	0.5	0.05	-0.8	5.0	0.01	1.0	0.02

From the baseline parameters in Scenario 1, we adjust the values of the mean-level for short-term variance factor (θ_2) and the correlation parameter of the long-term factor (ρ_1) in Scenarios 2 to 4 in order to produce various shapes of the implied volatility surface. The baseline parameter setting is motivated by the calibration results to the S&P500 index data in Section 5.

- **Scenario 1.** As shown in top-left panel of Figure 2, the implied volatility surface exhibits an moderate upward-sloping term structure given that $\theta_1 > \upsilon_{10}$ and $\theta_2 > \upsilon_{20}$. Given the negative correlations of the two factors ρ_1 and ρ_2, the short-term skewness is prominent and decays gradually with the time-to-maturity. It should be noted that this is the class of implied volatility surface that is commonly observed in the index option market. This is also the case in which a one-factor Heston model is able to provide a good fit.

- **Scenario 2.** To study the impact of the mean levels on the term structure, we adjust the value of θ_2 from 0.04 to 0.01. This generate a hump-shaped term structure as shown in the top-right panel of Figure 2. The generation of the hump-shaped term structure can be explained based on the variance swap pricing formula in (5): when $\tau = 0$, the variance swap rate is given by $VS(0) = \upsilon_{10} + \upsilon_{20}$; for $\tau > 0$, $\tau \approx 1/\kappa_2$ and $\tau << 1/\kappa_1$, i.e., at the short-to-medieum term, we have $VS(\tau) \approx \upsilon_{10} + \theta_2$. Hence, the slope of the term structure at the short-end can be approximated by $VS(\tau) - VS(0) \approx \theta_2 - \upsilon_{20}$. In a similar fashion, consider $\tau \approx 1/\kappa_1$ and $\tau >> 1/\kappa_2$, the term structure at medium-to-long term can be approximated as $\theta_1 - \upsilon_{10}$. As a result, by tuning the parameters θ_1 and θ_2 relative to υ_{10} and υ_{20}, one can generate a rich variation of the term structure of implied volatility. Moreover, it is worth the note that the change in θ_2 has minimal impact on the 1-month skewness because in this case the short-term variance factor takes roughly 3 months to mean-revert.

- **Scenario 3.** Then, we adjust the long-term correlation ρ_1 from -0.5 to slightly positive at 0.25 while keeping the short-term correlation the same. In that case, the long-term skew becomes flattened out much faster given the positive leverage effect of the long-term variance factor. This indicates the flexibility to control the long-term skew by adjusting the long-term factor. However, the change in ρ_1 also reduces the short-term skewness, indicating that its impact on the short-term smile is not entirely separable.

- **Scenario 4.** Finally, we combine Scenarios 2 and 3 in such a way that a hump-shaped implied volatility surface with a positive skew in long time-to-maturity can be generated - such a shape of the implied volatility surface is possible when market participants are expecting a medium-term recovery, while perceiving the possibility of a sudden market crash in the near term. Alternatively, it is often observed in the foreign-exchange market in which the implied volatility surface is usually more symmetric with its short-term and long-term smiles to be separately driven by short-term market expectations and long-term macroeconomics factors respectively.

4.2 Time-dependent Correlation

In this section, we illustrate the modeling of time-dependent correlation under the multifactor Heston model. Given the approximation formula, the put option price under the multifactor Heston model can be easily obtained by a direct numerical integration of (25) and (26). To compute the iterated integral, we break it down into nested integrals and apply the trapezoidal rule to convert them into multiple sums. For the characteristic function approach, we numerically solve the system of ODE using fourth-order Runga-Kutta method and then invert the Fourier transform accordingly. It is worth to note that in the characteristic function approach, for each strike price K, one needs to solve the system of ODE repeatedly at different grid points during the numerical inversion of the Fourier integral. In contrast, because the expansion coefficients of the approximation formula are independent of the strike price, one only needs to compute the expansion coefficients once for a given time-to-maturity to price option at an arbitrary strike.

In the following, we illustrate the computation of the put option prices under the time-dependent correlation coefficient.

Example 13 *We assume for the i^{th} variance factor, the correlation with the log stock price has the following formulation,*

$$\rho_{it} = \alpha_i e^{-\beta_i t} + \chi_i,$$

where

$$\rho_{i0} = \alpha_i + \chi_i, |\rho_{i0}| < 1, \quad \beta_i \geq 0, |\chi_i| \leq 1, \quad |\alpha_i| \leq 1 + |\chi_i|.$$

The parameter β_i governs the convergence speed of the time-dependent correlation to a long-term level of χ_i.

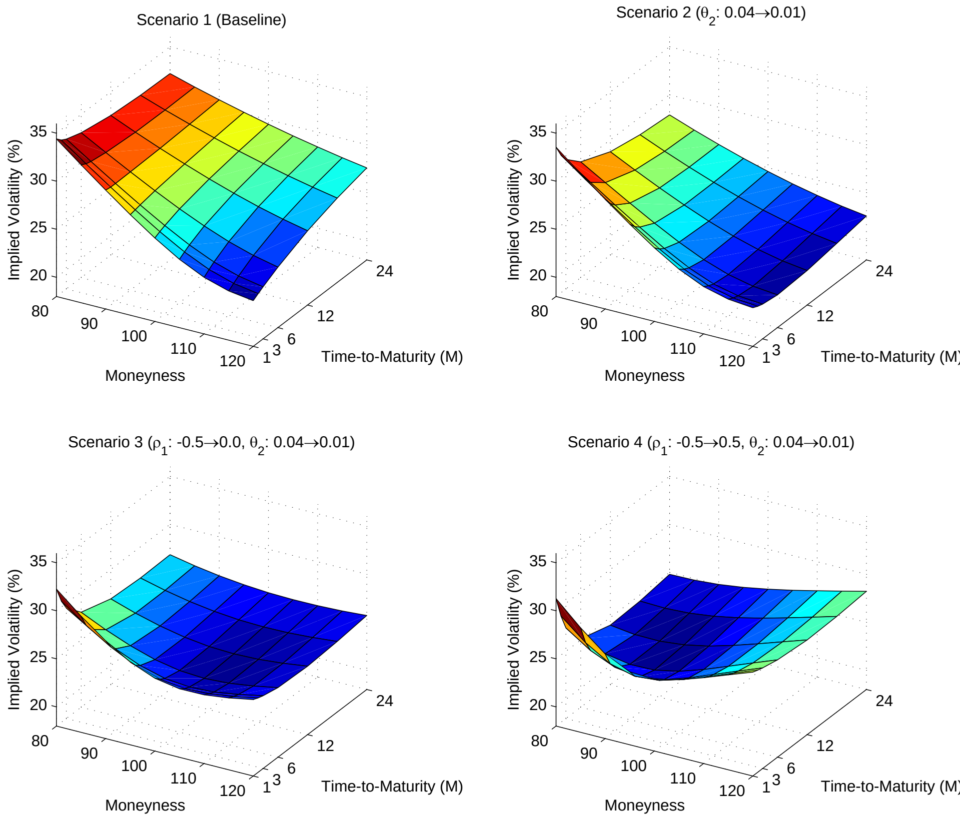

Figure 2: Various shapes of the implied volatility surfaces in Example 12.

The formulation of the time-dependent correlation is motivated by the literature on interest rate modeling, such as Piterberg (2005). Such functional form of the time-dependent correlation is simple and captures the salient fact that the correlation between stock price and volatility decouples as the time-to-maturity gets longer. Alternatively, the specification can be used to produce a persistent long-term skew by setting a high level of χ_i. The time-dependent correlation function allows a greater flexibility to model the short-term and long-term implied volatility smile separately.

Table 3 shows the accuracy of the approximation formula when correlation coefficients are time-dependent. We set the parameters $\alpha_1 = -0.15$, $\beta_1 = 0.5, \chi_1 = -0.1$ and $\alpha_2 = -0.25$, $\beta_2 = 5.0, \chi_2 = -0.25$, such that the initial correlation is consistent with Example 10 (i.e., $\rho_{10} = -0.25$ and $\rho_{20} = -0.5$). It is found that the approximation formula remains very accurate in the case of time-dependent parameters. For short-term options, the approximation formula is accurate up to the 2 decimal places, with the errors less than 50 bps, while the approximation error for long-term options remain in the order-of-magnitude of 200 bp as in the case of constant correlation. This indicates that the approximation formula is effective even in the extension to time-dependent model parameters.

5 Calibration

5.1 Data and the Calibration Procedure

To obtain the risk-neutral model parameters, we perform the daily calibration of the two-factor Heston model using the approximation formula to the cross-sectional market data of index option prices and the term structure of variance swap. We obtain from Bloomberg the interpolated data of implied volatilities of index options for the S&P 500 index (SPX) and Nikkei 225 index (NKY) with the fixed maturities of 1, 2, 3, 6, 12, 18 and 24 months and across the moneyness of 80%, 90%, 95%, 97.5%, 100%, 102.5%, 105%, 110% and 120%. The moneyness is defined by K/S, where K is the strike price and S is the current spot index level. While index options are exchange-traded

Table 3: Estimation of put option prices under two-factor Heston model in Example 13 with the time-dependent correlation to be set as: $\alpha_1 = -0.15, \beta_1 = 0.5, \chi_1 = -0.1$, $\alpha_2 = -0.25, \beta_2 = 5.0, \chi_2 = -0.25$.

Moneyness	80	90	100	110	120	80	90	100	110	120
	Time-to-Maturity = 3M					Time-to-Maturity = 1Y				
Numerical ODE	1.1716	3.4341	7.6517	13.9097	21.8071	6.0672	10.0196	15.1082	21.2389	28.2670
Approximation	1.1743	3.4342	7.6510	13.9082	21.8036	6.0642	10.0147	15.1042	21.2354	28.2619
Approximation Error	0.0026	0.0001	0.0007	0.0016	0.0034	0.0030	0.0049	0.0039	0.0035	0.0051
Error Estimate	0.0195					0.3125				
Monte-Carlo	1.1669	3.4284	7.6476	13.9065	21.8027	6.0606	10.0112	15.0976	21.2277	28.2531
MC Error	0.0038	0.0069	0.0104	0.0136	0.0161	0.0113	0.0149	0.0185	0.0220	0.0251
	Time-to-Maturity =6M					Time-to-Maturity = 2Y				
Numerical ODE	2.9716	6.1072	10.7644	16.8856	24.2415	10.8410	15.5735	21.1297	27.4193	34.3453
Approximation	2.9727	6.1056	10.7630	16.8842	24.2377	10.8301	15.5581	21.1120	27.4000	34.3240
Approximation Error	0.0011	0.0017	0.0014	0.0014	0.0037	0.0109	0.0154	0.0177	0.0193	0.0212
Error Estimate	0.0781					1.2500				
Monte-Carlo	2.9635	6.0992	10.7607	16.8863	24.2455	10.8292	15.5642	21.1229	27.4150	34.3394
MC Error	0.0070	0.0104	0.0140	0.0173	0.0202	0.0164	0.0202	0.0238	0.0273	0.0306

contracts such that their expiration dates are on fixed calendar days and the strike prices are on standardized grids, the Bloomberg converts and interpolates the option implied volatilities into constant maturities and relative moneyness to the spot index level on each trading day, taking care of the bid-ask spread and filtering of illiquid options. In addition, we obtain the term structure of variance swap for the fixed maturities of 1, 2, 3, 6, 12 and 24 months on each trading day, which is calculated from the Bloomberg implied volatility using the CBOE VIX index methodology. Hence, the variance swap rates are considered to be theoretical quotes. We obtain also the overnight-index-swap interest rate for the maturities 1, 2, 3, 6, 12, 18 and 24 months, which is considered to be a good proxy of the risk-free interest rate in the post-crisis scenario. The dividend yield is assumed to be zero. Given the implied volatility data, we compute the corresponding put option price (we call it the Bloomberg quoted price) using the Black-Scholes formula.

As noted in Christoffersen et al. (2009), the calibration of the multifactor Heston model involves the joint-identification of the structural parameters $(\rho_i, \theta_i, \kappa_i, \xi_i)$ and the unobserved initial variance υ_{i0}. They adopt an iterative two-step procedure that separately estimate the structural parameter and the initial variance. Gauthier and Rivaille (2009) note that the initial variance and the mean-reverting level have similar impact on the implied volatility smile, and suggest that one should avoid the joint-identification of the two parameters during the optimization procedure. Moreover, they mention the mean-reversion speed parameter is not sensitive to the option prices, and market participants commonly fix it at its long-term average during daily calibration. Cont and Tankov (2004) discuss the challenges involve in the calibration of an option pricing model to a finite set of market prices as an ill-posed problem, and suggest the use of a regularization function to improve the stability of the calibration across different trading days. The slight loss in precision due to the regularization function is justified by the existence of bid-ask spreads, discrete tick in price quote and measurement errors of illiquid options. Against this background, we implement the following two-step procedure to calibrate the model parameters for the two-factor Heston model.

Step 1: Calibration to the Term Structure of Variance Swap

As shown in (5), the fair strike of variance swap depends only on the structural parameters $\{\theta_1, \theta_2, \kappa_1, \kappa_2\}$ and the two unobserved initial variances $\{\upsilon_{10}, \upsilon_{20}\}$. Hence, we first calibrate these 6 parameters using the term stucture of variance swap by minimizing the sum-of-square (quadratic) pricing errors as

$$\widehat{\Theta}_t = \arg\min \left[\frac{1}{m} \sum_{k=1}^{m} \left(VS_{k,t}\left(\Theta_t\right) - VS_{k,t} \right)^2 + g\left(\Theta_t\right) \right], \tag{30}$$

where t denotes the trading day, $VS_{k,t}\left(\Theta_t\right)$ and $VS_{k,t}$ are the model-implied and Bloomberg quote of variance swap for the k^{th} time-to-maturity respectively (in volatility, the fair strike of 20% is taken to be 0.2 in the calibraion), $\Theta_t = \{\theta_1, \theta_2, \kappa_1, \kappa_2, \upsilon_{10}, \upsilon_{20}\}$ is the estimated parameters for step I. Here, $g\left(\Theta_t\right) = \alpha \left(\Theta_t - \Theta_t^{Int}\right)^2$ is the penalty function that is used to regularize the optimization, where Θ_t^{Int} is the initial guess and α is the loading coefficient of the penalty function (Cont and Tankov, 2004). It is worth to note that the penalty function is incorporated to produce stable estimates for some parameters which are difficult to identify, such as the mean levels $\{\theta_1, \theta_2\}$ and the mean-reversion speed $\{\kappa_1, \kappa_2\}$. We take the initial guess: $\kappa_1 = 0.5$, $\kappa_2 = 5.0, \theta_1 = \upsilon_{10} = 0.10$ and $\theta_2 = \upsilon_{20} = 0.05$.

These values are motivated by the average estimates from the trial calibrations that discard the penalty function. From this calibration step we can identify 6 out of the 10 parameters in the two-factor Heston model.

Step 2: Calibration to Option Price and Term structure of variance swap

In Step 2, we include the Bloomberg quoted prices of put options and calibrate the two-factor Heston model by minimizing the quadratic pricing error as

$$\widehat{\widetilde{\Theta}}_t = \arg\min \left[\frac{1}{n} \sum_{j=1}^{n} \omega_j \left(P_{j,t}\left(\widetilde{\Theta}_t\right) - P_{j,t} \right)^2 + \frac{1}{m} \sum_{k=1}^{m} \left(VS_{k,t}\left(\widetilde{\Theta}_t\right) - VS_{k,t} \right)^2 + g\left(\widetilde{\Theta}_t\right) \right], \tag{31}$$

where t denotes the trading day, $P_{j,t}\left(\widetilde{\Theta}_t\right)$ is the model-implied price for the j^{th} put option, $P_{j,t}$ is the Bloomberg quoted price for the j^{th} put option. Here, the option price is normalized by the spot price. For the calibration of option price, we select the weighting ω_j to be $(1/Vega_j)^2$, where $Vega_j$ is the Black-Scholes Vega normalized by the spot price as computed using the Bloomberg implied volatility. To avoid giving too much weights to deep in-the-money and out-of-the-money options with very small Vega, we impose a lower bound of $Vega_j$ by 0.01. As noted in Cont and Tankov (2004) and Christoffersen et al. (2009), such weighting scheme using the inverse of Black-Scholes Vega effectively converts the pricing error in option price into error in implied volatility. In our case, this makes the pricing errors for option and variance swap to be the same order of magnitude.

Following the suggestion in Gauthier and Rivaille (2009), we exclude the initial variance υ_{10} and υ_{20} in the calibration in Step 2 and fix them as the estimated values in Step I. As such, we only calibrate the remaining 8 structural parameters $\widetilde{\Theta}_t = \{\rho_1, \theta_1, \kappa_1, \xi_1; \rho_2, \theta_2, \kappa_2, \xi_2\}$ in Step 2. We do not iterative the two steps as in Christoffersen et al. (2009) because we have included variance swaps as additional market instruments to identify the initial variances υ_{10} and υ_{20}. For the initial guess, we take: $\rho_1 = \rho_2 = -0.5$, $\xi_1 = 0.5$ and $\xi_2 = 1.0$, and use the estimated parameter in Step I as the initial values for $\theta_1, \theta_2, \kappa_1$ and κ_2. For the optimization algorithm, we use the Levenberg-Marquardt algorithm to minimize the quadratic pricing error as a non-linear least-square problem.

Remark 14 *For the penalty function, one has to set a loading coefficient α that balances the stability and precision of the parameter estimates. Cont and Tankov (2004) propose the use of the Morozov discrepancy principle, which authorize the loss of precision in the optimization procedure that is of the same order of magnitude of the model error when applied to a given data set. In particular, Cont and Tankov (2004) suggest that one can first estimate a priori error level e_0 of the optimization problem (31) with $\alpha = 0$. Then, the value of α can be selected in a way such that the calibration error $e_\alpha \approx e_0$ and $e_\alpha > e_0$. Following such procedure, we perform a number of trial calibrations by taking different values of α. We take $\alpha = 0.02$ for SPX market and $\alpha = 0.04$ for NKY market as reasonable parameters that meet the criteria.*

5.2 S&P 500 Index Option

5.2.1 Calibration Results

Table 4 reports the estimated model parameters from the monthly calibration of the implied volatility surface and term structure of variance swap for the sampling period from Jan-2010 to Dec-2012. The instantaneous variance and correlation based on (2) and (3) are also reported as reference. We choose calibrate the model at the last Wednesday of a month to minimize the month-end liquidity effect that may influence the implied volatility surface. We also report the corresponding calibration errors to the implied volatility surface. As we noted in Remark (8), the approximation formula could give option value that bleach the no-arbitrage condition for some parameter range and cannot be inverted to the corresponding a Black-Scholes implied volatility. Therefore, from the estimated parameters using the approximation formula, we then compute the corresponding model-implied volatility surface by plugging in the model parameters into the exact formula of multifactor Heston model using the characteristic function approach.

1. **Initial Variance Factors:** The left panel in Figure 3 shows the time series of the two initial variance factors υ_{10} and υ_{20} based on the month-end calibration. Given the two-step procedure, the identification of the initial variance parameters is very robust with respect to different initial guess and the penalty's loading coefficient α. This suggests that the term structure of variance swap contains rich information about the variance process. The two variance factors can be distinguished as a long-term variance factor which has a mean-reversion speed of $0.3 - 0.6$, implying a half-life of around 2 to 3 years, and a short-term variance factor, with a mean-reversion speed of 5.0 (i.e., half-life of around 2 to 3 months). Moreover, the time-series dynamics of the two variance

factors and the instantaneous volatility (which is calculated as the square-root of the sum of initial variances) matches closely to the short-term volatility such as the 1-month variance swap rate.

2. **Volatility-of-Volatility and Correlation:** It is well-known that the Vol-of-Vol parameters ξ_1 and ξ_2 capture the level and curvature of the implied volatility surface, while the correlation coefficients ρ_1 and ρ_2 control the skew of the smile. Therefore, the magnitudes of these parameters are expected to be higher during stressed market scenarios. The short-term Vol-of-Vol experiences a sharp increase during Apr-Jun 2010 and Jul-Sep 2011, which correspond to the outbreak of the European debt crisis and the stock market crash amid the US debt ceiling concerns. In contrast, the long-term Vol-of-Vol remains relatively stable, which reflects the dynamics of a slower time-scale. Similar to the dynamics of the Vol-of-Vol parameters, the short-term correlation ρ_2 become highly negative at -0.8 and -0.9 during Apr-Jun 2010 and Jul-Sep 2011 respectively, reflecting the steepening of the short-term implied volatility skew when market participants perceive a higher downside risk during a distress market.

3. **Mean Level and Mean-Reversion Speed:** As shown in the right panel of Figure 3, the mean levels θ_1 and θ_2 move in tandem (with $\theta_1 > \theta_2$), reflecting the parallel shift of the implied volatility surface with an upward sloping term structure. It is interesting to note that the two parameters move in opposite direction during Apr-Jun 2010 and Jul-Aug 2011, in which the short-term mean level θ_2 experiences a drop while the long-term mean θ_1 moves upward, indicating its freedom to separately control the short-end and long-end of the level of implied volatility surface. Indeed, when we compare the estimated mean levels θ_1 and θ_2 with the variance swap rates of different tenors, we notice that the mean level θ_1 (the long-term factor) is closely linked to the long-term variance swap rate (e.g., the 12-month rate), while the mean level θ_2 appears to control slope of the term structure (e.g., the 12-month rate minus the 1-month rate). On the other hand, the mean-reversion speed parameters κ_1 and κ_2 are very stable across time and is very close to the initial values when the penalty function is imposed. Actually, the estimates of other model parameters are robust with respect to alternative choices of the initial guess of κ_1 and κ_2. This indicates the cross-sectional data of option prices at a single trading day does not contain enough information to identify the value of mean-reversion speed. In practice, the mean-reversion speed parameters should be estimated using historical data (e.g., using econometrics technique) and fix them during the daily calibration exercise.

4. **Calibration Errors:** We compute the calibration error for option price by subtracting the model implied volatility by the Bloomberg implied volatility. The average calibration error in terms of implied volatility ranges from 1% to 2% on different trading days, with the maximum calibration errors ranges from 5% to 7%. It is worth to note that the calibration error is primarily contributed by the pricing error for options in extreme strike, whereas the average calibration error for around at-the-money options are less than 0.5%, indicating an excellent fit to the implied volatility surface. The poor fit to deep moneyness options can be explained by the model restriction of stochastic volatility model and the approximation formula: i.) it is known that the short-term skewness at extreme strikes can be best explained by a model with jumps in asset price, such as a jump-diffusion or jump-to-default model; ii.) the approximation formula is less accurate for extreme strikes (in percentage terms), making it difficult to fit the implied volatility for these options.

5.2.2 Implied Volatility Surface

We present the implied volatility surface of the two consecutive month-end calibration during April 2010 and May 2010, which corresponds to the outbreak of the European debt crisis.

1. **The Leverage Effect:** Figure 4 show the calibration result for 28-April-2010. The implied volatility surface shows a steep short-term skewness, with the 1-month implied volatility going from 15% at 105% moneyness to 30% at 80% moneyness. As can be seen, the two-factor Heston model is able to reproduce the short-term skewness with the moderate leverage effect with the instantaneous correlation of -0.56. In terms of the calibration quality, the pricing errors are overall within 1-2%, with the discrepancy more significant for short-term and long-term deep in-the-money put options.

2. **The Short-Term and Long-Term Smile:** Figure 5 show the calibration result for 26–May-2011. In comparison to the upward sloping term structure in Figure 4, the term structure of implied volatility shows an inverted hump-shape which a significant short-term skewness. This indicates that market participants are expecting a recede of the debt crisis in the medium-to-long term, while perceiving the possibility of a market crash in the near term which can be caused by a sudden change in central bank policy. On the other hand,

Table 4: Calibrated model parameters and absolute errors (in volatility points) for SPX market of the two-factor Heston model. The numbers shown are the estimated parameters obtained from monthly calibration (the last Wednesday of a month) to the Bloomberg implied volatility surface and term structure of variance swap. The columns Vol. and Corr. are the instantaneous volatility (square-root of the variance) and instantaneous correlation.

	Factor 1					Factor 2							Error		
Date	ρ_1	κ_1	θ_1	ξ_1	υ_{10}	ρ_2	κ_2	θ_2	ξ_2	υ_{20}	Vol.	Corr.	Mean	Min	Max
Year 2010															
Jan	-0.54	0.52	0.069	0.59	0.035	-0.61	5.00	0.025	1.11	0.015	22.3	-0.54	1.27	0.05	3.82
Feb	-0.57	0.46	0.056	0.60	0.024	-0.52	5.00	0.034	0.98	0.010	18.3	-0.53	1.18	0.06	3.21
Mar	-0.61	0.43	0.065	0.56	0.016	-0.52	5.01	0.031	0.86	0.007	15.5	-0.56	1.26	0.07	3.16
Apr	-0.59	0.50	0.087	0.63	0.026	-0.56	5.00	0.029	1.02	0.011	19.1	-0.56	1.49	0.11	3.30
May	-0.55	0.53	0.214	0.77	0.058	-0.80	4.99	0.015	1.45	0.059	34.2	-0.68	1.88	0.03	6.82
Jun	-0.65	0.56	0.207	0.91	0.075	-0.72	4.99	0.020	1.27	0.035	33.3	-0.67	2.16	0.00	5.67
Jul	-0.65	0.44	0.110	0.85	0.031	-0.56	5.00	0.056	1.12	0.012	20.8	-0.61	1.90	0.10	5.14
Aug	-0.73	0.46	0.132	0.83	0.041	-0.61	4.99	0.061	1.09	0.016	23.9	-0.69	1.63	0.00	4.84
Sep	-0.68	0.38	0.124	0.84	0.024	-0.52	5.01	0.062	1.00	0.010	18.4	-0.63	1.78	0.04	5.81
Oct	-0.63	0.37	0.091	0.76	0.020	-0.47	5.01	0.051	0.94	0.008	16.9	-0.58	1.52	0.02	5.08
Nov	-0.63	0.28	0.127	0.69	0.019	-0.51	4.99	0.043	0.94	0.008	16.2	-0.58	1.69	0.00	4.53
Dec	-0.70	0.34	0.083	0.77	0.011	-0.52	5.04	0.053	0.83	0.005	12.6	-0.64	1.79	0.08	5.44
Year 2011															
Jan	-0.64	0.38	0.085	0.66	0.011	-0.50	5.02	0.035	0.81	0.005	12.7	-0.59	1.62	0.05	4.36
Feb	-0.63	0.50	0.097	0.66	0.028	-0.59	5.00	0.020	1.04	0.012	20.1	-0.60	1.71	0.10	3.72
Mar	-0.69	0.38	0.074	0.64	0.014	-0.55	5.02	0.036	0.85	0.006	14.1	-0.63	1.58	0.05	4.53
Apr	-0.66	0.37	0.091	0.65	0.009	-0.49	5.03	0.034	0.74	0.004	11.4	-0.60	1.57	0.11	4.97
May	-0.67	0.43	0.109	0.60	0.014	-0.52	5.01	0.025	0.84	0.007	14.5	-0.60	1.40	0.00	3.96
Jun	-0.67	0.41	0.080	0.65	0.012	-0.53	5.01	0.039	0.82	0.005	13.4	-0.62	1.63	0.10	4.53
Jul	-0.65	0.52	0.110	0.55	0.026	-0.62	5.01	0.011	0.99	0.021	21.6	-0.61	1.22	0.02	4.14
Aug	-0.57	0.56	0.133	0.76	0.066	-0.79	4.99	0.010	1.32	0.038	32.2	-0.65	2.04	0.01	5.67
Sep	-0.63	0.58	0.169	0.83	0.096	-0.93	4.99	0.006	1.47	0.065	40.1	-0.76	2.08	0.01	6.87
Oct	-0.72	0.58	0.105	0.83	0.053	-0.73	4.99	0.042	1.22	0.021	27.2	-0.71	1.90	0.04	4.27
Nov	-0.66	0.50	0.054	0.86	0.045	-0.59	5.00	0.073	1.15	0.017	24.9	-0.63	1.99	0.20	4.62
Dec	-0.67	0.46	0.091	0.74	0.034	-0.57	5.00	0.049	1.05	0.013	21.6	-0.63	1.65	0.02	3.97
Year 2012															
Jan	-0.67	0.39	0.081	0.74	0.014	-0.54	5.02	0.048	0.93	0.006	14.1	-0.62	1.85	0.07	4.92
Feb	-0.67	0.40	0.126	0.73	0.014	-0.50	5.01	0.039	0.90	0.006	14.4	-0.61	1.98	0.12	4.93
Mar	-0.69	0.39	0.099	0.69	0.007	-0.51	5.04	0.038	0.73	0.004	10.3	-0.62	1.80	0.06	4.91
Apr	-0.71	0.44	0.133	0.66	0.014	-0.55	5.01	0.027	0.86	0.007	14.4	-0.64	1.65	0.02	4.22
May	-0.64	0.52	0.138	0.74	0.035	-0.61	4.99	0.025	1.11	0.015	22.4	-0.61	1.93	0.06	4.97
Jun	-0.66	0.39	0.135	0.69	0.021	-0.51	5.00	0.035	0.92	0.009	17.2	-0.60	1.73	0.06	4.49
Jul	-0.64	0.44	0.121	0.65	0.022	-0.51	5.00	0.029	0.93	0.009	17.6	-0.58	1.61	0.01	4.48
Aug	-0.67	0.44	0.113	0.65	0.014	-0.53	5.01	0.036	0.87	0.006	14.0	-0.61	1.53	0.00	4.43
Sep	-0.64	0.45	0.137	0.56	0.015	-0.51	5.01	0.015	0.83	0.007	14.8	-0.58	1.46	0.01	3.82
Oct	-0.63	0.47	0.122	0.54	0.020	-0.52	5.00	0.009	0.88	0.010	17.3	-0.56	1.35	0.02	3.42
Nov	-0.58	0.46	0.090	0.49	0.014	-0.48	5.01	0.016	0.80	0.007	14.6	-0.52	1.22	0.03	3.35
Dec	-0.63	0.50	0.108	0.49	0.020	-0.56	5.01	0.008	0.90	0.014	18.4	-0.56	1.16	0.02	3.64
Summary	ρ_1	κ_1	θ_1	ξ_1	υ_{10}	ρ_2	κ_2	θ_2	ξ_2	υ_{20}	Vol.	Corr.	Mean	Min	Max
Mean	-0.64	0.45	0.110	0.690	0.028	-0.57	5.00	0.033	0.988	0.014	19.3	-0.61	1.645	0.049	4.556
Median	-0.65	0.45	0.109	0.675	0.021	-0.53	5.00	0.034	0.935	0.010	17.5	-0.61	1.641	0.040	4.508
Min	-0.73	0.28	0.054	0.490	0.007	-0.93	4.99	0.006	0.732	0.004	10.3	-0.76	1.162	0.003	3.163
Max	-0.54	0.58	0.214	0.908	0.096	-0.47	5.04	0.073	1.467	0.065	40.1	-0.52	2.165	0.201	6.867

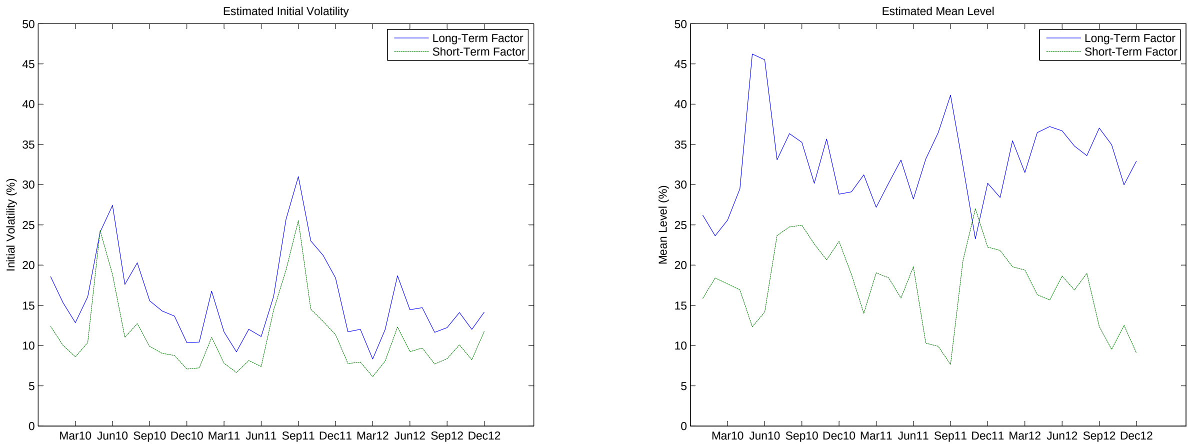

Figure 3: The time-series dynamics of the estimated initial volatility and long-term mean level in volatility points (computed as square-root of the estimates) from monthly calibration.

the short-term skewness decays much faster than in the case of Figure 4. This is because the short-term variance factor v_{2t} reverts to a lower mean-level θ_2 such that the short-term leverage effect is suppressed. This market scenario corresponds to Figure 3 (right panel) when the mean levels of the two variance factors move in opposite direction.

In terms of the model flexibility, the calibrated implied volatility surface shows that the two-factor model ia able to separately control the short-term and long-term term structure and volatility smile during these stress market scenarios. In particular, it should be noted that the two-factor model is able to generate the hump-shaped term structure of variance swap, which is not fleasible in the case of one-factor model. This indicates the necessity to adopt multifactor modeling in order to consistently price European options and volatility derivatives such as variance swaps.

5.3 Nikkei 225 Index Option

We perform similar monthly calibration using the NKY market data as obtained from Bloomberg. In contrast to the SPX option market, the NKY option market is less liquid in which deep out-of-the money and long-maturity trades are rare (Fukasawa et al., 2011). As a result, we include only the options with moneyness 90%, 95%, 97.5%, 100%, 102.5%, 105%, and 110% in the calibration.The paramter settings and procedures are similar to the case of SPX options.

5.3.1 Calibration Results

The monthly calibration result to the NKY data is presented in Table 5. As the implied volatility surface is more flat, the esimate of the short-term mean level θ_1 is found to be small, reflecting that the term structure at the short-term is usually inverted or moderately upward. In comparison to the SPX market, the estimated correlations are lower with the average instantaneous correlation of -0.48, suggesting the NKY implied volatility surface is more flat. The time-series variations of other model parameters are similar to the SPX calibration.

Given the two-step calibration procedure, the identification of the initial variance factors are robust. Nevertheless, we find a number of occasions in the data set that the term structure of variance swap are inconsistent to the implied volatility surface, in particular for long time-to-maturity options. Indeed, for the NKY options traded in the Osaka Securities Exchange, most of the contracts are traded with a duration less than 1 year in which only the June and December contracts are traded with time-to-maturity over 1 years.[1] This is in contrast to the case of SPX market in which the actively traded long-term options in the Long-term Equity Anticipation Securities (LEAPS) market helps market participants to pin down the long-end of the implied volatility surface. The poor liquidity of long-term options in the NKY market may renders the interpolation procedure by Bloomberg unreliable.

[1] See http://www.ose.or.jp/e/derivative/225options/.

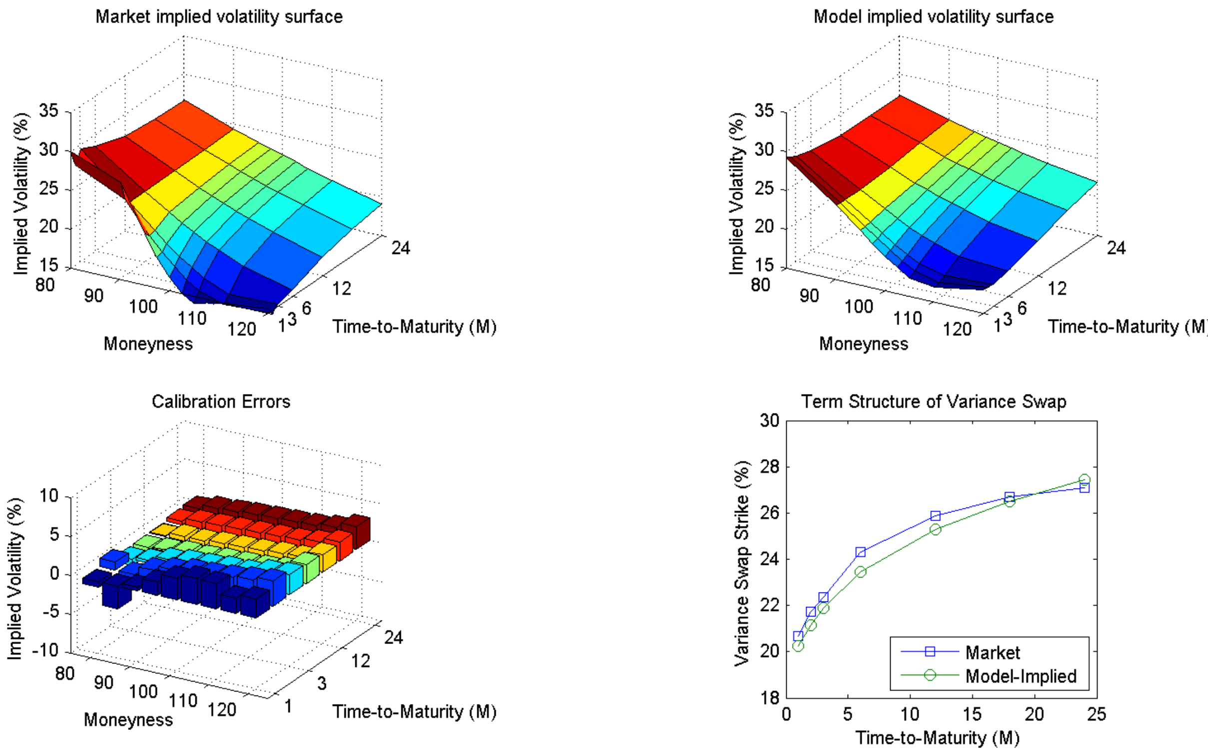

Figure 4: SPX Index on 28-Apr-2010: the plot of the Bloomberg implied volatility surface, calibrated model-implied volatility surface, calibration errors, and calibration result to the Bloomberg theoritical term structure of variance swap. The calibrated model parameters are: $\rho_1 = -0.59, \kappa_1 = 0.50, \theta_1 = 0.087, \xi_1 = 0.63, \upsilon_{10} = 0.026, \rho_2 = -0.56, \kappa_2 = 5.00, \theta_2 = 0.029, \xi_2 = 1.02, \upsilon_{20} = 0.011$.

Therefore, one should be cautious in interpreting the calibrated results in these cases. Fortunately, in the presence of the regularization procedure, the calibrated estimates are not very sensitive to the outliers.

5.3.2 Implied Volatility Surface

Figure 6 shows the calibrated implied volatility surface for 30-March-2011, which captures the stress market after the earthquake and concerns about the Fukushima nuclear disaster. The overall fit of the two-factor for around at-the-money and medium time-to-maturity options are excellent, and is able to capture the inverted term structure and some of the skew of implied volatility. Nevertheless, the model has difficulty to reproduce the short-term skew of deep moneyness options which is better to be captured by a jump-diffusion model given its disaster nature.

5.4 Computational Time

In terms of computational time, the calibration using the approximation formula is very efficient. For example, when we perform the calibration using the Matlab routine for Levenberg-Marquardt algorithm (running on a Laptop with an Intel(R) Core(TM) i7-3520 CPU at 2.90 Ghz), and set the convergence tolerance of the objective function is set to be 1e-05, the total computational time to calibrate the 36 snapshots of end-of-month implied volatility surface is around 100-150 seconds. In contrast, when the characteristic function is used to compute the exact option price, the corresponding computational time is 2000 to 2500 seconds. The computational speed improved signifcantly by a factor of 20. Indeed, the calibration to a snapshot of the implied volatility surface is almost instantaneous when the approximation formula is used. In addition, we found that the calibration using the approximation formula gives more stable estimated parameters across time. This can be explained by that fact that the computation of the exact option price using the characteristic function approach may encounter numerical instability during the calibration process at different parameter ranges (e.g., the selected contour for Fourier inversion may not be suitable for some extreme parameter ranges). In practice, it is difficult for the researcher to ensure the numerical stability

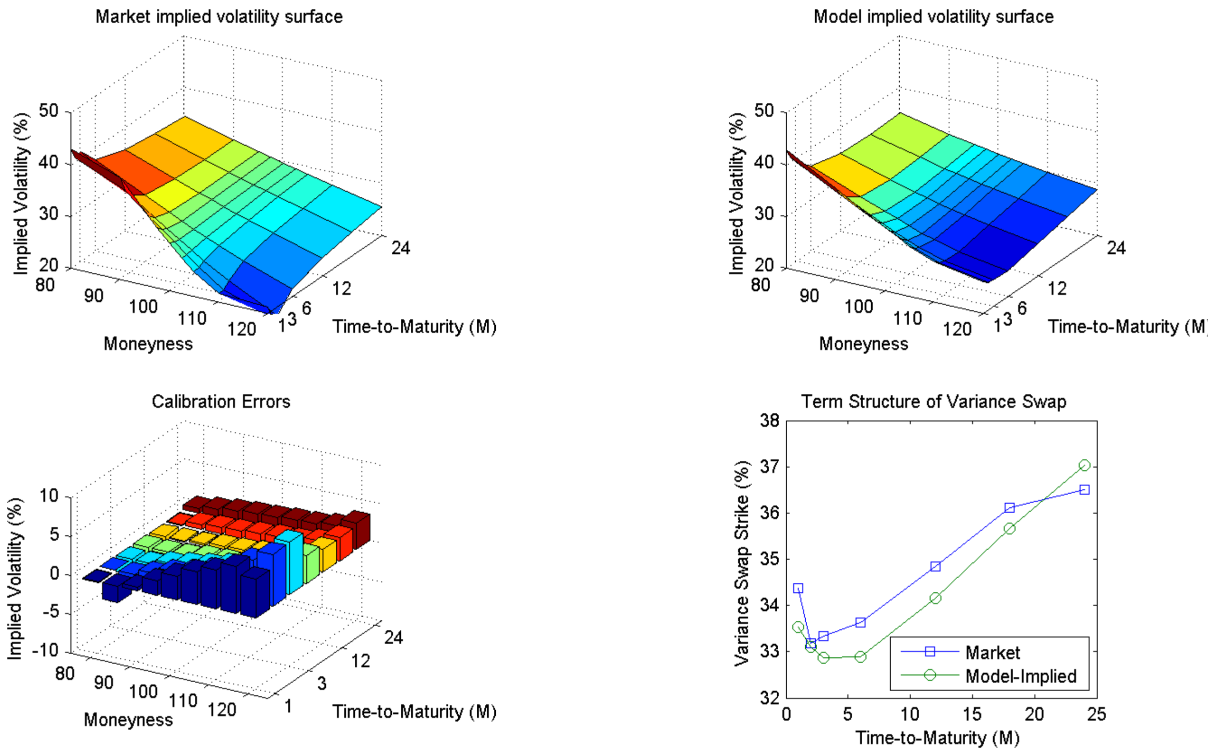

Figure 5: SPX Index on 26-May-2010: the plot of the Bloomberg implied volatility surface, calibrated model-implied volatility surface, calibration errors, and calibration result to the Bloomberg theoritical term structure of variance swap. The calibrated model parameters are: $\rho_1 = -0.55, \kappa_1 = 0.53, \theta_1 = 0.214, \xi_1 = 0.77, \upsilon_{10} = 0.058, \rho_2 = -0.80, \kappa_2 = 4.99, \theta_2 = 0.015, \xi_2 = 1.45, \upsilon_{20} = 0.059$.

of the Fourier inversion at every single iteration of the optimization procedure. The ease of implementation of the approximation formula suggests that the calibration can be done and visualized even on an excel spreadsheet environment. Moreover, given the gain in computation efficiency, the approximation formula is very useful for econometrics estimation, back-testing of the model, as well as evaluation of portfolio risk (e.g., calculation of Value-at-Risk or Counterparty Credit Exposure), in which one has to evaluate a large number of option prices while the requirement on precision is of less concerns.

6 Conclusion

In this paper, we develop an asymptotic approach to the multifactor Heston option-pricing model under time-dependent model parameters. The expansion terms under constant parameter are explicitly computed, while the incorporation of time-dependent parameters can be achieved in straight-forward manner. We show that the error bound of the approximation formula for the multifactor case can be formulated as the sum of error in the one-factor case in Benhamou et al. (2010). For illustration, we calibrate a two-factor Heston model to the option price and term structure of variance swap of the S&P 500 index. The calibration result shows that it is possible to distinguish a short-term and a long-term variance factor with different mean-reversion speed and level. In particular, the two-factor model provides the flexibility to separately control the short-end and long-end of the implied volatility in order to fit various shapes of the implied volatility surface during stress market scenarios. In terms of computational time, the approximation formula speed up the calibration procedure by at least a factor of 20 in comparison to the case when the characteristic function approach is used to compute the model prices. As the approximation formula allows one to compute option prices under Heston model with multifactor extension and time-dependent parameters in an unified framework, it would be interesting to perform the empirical study that compares the parsimoniousness of multifactor extension and time-dependent parameters extension. Finally, it is worth to note that the asymptotic approach developed in this paper can be readily applied to other multifactor models, such as a jump-to-default

Table 5: Calibrated model parameters and absolute errors (in volatility points) for NKY market of the two-factor Heston model. The numbers shown are the estimated parameters obtained from monthly calibration (the last Wednesday of a month) to the Bloomberg implied volatility surface and term structure of variance swap. The columns Vol. and Corr. are the instantaneous volatility (square-root of the variance) and instantaneous correlation.

	Factor 1					Factor 2							Error		
Date	ρ_1	κ_1	θ_1	ξ_1	υ_{10}	ρ_2	κ_2	θ_2	ξ_2	υ_{20}	Vol.	Corr.	Mean	Min	Max
Year 2011															
Jan	-0.48	0.51	0.054	0.48	0.016	-0.50	5.00	0.040	1.01	0.006	14.6	-0.45	0.93	0.02	4.07
Feb	-0.46	0.52	0.066	0.49	0.030	-0.50	5.00	0.016	1.03	0.013	20.6	-0.45	1.18	0.02	4.58
Mar	-0.52	0.54	0.100	0.47	0.041	-0.70	5.01	0.001	1.21	0.072	33.6	-0.62	1.96	0.14	6.86
Apr	-0.56	0.53	0.093	0.56	0.038	-0.58	5.00	0.014	1.08	0.016	23.1	-0.54	1.33	0.00	4.24
May	-0.57	0.55	0.105	0.52	0.038	-0.62	5.00	0.001	1.11	0.018	23.6	-0.55	1.61	0.00	5.15
Jun	-0.48	0.53	0.104	0.58	0.040	-0.56	5.00	0.002	1.08	0.018	24.1	-0.49	1.76	0.10	4.17
Jul	-0.40	0.50	0.060	0.53	0.030	-0.46	5.00	0.024	1.02	0.012	20.7	-0.41	1.59	0.00	4.73
Aug	-0.72	0.57	0.141	0.81	0.063	-0.60	5.00	0.001	1.11	0.023	29.3	-0.67	2.57	0.44	9.74
Sep	-0.60	0.49	0.116	0.80	0.079	-0.62	5.01	0.006	1.16	0.048	35.8	-0.60	3.40	0.10	6.89
Oct	-0.57	0.48	0.135	0.75	0.049	-0.54	5.00	0.022	1.06	0.021	26.5	-0.55	1.89	0.27	4.53
Nov	-0.59	0.53	0.154	0.71	0.063	-0.60	5.00	0.005	1.11	0.032	30.8	-0.58	2.26	0.13	5.72
Dec	-0.47	0.55	0.036	0.45	0.030	-0.53	4.99	0.043	1.05	0.009	19.7	-0.46	1.84	0.08	7.94
Year 2012															
Jan	-0.43	0.51	0.058	0.50	0.029	-0.47	5.00	0.027	1.03	0.012	20.2	-0.42	1.17	0.13	3.45
Feb	-0.44	0.43	0.180	0.85	0.027	-0.43	5.00	0.019	1.00	0.011	19.6	-0.44	2.28	0.28	5.63
Mar	-0.44	0.46	0.069	0.64	0.023	-0.44	5.00	0.031	1.01	0.009	17.8	-0.43	1.50	0.01	4.31
Apr	-0.48	0.47	0.057	0.63	0.025	-0.48	5.00	0.033	1.03	0.010	18.8	-0.47	1.30	0.14	2.92
May	-0.35	0.41	0.227	0.99	0.037	-0.43	5.00	0.016	1.01	0.017	23.3	-0.38	3.30	0.16	8.26
Jun	-0.55	0.44	0.100	0.80	0.025	-0.48	5.00	0.037	1.04	0.010	18.5	-0.52	2.14	0.17	4.43
Jul	-0.51	0.48	0.101	0.72	0.031	-0.52	4.99	0.021	1.06	0.012	20.9	-0.51	2.01	0.07	4.49
Aug	-0.37	0.48	0.108	0.65	0.021	-0.41	4.99	0.022	1.01	0.008	17.1	-0.38	1.67	0.04	4.05
Sep	-0.37	0.45	0.133	0.76	0.019	-0.37	4.99	0.021	0.99	0.008	16.5	-0.37	2.32	0.31	6.41
Oct	-0.40	0.44	0.134	0.67	0.020	-0.44	5.00	0.011	1.00	0.012	17.8	-0.41	1.70	0.00	4.77
Nov	-0.32	0.48	0.058	0.50	0.021	-0.37	5.00	0.019	0.96	0.009	17.2	-0.32	1.67	0.05	3.99
Dec	-0.48	0.48	0.101	0.63	0.029	-0.49	5.00	0.021	1.02	0.012	20.2	-0.47	1.34	0.02	4.18
Summary	ρ_1	κ_1	θ_1	ξ_1	υ_{10}	ρ_2	κ_2	θ_2	ξ_2	υ_{20}	Vol.	Corr.	Mean	Min	Max
Mean	-0.48	0.49	0.104	0.645	0.034	-0.51	5.00	0.019	1.051	0.017	22.1	-0.48	1.865	0.112	5.230
Median	-0.48	0.48	0.101	0.638	0.030	-0.49	5.00	0.020	1.029	0.012	20.4	-0.46	1.728	0.089	4.558
Min	-0.72	0.41	0.036	0.451	0.016	-0.70	4.99	0.001	0.963	0.006	14.6	-0.67	0.931	0.000	2.915
Max	-0.32	0.57	0.227	0.991	0.079	-0.37	5.01	0.043	1.211	0.072	35.8	-0.32	3.396	0.439	9.739

model with stochastic default intensity, or a mixture stochastic volatility model in which one factor is driven by a Brownian motion and another factor driven by a fractional Brownian motion. These extensions are left for further research.

References

[1] Alos,E., J.Leon and J.Vives (2007) On the Short-Time Behavior of the Implied Volatility for Jump-Diffusion Models with Stochastic Volatility, Finance and Stochastics 11, 4:571-589.

[2] Ait-Sahalia,Y. and R.Kimmel (2007) Maximum Likelihood Estimation of Stochastic Volatility Models, Journal of Financial Economics 83, 413-452.

[3] Antonelli,F. and S.Scarlatti (2009) Pricing options under stochastic volatility: A Power Series Approach, Finance and Stochastics 13, 2:269-303.

[4] Benhamou,E., E.Gobet and M.Miri (2010b) Time Dependent Heston Model, SIAM Journal on Financial Mathematics 1:289-325.

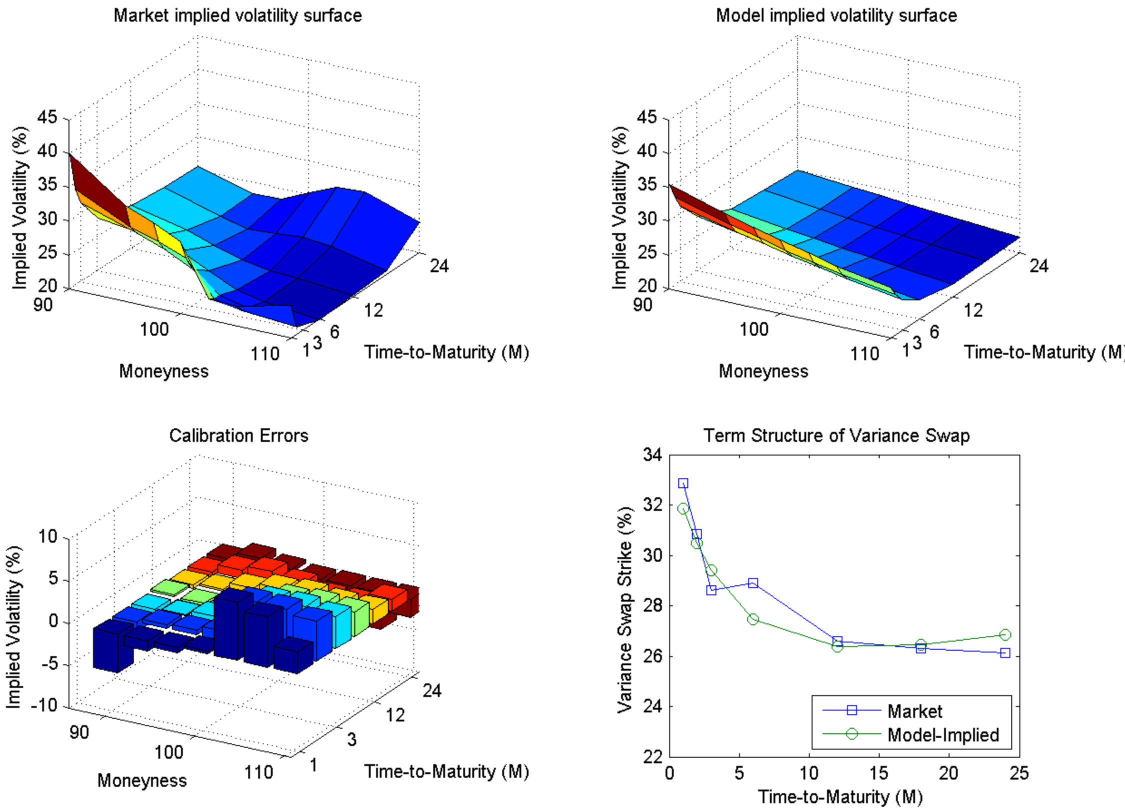

Figure 6: NKY Index on 26-Jan-2010: the plot of the Bloomberg implied volatility surface, calibrated model-implied volatility surface, calibration errors, and calibration result to the Bloomberg theoritical term structure of variance swap. The calibrated model parameters are: $\rho_1 = -0.52, \kappa_1 = 0.54, \theta_1 = 0.100, \xi_1 = 0.47, \upsilon_{10} = 0.041, \rho_2 = -0.70, \kappa_2 = 5.01, \theta_2 = 0.001, \xi_2 = 1.21, \upsilon_{20} = 0.072$.

[5] Bengomi,L. (2009). Dynamic Properties of Smile Models. Frontiers in Quantitative Finance: Volatility and Credit Risk Modeling, Wiley.

[6] Buehler,H. (2006) Consistent Variance Curve Model. Finance and Stochastic, 10:178-203.

[7] Bayraktar,E. and B.Yang (2011) A Unified Framework for Pricing Credit and Equity Derivatives, Mathmatical Finance 21, 3:493-517.

[8] Carr,P. and D.Madan (1999) Option Valuation using the Fast Fourier Transform, Journal of Computational Finance 2, 4:61-73.

[9] Christoffersen,P., S.Heston and K.Jacobs (2009) The Shape and Term Structure of the Index Option Smirk: Why Multifactor Stochastic Volatility Models Work so Well, Management Science 55, 12:1914-1932.

[10] Chung,T.K. and Y.K.Kwok (2012) Equity-Credit Modeling under Affine Jump-Diffusion-Models with Jump-to-Default, to appear in Handbook on Computational Economics and Finance, Oxford University Press.

[11] Cont,R. and Tankov,P. (2004) Non-Parametric Calibration of Jump-Diffusion Option Pricing Models, Journal of Computational Finance, 7, 3:1-49.

[12] Duffie,D., Pan,J. and K.Singleton (2000) Transform Analysis and Asset Pricing for Affine Jump-Diffusions, Econometrica 68, 6:1343-1376.

[13] Fonseca,J., M. Grasselli and C.Tebaldi (2008) A Multifactor Volatility Heston Model, Quantitative Finance 8, 6:591-604.

[14] Fouque,J-P., G.Papanicolaou and R.Sircar (2000) Derivatives in Financial Markets with Stochastic Volatility, Cambridge University Press, Cambridge, UK.

[15] Fouque,J-P., G.Papanicolaou, R.Sircar and K.Solna (2003) Multiscale Stochastic Volatility Asymptotics, SIAM Journal on Multiscale Modeling and Simulations 2, 1:22-42.

[16] Fouque,J-P., G.Papanicolaou, R.Sircar and K.Solna (2004) Maturity Cycles in Implied Volatility, Finance and Stochastics 8, 4:451-477.

[17] Froque,J-P and M.J.Lorig (2011) A Fast Mean-Reverting Correction to Heston's Stochastic Volatility Model, SIAM Journal on Financial Mathematics 2, 221-254.

[18] Fukasawa,M. (2011) Asymptotic Analysis for Stochastic Volatility: Martingale Expansion, Finance and Stochastic 15, 4:635-654.

[19] Fukasawa,M., I.Ishida. N.Maghrebi, K.Oya, M.Ubukata and K.Yamazaki (2011) Model-Free Implied Volatility: from Surface to Index. International Journal of Theoretical and Applied Finance 14, 4:433-463.

[20] Gatheral,J., E.Hsu, P.Laurence, C.Ouyang and T-H.Wang (2009) Asymptotics of Implied Volatility in Local Volatility Models, Mathematical Finance 22, 4:591-620.

[21] Gauthier,P. and P-Y.H.Rivaille (2009) Fitting the Smile, Smart Parameters for SABR and Heston, Working Paper.

[22] Hagan,P., D.Kumar, A,Lesniewski and D.Woodward (2002) Managing Smile Risk, Wilmott Magazine, 15:84-108.

[23] Heston,S. (1993) A Closed-Form Solution for Options with Stochastic Volatility with Applications to Bond and Currency Options, Review of Financial Studies 6, 2:327-343.

[24] Labordere,P.H. (2005) A General Asymptotic Implied Volatility for Stochastic Volatility Models, Working Paper.

[25] Lee,R.W. (2004) Option Pricing by Transform Methods: Extensions, Unification and Error Control, Journal of Computational Finance 7, 3:51-86.

[26] Lewis,A. (2007) Geometries and Smile Asymptotics for a Class of Stochastic Volatility Models, Working Paper.

[27] Li,G. and C.Zhang (2010) On the Number of State Variables in Option Pricing, Management Science 56, 11:2058-2075.

[28] Lord,R. and C.Kahl (2007) Optimal Fourier Inversion in Semi-Analytical Option Pricing, Journal of Computational Finance 10, 4:1-30.

[29] Lord,R. and C.Kahl (2010) Complex Logarithms in Heston-like Models. Mathematical Finance 20, 4:671-694.

[30] Nualart,D. (2006) The Malliavin Calculus and Related Topics, 2nd ed., Springer.

[31] Osajima,Y. (2007) The Asymptotic Expansion Formula of Implied Volatility for Dynamic SABR Model and FX Hybrid Model, Working Paper.

[32] Sircar,R. and Papageorgiou,E. (2009) Multiscale Intensity Models and Name Grouping for Valuation of Multi-name Credit Derivatives, Applied Mathematical Finance 16, 4:353-383.

[33] Piterbarg,V. (2005) Time to smile, Risk Magazine 18, 5:71-75.

[34] Takahashi,A. and T.Yamada (2012) An Asymptotic Expansion with Push-Down of Malliavin Weights, SIAM Journal on Financial Mathematics 3, 1:95-136.

[35] Tanaka,K., T.Yamada and T.Watanabe (2010) Applications of Gram-Charlier Expansion and Bond Moments for Pricing of Interest Rates and Credit Risk, Quantitative Finance 10, 6:645-662.

[36] Yu,C., Li,H. and M.Wells (2010) Estimation of Levy Jump Models Under the Risk Neutral and Physical Measure Using Stock and Option Prices, Mathematical Finance 21, 3:383–422

[37] Zheng,W. and Y.K.Kowk (2013) Closed Form Pricing Formulas for Discretely Sampled Generalized Variance Swaps, forthcoming in Mathematical Finance.

A Multifactor Heston Model under AD framework

In this Appendix, we derive the closed-form solution of the characteristic function for the multifactor Heston model under the AD framework in Duffie et al. (2000). Consider the filtered probability space $(\Omega, F, \{\mathcal{F}_t\}, P)$, the multifactor Heston model is defined in some state space $D \subset \mathbb{R}^{2n}$:

$$dY_t = \mu(Y_t)\,dt + \sigma(Y_t)\,dZ_t$$

with the $2n$-dimensional Brownian motions $Z_t = \left\{W_t^1, ..., W_t^n, B_t^1, ..., B_t^n\right\}$ and the state variables $Y_t = (x_t, \upsilon_t)$ where $x_t = (X_t, 0, ..., 0)^T$ and $\upsilon_t = (\upsilon_{1t}, \upsilon_{2t}, ..., \upsilon_{nt})^T$, with X_t is the log-forward price in (1). The drift coefficient is given by $\mu(Y_t) = (\mu_x(Y_t), \mu_\upsilon(Y_t))$ with

$$\mu_x(Y_t) = \left(-\frac{1}{2}\sum_{i=1}^{n}\upsilon_{it}, 0, ..., 0\right)^T, \ \mu_\upsilon(Y_t) = (\kappa_1(\theta_1 - \upsilon_{1t}), ..., \kappa_n(\theta_n - \upsilon_{nt}))^T,$$

and the volatility matrix is formulated as

$$\sigma(Y_t) = \begin{pmatrix} \sqrt{\upsilon_{1t}} & \cdots & 0 & 0 & \cdots & 0 \\ \vdots & \ddots & \vdots & \vdots & \ddots & \vdots \\ 0 & \cdots & \sqrt{\upsilon_{nt}} & 0 & \cdots & 0 \\ \rho_1\xi_1\sqrt{\upsilon_{1t}} & \cdots & 0 & \xi_1\sqrt{1-\rho_1^2}\sqrt{\upsilon_{2t}} & \cdots & 0 \\ \vdots & \ddots & \vdots & \vdots & \ddots & \vdots \\ 0 & \cdots & \rho_n\xi_n\sqrt{\upsilon_{nt}} & 0 & \cdots & \xi_n\sqrt{1-\rho_n^2}\sqrt{\upsilon_{nt}} \end{pmatrix}.$$

Following Duffie et al. (2000), the marginal characteristic function with $u = (u_0, 0, ..., 0)$ is readily obtained as

$$\phi(Y_t; t, T; u) = \mathbb{E}\left[\exp(u_0 X_T)|\,\mathcal{F}_t\right] = \mathbb{E}_t\left[\exp(u \cdot Y_T)\right] = \exp\left[A(T-t) + B(T-t)\,x_t + \sum_{i=1}^{n} D_i(T-t)\,\upsilon_{i0}\right], \quad \text{(A.1)}$$

in which the coefficients $A(\tau)$, $B(\tau)$ and $D(\tau) = (D_1(\tau), ..., D_n(\tau))^T$ solve the system of ODEs

$$\begin{aligned} \frac{\partial A(\tau)}{\partial \tau} &= \sum_{i=1}^{n}\kappa_i\theta_i D_i(\tau), \quad \frac{\partial B(\tau)}{\partial \tau} = 0, \\ \frac{\partial D_i(\tau)}{\partial \tau} &= \frac{1}{2}\xi_i^2 D_i^2(\tau) + \rho_i\xi_i B(\tau) D_i(\tau) - \kappa_i D_i(\tau) + \frac{1}{2}B^2(\tau) - \frac{1}{2}B(\tau), \end{aligned}$$

for $i = 1, 2, ..., n$ and $\tau \in [0, T-t]$, with the initial conditions given by $A(0) = 0$, $B(0) = u_0$ and $D_i(0) = 0$. It is noted that the ODEs governing $D_i(\tau)$ can be recasted as a Riccati equation

$$\frac{\partial D_i(\tau)}{\partial \tau} = c_{i,0} + c_{i,1}D_i(\tau) + c_{i,2}D_i^2(\tau),$$

for $i = 1, 2, ..., n$, by expressing the coefficients

$$c_{i,0} = \frac{1}{2}u_0(u_0 - 1), \quad c_{i,1} = \rho_i\xi_i u_0 - \kappa_i, \quad c_{i,2} = \frac{1}{2}\xi_i^2,$$

with the boundary condition $D_i(0) = 0$. By direct integration, the system of ODEs has the explicit solution

$$\begin{aligned} A(\tau) &= \sum_{i=1}^{n}\kappa_i\theta_i\left\{r_{i,-}\tau - \frac{2}{\xi_i^2}\ln\left[\frac{1 - g_i\exp[-d_i\tau]}{1 - g_i}\right]\right\}, \\ B(\tau) &= u_0, \quad D_i(\tau) = r_{i,-}\frac{1 - \exp[-d_i\tau]}{1 - g_i\exp[-d_i\tau]}, \end{aligned} \quad \text{(A.2)}$$

where

$$r_{i,\pm} = \frac{1}{2c_{i,2}}\left[-c_{i,1} \pm d_i\right], \quad g_i = \frac{r_{i,-}}{r_{i,+}}, \quad d_i = \sqrt{c_{i,1}^2 - 4c_{i,0}c_{i,2}}.$$

In the case when the model parameters are time-dependent, we do not have closed-form solution and one has to resort numerical method such as the fourth-order Runga-Kutta method to solve the system of ODEs. By taking $u_0 = i_0\omega$ gives (6) in Section 2.

B Asymptotic Expansion Formula

Recall that the put option price under the perturbed Heston model is given by

$$g(\epsilon)=\mathbb{E}\left[e^{-\int_0^T r_t dt}\mathbb{E}\left[\left(K-e^{\int_0^T (r_t-q_t)dt+X_T^{\epsilon}}\right)_+\middle|\mathcal{F}_T^B\right]\right]=\mathbb{E}[P(x'+\Delta x\left(\epsilon\right),y'+\Delta y\left(\epsilon\right))]. \tag{B.1}$$

Now, we expand $P(x'+\Delta x\left(\epsilon\right),y'+\Delta y\left(\epsilon\right))$ with respect to ϵ around $\epsilon=0_n$ up to second order,

$$P(x'+\Delta x\left(\epsilon\right),y'+\Delta y\left(\epsilon\right))=P(x',y')+\sum_{i=1}^n \epsilon_i\,\frac{\partial P}{\partial \epsilon_i}(x\left(\epsilon\right),y\left(\epsilon\right))\bigg|_{\epsilon=0_n}+\frac{1}{2}\sum_{i=1}^n\sum_{j=1}^n \epsilon_i\epsilon_j\,\frac{\partial^2 P}{\partial\epsilon_i\partial\epsilon_j}(x\left(\epsilon\right),y\left(\epsilon\right))\bigg|_{\epsilon=0_n}+\varepsilon \tag{B.2}$$

where ε is the expansion error. The partial derivatives are given by chain rules as

$$\begin{aligned}
\frac{\partial P}{\partial \epsilon_i}(x\left(\epsilon\right),y\left(\epsilon\right)) &= P_x\partial_i x+P_y\partial_i y\\
\frac{\partial^2 P}{\partial \epsilon_i^2}(x\left(\epsilon\right),y\left(\epsilon\right)) &= P_{xx}(\partial_i x)^2+P_x\partial_i^2 x+P_{yy}(\partial_i y)^2+P_y\partial_i^2 y+2P_{xy}(\partial_i x)(\partial_i y)\\
\frac{\partial^2 P}{\partial \epsilon_i\partial\epsilon_j}(x\left(\epsilon\right),y\left(\epsilon\right)) &= P_{xx}\left(\partial_i x\right)\left(\partial_j x\right)+P_{xy}\left(\partial_i x\right)\left(\partial_j y\right)+P_{yy}\left(\partial_i y\right)\left(\partial_j y\right)+P_{xy}\left(\partial_j x\right)\left(\partial_i y\right)
\end{aligned}$$

with the notation $P_x=\frac{\partial P}{\partial x}(x',y')$, $\partial_i x=\frac{\partial x(\epsilon)}{\partial\epsilon_i}\Big|_{\epsilon=0_n}$ and $\partial_i\partial_j x=\frac{\partial^2 x(\epsilon)}{\partial\epsilon_i\partial\epsilon_j}\Big|_{\epsilon=0_n}$, where we have used the relationship

$$\partial_i\partial_j x\left(\epsilon\right)=\partial_i\partial_j y\left(\epsilon\right)=0.$$

Plugging in these derivatives to the expansion formula (B.2), we have

$$\begin{aligned}
P(x'+\Delta x\left(\epsilon\right),y'+\Delta y\left(\epsilon\right))= \quad & P(x',y')+\sum_{i=1}^n\left[P_x\left(\epsilon_i\partial_i x+\frac{1}{2}\epsilon_i^2\partial_i^2 x\right)+P_y\left(\epsilon_i\partial_i y+\frac{1}{2}\epsilon_i^2\partial_i^2 y\right)\right]\\
&+\frac{1}{2}\sum_{i=1}^n\sum_{j=1}^n\epsilon_i\epsilon_j\left[P_{xx}(\partial_i x)(\partial_j x)+P_{yy}(\partial_i y)(\partial_j y)+2P_{xy}(\partial_i x)(\partial_j y)\right]+\varepsilon.
\end{aligned}$$

By noting that

$$\begin{aligned}
\partial_i x\left(\epsilon\right) &= \partial_i\Gamma_{iT}^{\epsilon_i}=\Gamma_{i1,T}, \quad \partial_i^2 x\left(\epsilon\right)=\partial_i^2\Gamma_{iT}^{\epsilon_i}=\Gamma_{i2,T}\\
\partial_i y\left(\epsilon\right) &= \partial_i\Xi_{iT}^{\epsilon_i}=\Xi_{i1,T}, \quad \partial_i^2 y\left(\epsilon\right)=\partial_i^2\Xi_{iT}^{\epsilon_i}=\Xi_{i2,T},
\end{aligned}$$

the expansion is written as

$$\begin{aligned}
& P(x'+\Delta x\left(\epsilon\right),y'+\Delta y\left(\epsilon\right))\\
= \quad & P(x',y')+\sum_{i=1}^n\left[P_x\left(\epsilon_i\Gamma_{i1,T}+\frac{\epsilon_i^2}{2}\Gamma_{i2,T}\right)+P_y\left(\epsilon_i\Xi_{i1,T}+\frac{\epsilon_i^2}{2}\Xi_{i2,T}\right)\right]\\
& +\frac{1}{2}\sum_{i=1}^n\sum_{j=1}^n\epsilon_i\epsilon_j\left[P_{xx}\Gamma_{i1,T}\Gamma_{j1,T}+P_{yy}\Xi_{i1,T}\Xi_{j1,T}+2P_{xy}\Gamma_{i1,T}\Xi_{j1,T}\right]+\varepsilon,\\
= \quad & P(x',y')+P_x\sum_{i=1}^n\left(\epsilon_i\Gamma_{i1,T}+\frac{\epsilon_i^2}{2}\Gamma_{i2,T}\right)+P_y\sum_{i=1}^n\left(\epsilon_i\Xi_{i1,T}+\frac{\epsilon_i^2}{2}\Xi_{i2,T}\right)\\
& +\frac{1}{2}\left[P_{xx}\left(\sum_{i=1}^n\epsilon_i\Gamma_{i1,T}\right)^2+P_{yy}\left(\sum_{i=1}^n\epsilon_i\Xi_{i1,T}\right)^2+2P_{xy}\left(\sum_{i=1}^n\epsilon_i\Gamma_{i1,T}\right)\left(\sum_{i=1}^n\epsilon_i\Xi_{i1,T}\right)\right]+\varepsilon.
\end{aligned}$$

Then, by taking the expectations on the both sides, the second-order expansion of $g(\epsilon)$ with respect to ϵ around $\epsilon = 0_n$ is given by

$$\begin{aligned} g(\epsilon) &= \mathbb{E}\left[P(x',y')\right] + \mathbb{E}\left[\frac{\partial P(x',y')}{\partial x}\sum_{i=1}^{n}\left(\epsilon_i\Gamma_{i1,T} + \frac{\epsilon_i^2}{2}\Gamma_{i2,T}\right)\right] \\ &+\mathbb{E}\left[\frac{\partial P(x',y')}{\partial y}\left(\epsilon_i\Xi_{i1,T} + \frac{\epsilon_i^2}{2}\Xi_{i2,T}\right)\right] \\ &+\frac{1}{2}\mathbb{E}\left[\frac{\partial^2 P(x',y')}{\partial x^2}\left(\sum_{i=1}^{n}\epsilon_i\Gamma_{i1,T}\right)^2\right] + \frac{1}{2}\mathbb{E}\left[\frac{\partial^2 P(x',y')}{\partial y^2}\left(\sum_{i=1}^{n}\epsilon_i\Xi_{i1,T}\right)^2\right] \\ &+\mathbb{E}\left[\frac{\partial^2 P(x',y')}{\partial x\partial y}\left(\sum_{i=1}^{n}\epsilon_i\Gamma_{i1,T}\right)\left(\sum_{i=1}^{n}\epsilon_i\Xi_{i1,T}\right)\right] + \tilde{\varepsilon}, \end{aligned} \tag{B.3}$$

where $\tilde{\varepsilon} = \mathbb{E}[\varepsilon]$. By plugging in the explicit expressions in (17) and (18), we obtain the expansion formula in Section 3.2. It is noted that the result (B.3) is obtained via the expansion with respect to ϵ while we consider an expansion with respect to a different parameter λ with keeping ϵ fixed later in Appendix D.

C Expansion Coefficients with Malliavin Calculus

We set out the following definitions and lemmas by following Benhamou et al. (2010).

Definition 15 *(Integral Operator)*

1. For any real number k and any integrable function $l = l(u)$, for $u \in [0,T]$, we denote

$$\omega_{t,T}^{(k,l)} \triangleq \int_t^T e^{ku} l(u)\, du \tag{C.1}$$

for $\forall t \in [0,T]$.

2. For any real numbers $(k_1, k_2, ..., k_n)$ and any integrable functions $(l_1, l_2, ..., l_n)$, $l_i = l_i(u)$ for $u \in [0,T]$, we denote the n-times iterated integral as

$$\omega_{t,T}^{(k_1,l_1),(k_2,l_2),...,(k_n,l_n)} \triangleq \omega_{t,T}^{\left(k_1, l_1\omega_{\cdot,T}^{(k_2,l_2),...,(k_n,l_n)}\right)} \tag{C.2}$$

for $\forall t \in [0,T]$.

Lemma 16 *(Duality Formula) For $G \in \mathbb{D}^{1,\infty}(\Omega)$ and a square integrable and predictable process γ, we have*

$$\mathbb{E}\left[G\int_0^t \gamma_s dB_s\right] = \mathbb{E}\left[\int_0^t \gamma_s D_s^B(G) ds\right] \tag{C.3}$$

where $D_s^B(G) = \left(D_s^B(G)\right)_{s\geq 0}$ is the first Malliavin derivative of G with respect to a one-dimensional standard Brownian motion B.
Proof. *See Nualart (2006).* ■

As an application of the result above, an expectation of a random variable with a stochastic integral with respect to B^α can be transformed by the duality formula to pick up only the diffusion coefficient of B^α. The technique plays an important role as a building block in the following calculations.

Lemma 17 *Suppose a random variable is given in a form of $G(V_T) \in \mathbb{D}^{1,\infty}(\Omega)$, where G is a smooth function, $V_T = \sum_{i=1}^{n}\int_0^T \rho_{it}\sqrt{\upsilon_{i0,t}}dB_t^i$ and B^i are independent standard Brownian motions for $i = 1, 2, ..., n$. Let γ be a square integrable and predictable process. Then we have*

$$\mathbb{E}\left[G(V_T)\int_0^t \gamma_s dB_s^\alpha\right] = \mathbb{E}\left[G^{(1)}(V_T)\int_0^t \gamma_s\rho_{\alpha t}\sqrt{\upsilon_{\alpha 0,t}}ds\right] \tag{C.4}$$

for all $\alpha = 1, 2, ..., n$, where $G^{(k)}$ is the k-th derivative of G.

Proof. Let us denote by $D^\alpha = (D_s^\alpha(\cdot))_{s\geq 0}$ the first Malliavin derivative with respect to the Brownian motion B^α, for $\alpha = 1, 2, ..., n$. Note that

$$D_s^\alpha \left(\int_0^T \rho_{it} \sqrt{\upsilon_{i0,t}} dB_t^i \right) = \delta_{i\alpha} \rho_{\alpha s} \sqrt{\upsilon_{\alpha s}} \mathbf{1}_{\{s\leq T\}},$$

where δ_{ij} is the Kronecker's delta. By the chain rule of Malliavin derivative (see Nualart, 2006, Proposition 1.2.3), we have

$$D_s^\alpha (G(V_T)) = G^{(1)}(V_T) \sum_{i=1}^n D_s^\alpha \left(\int_0^T \rho_{it} \sqrt{\upsilon_{i0,t}} dB_t^i \right) = G^{(1)}(V_T) \rho_{\alpha s} \sqrt{\upsilon_{\alpha s}} \mathbf{1}_{\{s\leq T\}}. \tag{C.5}$$

Then Lemma 16 yields the result. ■

Lemma 18 *For any deterministic integrable function f on $[0,T]$ and any continuous semimartingale Z with $Z(0) = 0$, we have*

$$\int_0^T f(t) Z(t) dt = \int_0^T \omega_{t,T}^{(0,f)} dZ(t).$$

Proof. Applying Ito's formula on $\omega_{t,T}^{(0,f)} Z(t)$, we have $d\left(\omega_{t,T}^{(0,f)} Z(t)\right) = -f(t) Z(t) dt + \omega_{t,T}^{(0,f)} dZ(t)$. Note that $Z(0) = 0$ and $\omega_{T,T}^{(0,f)} = 0$. A direct integration on both side from $t = 0$ to $t = T$ gives the result. ■

Lemma 19 *Let $P = P(x, y)$ to be the Black-Scholes formula of a put option, we have*

$$\left[\frac{\partial}{\partial y} - \frac{1}{2} \left[\frac{\partial^2}{\partial x^2} - \frac{\partial}{\partial x} \right] \right] P(x, y) = 0 \tag{C.6}$$

for all $x \in \mathbb{R}$ and $y \in \mathbb{R}^+$.
Proof. *This can be proved by direct differentiation of the Black-Scholes formula.* ■

To proceed, we state the following Lemma, which is an extension of Lemma 5.5 in Benhamou et al. (2010).

Lemma 20 *Let $G(V_T) = G\left(\sum_{i=1}^n \int_0^T \rho_{it} \sqrt{\upsilon_{i0,t}} dB_t^i \right) \in \mathbb{D}^{1,\infty}(\Omega)$ as in Lemma 17, h be a deterministic function which is integrable, and $\upsilon_{i1,t} = e^{-\kappa_i t} \int_0^t e^{\kappa_i s} \xi_{is} \sqrt{\upsilon_{i0,s}} dB_s^i$ as defined in (15) for $i = 1, 2, ..., n,$. Then,we have*

$$\begin{aligned}
\mathbb{E}\left[G(V_T) \int_0^T h(t) \upsilon_{\alpha 1,t} dt \right] &= \omega_{0,T}^{(\kappa_\alpha,\phi_{\alpha 1}),(-\kappa_\alpha,h)} \mathbb{E}\left[G^{(1)}(V_T) \right], \qquad (C.7)\\
\mathbb{E}\left[G(V_T) \int_0^T h(t) \upsilon_{\alpha 1,t} \upsilon_{\beta 1,t} dt \right] &= \omega_{0,T}^{(\kappa_\alpha,\phi_{\alpha 1}),(\kappa_\beta,\phi_{\beta 1}),(-(\kappa_\alpha+\kappa_\beta),h)} \mathbb{E}\left[G^{(2)}(V_T) \right] \\
&\quad + \omega_{0,T}^{(\kappa_\beta,\phi_{\beta 1}),(\kappa_\alpha,\phi_{\alpha 1}),(-(\kappa_\alpha+\kappa_\beta),h)} \mathbb{E}\left[G^{(2)}(V_T) \right], \quad \alpha \neq \beta, \qquad (C.8)
\end{aligned}$$

where

$$\phi_{\alpha 1}(s) = \rho_{\alpha s} \xi_{\alpha s} \upsilon_{\alpha 0,s}, \quad \phi_{\beta 1}(s) = \rho_{\beta s} \xi_{\beta s} \upsilon_{\beta 0,s}.$$

Proof. *For the equation (C.7), we have*

$$\begin{aligned}
\mathbb{E}\left[G(V_T) \int_0^T h(t) \upsilon_{\alpha 1,t} dt \right] &= \mathbb{E}\left[G(V_T) \int_0^T h(t) e^{-\kappa_\alpha t} \left[\int_0^t e^{\kappa_\alpha s} \xi_{\alpha s} \sqrt{\upsilon_{\alpha 0,s}} dB_s^\alpha \right] dt \right] \\
&= \mathbb{E}\left[G(V_T) \int_0^T e^{\kappa_\alpha s} \xi_{\alpha s} \sqrt{\upsilon_{\alpha 0,s}} \left[\int_s^T h(t) e^{-\kappa_\alpha t} dt \right] dB_s^\alpha \right] \\
&= \mathbb{E}\left[G(V_T) \int_0^T \omega_{s,T}^{(-\kappa_\alpha,h)} e^{\kappa_\alpha s} \xi_{\alpha s} \sqrt{\upsilon_{\alpha 0,s}} dB_s^\alpha \right] \\
&= \mathbb{E}\left[G^{(1)}(V_T) \int_0^T \omega_{t,T}^{(-\kappa_\alpha,h)} e^{\kappa_\alpha t} \rho_{\alpha t} \xi_{\alpha t} \upsilon_{\alpha 0,t} dt \right] \\
&= \mathbb{E}\left[G^{(1)}(V_T) \right] \omega_{0,T}^{(\kappa_\alpha,\phi_{\alpha 1}),(-\kappa_\alpha,h)},
\end{aligned}$$

where we applied the Fubini theorem on the second equality and Lemma 17 on the fourth equality.

For the second equation (C.8), let us denote $Y_t^i = e^{\kappa_i t}\upsilon_{i1,t}$. *Since it holds that due to* $d\langle Y^\alpha, Y^\beta\rangle = 0$ *when* $\alpha \neq \beta$

$$\upsilon_{\alpha 1,t}\upsilon_{\beta 1,t} = e^{-(\kappa_\alpha+\kappa_\beta)t}Y_t^\alpha Y_t^\beta = e^{-(\kappa_\alpha+\kappa_\beta)t}\left[\int_0^t Y_s^\alpha dY_s^\beta + \int_0^t Y_s^\beta dY_s^\alpha\right],$$

we observe

$$\mathbb{E}\left[G(V_T)\int_0^T h(t)\,\upsilon_{\alpha 1,t}\upsilon_{\beta 1,t}dt\right] = \mathbb{E}\left[G(V_T)\int_0^T h(t)\,e^{-(\kappa_\alpha+\kappa_\beta)t}\left(\int_0^t Y_s^\alpha dY_s^\beta + \int_0^t Y_s^\beta dY_s^\alpha\right)dt\right].$$

For the first term on the right-hand side

$$\mathcal{Y}_1 = \mathbb{E}\left[G(V_T)\int_0^T h(t)\,e^{-(\kappa_\alpha+\kappa_\beta)t}\left(\int_0^t Y_s^\alpha dY_s^\beta\right)dt\right],$$

in a similar way as the previous discussion we have

$$\begin{aligned}
\mathcal{Y}_1 &= \mathbb{E}\left[G(V_T)\int_0^T h(t)\,e^{-(\kappa_\alpha+\kappa_\beta)t}\left(\int_0^t Y_s^\alpha e^{\kappa_\beta s}\xi_{\beta s}\sqrt{\upsilon_{\beta 0,s}}dB_s^\beta\right)dt\right] \\
&= \mathbb{E}\left[G(V_T)\int_0^T \omega_{s,T}^{(-(\kappa_\alpha+\kappa_\beta),h)}Y_s^\alpha e^{\kappa_\beta s}\xi_{\beta t}\sqrt{\upsilon_{\beta 0,s}}dB_s^\beta\right] \\
&= \mathbb{E}\left[G^{(1)}(V_T)\int_0^T \omega_{t,T}^{(-(\kappa_\alpha+\kappa_\beta),h)}e^{\kappa_\beta t}\rho_{\beta t}\xi_{\beta t}\upsilon_{\beta 0,t}Y_t^\alpha dt\right] \\
&= \mathbb{E}\left[G^{(1)}(V_T)\int_0^T \omega_{t,T}^{(-(\kappa_\alpha+\kappa_\beta),h)}e^{\kappa_\beta t}\phi_{\beta 1}(t)Y_t^\alpha dt\right],
\end{aligned}$$

where we applied Lemma 17 on the third equality. To further simplify, we use Lemma 18 by taking $f(t) = \omega_{t,T}^{(-(\kappa_\alpha+\kappa_\beta),h)}e^{\kappa_\beta t}\phi_{\beta 1}(t)$, $Z(t) = Y_t^\alpha$ *i.e.,* $dZ(t) = e^{\kappa_\alpha t}\xi_{\alpha t}\sqrt{\upsilon_{\alpha 0,t}}dB_t^\alpha$. *Then by noting that*

$$\omega_{t,T}^{(0,f)} = \int_t^T \omega_{s,T}^{(-(\kappa_\alpha+\kappa_\beta),h)}e^{\kappa_\beta s}\phi_{\beta 1}(s)ds = \omega_{t,T}^{(\kappa_\beta,\phi_{\beta 1}),(-(\kappa_\alpha+\kappa_\beta),h)},$$

Lemma 18 and Lemma 17 yields

$$\begin{aligned}
\mathcal{Y}_1 &= \mathbb{E}\left[G^{(1)}(V_T)\int_0^T \omega_{t,T}^{(\kappa_\beta,\phi_{\beta 1}),(-(\kappa_\alpha+\kappa_\beta),h)}e^{\kappa_\alpha t}\xi_{\alpha t}\sqrt{\upsilon_{\alpha 0,t}}dB_t^\alpha\right] \\
&= \mathbb{E}\left[G^{(2)}(V_T)\int_0^T \omega_{t,T}^{(\kappa_\beta,\phi_{\beta 1}),(-(\kappa_\alpha+\kappa_\beta),h)}e^{\kappa_\alpha t}\rho_{\alpha t}\xi_{\alpha t}\upsilon_{\alpha 0,t}dt\right] \\
&= \omega_{t,T}^{(\kappa_\alpha,\phi_{\alpha 1}),(\kappa_\beta,\phi_{\beta 1}),(-(\kappa_\alpha+\kappa_\beta),h)}\mathbb{E}\left[G^{(2)}(V_T)\right].
\end{aligned}$$

By similar argument, the second term is obtained as

$$\begin{aligned}
\mathcal{Y}_2 &= \mathbb{E}\left[G(V_T)\int_0^T h(t)\,e^{-(\kappa_\alpha+\kappa_\beta)t}\left(\int_0^t Y_s^\beta dY_s^\alpha\right)dt\right] \\
&= \omega_{0,T}^{(k_\beta,\phi_{\beta 1}),(k_\alpha,\phi_{\alpha 1}),(-(\kappa_\alpha+\kappa_\beta),h)}\mathbb{E}\left[G^{(2)}(V_T)\right].
\end{aligned}$$

■

C.1 Proof of equation (22) in Proposition 1

From the expansion formula, it is easy to verify that when $\epsilon = 1_n$, take $i = \alpha$ and $j = \beta$ such that $\alpha \neq \beta$, we have

$$\Gamma_T^{\alpha,\beta} = \mathbb{E}\left[\frac{\partial^2 P}{\partial x^2}H_{\alpha T}H_{\beta T}\right] + \mathbb{E}\left[\frac{\partial^2 P}{\partial y^2}L_{\alpha T}L_{\beta T}\right] + \mathbb{E}\left[\frac{\partial^2 P}{\partial x \partial y}H_{\alpha T}L_{\beta T}\right] + \mathbb{E}\left[\frac{\partial^2 P}{\partial x \partial y}H_{\beta T}L_{\alpha T}\right],$$

where

$$\begin{aligned} H_{\alpha t} &= \int_0^t \rho_{\alpha s} \frac{\upsilon_{\alpha 1,s}}{2(\upsilon_{\alpha 0,s})^{1/2}} dB_s^\alpha - \frac{1}{2}\int_0^t \rho_{\alpha s}^2 \upsilon_{\alpha 1,s} ds, \\ L_{\alpha t} &= \int_0^T \left(1-\rho_{\alpha s}^2\right) \upsilon_{\alpha 1,s} ds. \end{aligned}$$

By the application of Ito's Lemma and the independence of $\left\{B_t^i : i = 1,2,...,n\right\}$, we can express

$$\begin{aligned} \Gamma_T^{\alpha,\beta} &= \mathbb{E}\left[\frac{\partial^2 P}{\partial x^2}\int_0^T H_{\alpha t} dH_{\beta t}\right] + \mathbb{E}\left[\frac{\partial^2 P}{\partial x^2}\int_0^T H_{\beta t} dH_{\alpha t}\right] + \mathbb{E}\left[\frac{\partial^2 P}{\partial y^2}\int_0^T L_{\alpha t} dL_{\beta t}\right] + \mathbb{E}\left[\frac{\partial^2 P}{\partial y^2}\int_0^T L_{\beta t} dL_{\alpha t}\right] \\ &+\mathbb{E}\left[\frac{\partial^2 P}{\partial x \partial y}\int_0^T H_{\alpha t} dL_{\beta t}\right] + \mathbb{E}\left[\frac{\partial^2 P}{\partial x \partial y}\int_0^T L_{\beta t} dH_{\alpha t}\right] + \mathbb{E}\left[\frac{\partial^2 P}{\partial x \partial y}\int_0^T H_{\beta t} dL_{\alpha t}\right] + \mathbb{E}\left[\frac{\partial^2 P}{\partial x \partial y}\int_0^T L_{\alpha t} dH_{\beta t}\right]. \end{aligned}$$

Let us denote the k-th term on the right-hand side by I_k. It is observed that the following pair of terms are symmetric in α and β : $I_1\&I_2$, $I_3\&I_4$, $I_5\&I_7$, and $I_6\&I_8$. We make use of Lemma 17 and Lemma 19 repeatedly in what follows in order to transform the terms of the partial derivatives with respect to x and y inside the expectations above to the partial derivatives with respect to y only.

i.) $I_1\&I_2$**:**

Noting that

$$dH_{\beta t} = \rho_{\beta t}\frac{\upsilon_{\beta 1,t}}{2(\upsilon_{\beta 0,t})^{1/2}} dB_t^\beta - \frac{1}{2}\rho_{\beta t}^2 \upsilon_{\beta 1,t} dt,$$

we have

$$I_1 \triangleq \mathbb{E}\left[\frac{\partial^2 P}{\partial x^2}\int_0^T H_{\alpha t} dH_{\beta t}\right] = \mathbb{E}\left[\frac{\partial^2 P}{\partial x^2}\int_0^T H_{\alpha t}\rho_{\beta t}\frac{\upsilon_{\beta 1,t}}{2(\upsilon_{\beta 0,t})^{1/2}} dB_t^\beta\right] - \mathbb{E}\left[\frac{\partial^2 P}{\partial x^2}\int_0^T H_{\alpha t}\rho_{\beta t}^2\frac{\upsilon_{\beta 1,t}}{2} dt,\right].$$

Since by Lemma 17 the first term is

$$\mathbb{E}\left[\frac{\partial^2 P}{\partial x^2}\int_0^T H_{\alpha t}\rho_{\beta t}\frac{\upsilon_{\beta 1,t}}{2(\upsilon_{\beta 0,t})^{1/2}} dB_t^\beta\right] = \mathbb{E}\left[\frac{\partial^3 P}{\partial x^3}\int_0^T H_{\alpha t}\rho_{\beta t}^2\frac{\upsilon_{\beta 1,t}}{2} dt\right],$$

we have

$$I_1 = \mathbb{E}\left[\left(\frac{\partial^3}{\partial x^3} - \frac{\partial^2}{\partial x^2}\right) P \int_0^T H_{\alpha t}\rho_{\beta t}^2\frac{\upsilon_{\beta 1,t}}{2} dt\right] = \mathbb{E}\left[\frac{\partial^2 P}{\partial x \partial y}\int_0^T H_{\alpha t}\rho_{\beta t}^2 \upsilon_{\beta 1,t} dt\right],$$

where Lemma 19 is applied on the second equality. To further simplify, we substitute the definition of $H_{\alpha t}$, such that

$$I_1 = \frac{1}{2}\mathbb{E}\left[\frac{\partial^2 P}{\partial x \partial y}\int_0^T \rho_{\beta t}^2 \upsilon_{\beta 1,t}\left(\int_0^t \rho_{\alpha s}\frac{\upsilon_{\alpha 1,s}}{(\upsilon_{\alpha 0,s})^{1/2}} dB_s^\alpha\right) dt\right] - \frac{1}{2}\mathbb{E}\left[\frac{\partial^2 P}{\partial x \partial y}\int_0^T \rho_{\beta t}^2 \upsilon_{\beta 1,t}\left(\int_0^t \rho_{\alpha s}^2 \upsilon_{\alpha 1,s} ds\right) dt\right], \quad \text{(C.9)}$$

and by applying Fubini Theorem and Lemma 17 on the first term, we have

$$\begin{aligned} \mathbb{E}\left[\frac{\partial^2 P}{\partial x \partial y}\int_0^T \rho_{\beta t}^2 \upsilon_{\beta 1,t}\left(\int_0^t \rho_{\alpha s}\frac{\upsilon_{\alpha 1,s}}{2(\upsilon_{\alpha 0,s})^{1/2}} dB_s^\alpha\right) dt\right] &= \frac{1}{2}\mathbb{E}\left[\frac{\partial^2 P}{\partial x \partial y}\int_0^T \rho_{\alpha s}\frac{\upsilon_{\alpha 1,s}}{(\upsilon_{\alpha 0,s})^{1/2}}\left(\int_s^T \rho_{\beta t}^2 \upsilon_{\beta 1,t} dt\right) dB_s^\alpha\right] \\ &= \frac{1}{2}\mathbb{E}\left[\frac{\partial^3 P}{\partial x^2 \partial y}\int_0^T \rho_{\alpha s}^2 \upsilon_{\alpha 1,s}\left(\int_s^T \rho_{\beta t}^2 \upsilon_{\beta 1,t} dt\right) ds\right] \\ &= \frac{1}{2}\mathbb{E}\left[\frac{\partial^3 P}{\partial x^2 \partial y}\int_0^T \rho_{\beta t}^2 \upsilon_{\beta 1,t}\left(\int_0^t \rho_{\alpha s}^2 \upsilon_{\alpha 1,s} ds\right) dt\right]. \end{aligned}$$

Finally, by Lemma 19 we have

$$I_1 = \mathbb{E}\left[\frac{\partial^2 P}{\partial y^2}\int_0^T \rho_{\beta t}^2 \upsilon_{\beta 1,t}\left(\int_0^t \rho_{\alpha s}^2 \upsilon_{\alpha 1,s} ds\right) dt\right]. \quad \text{(C.10)}$$

As term (2) is symmetric in (α,β) with term (1), by similar argument, we have

$$I_2=\mathbb{E}\left[\frac{\partial^2 P}{\partial x^2}\int_0^T H_{\beta t}dH_{\alpha t}\right]=\mathbb{E}\left[\frac{\partial^2 P}{\partial y^2}\int_0^T \rho_{\alpha t}^2\upsilon_{\alpha 1,t}\left(\int_0^t \rho_{\beta s}^2\upsilon_{\beta 1,s}ds\right)dt\right]. \tag{C.11}$$

ii.) I_3&I_4:
We express I_3&I_4 as

$$\begin{aligned} I_3 &= \mathbb{E}\left[\frac{\partial^2 P}{\partial y^2}\int_0^T L_{\alpha t}dL_{\beta t}\right]=\mathbb{E}\left[\frac{\partial^2 P}{\partial y^2}\int_0^T \left(1-\rho_{\beta t}^2\right)\upsilon_{\beta 1,t}\left(\int_0^t \left(1-\rho_{\alpha s}^2\right)\upsilon_{\alpha 1,s}ds\right)dt\right] && \text{(C.12)}\\ I_4 &= \mathbb{E}\left[\frac{\partial^2 P}{\partial y^2}\int_0^T L_{\beta t}dL_{\alpha t}\right]=\mathbb{E}\left[\frac{\partial^2 P}{\partial y^2}\int_0^T \left(1-\rho_{\alpha t}^2\right)\upsilon_{\alpha 1,t}\left(\int_0^t \left(1-\rho_{\beta s}^2\right)\upsilon_{\beta 1,s}ds\right)dt\right] && \text{(C.13)}\end{aligned}$$

for later use.

iii.) I_5, I_6, I_7 and I_8:
By the definition of $H_{\alpha t}$ and $L_{\beta t}$, we have

$$\begin{aligned} I_5 &= \mathbb{E}\left[\frac{\partial^2 P}{\partial x\partial y}\int_0^T H_{\alpha t}dL_{\beta t}\right]\\ &= \frac{1}{2}\mathbb{E}\left[\frac{\partial^2 P}{\partial x\partial y}\int_0^T \left(1-\rho_{\beta t}^2\right)\upsilon_{\beta 1,t}\left(\int_0^t \rho_{\alpha s}\frac{\upsilon_{\alpha 1,s}}{(\upsilon_{\alpha 0,s})^{1/2}}dB_s^\alpha\right)dt\right]-\frac{1}{2}\mathbb{E}\left[\frac{\partial^2 P}{\partial x\partial y}\int_0^T \left(1-\rho_{\beta t}^2\right)\upsilon_{\beta 1,t}\left(\int_0^t \rho_{\alpha s}^2\upsilon_{\alpha 1,s}ds\right)dt\right],\end{aligned}$$

which is similar to (C.9). Thus, in the same way as the derivation of (C.10), we are ready to obtain

$$I_5=\left[\frac{\partial^2 P}{\partial y^2}\int_0^T \left(1-\rho_{\beta t}^2\right)\upsilon_{\beta 1,t}\left(\int_0^t \rho_{\alpha s}^2\upsilon_{\alpha 1,s}ds\right)dt\right]. \tag{C.14}$$

As I_5 is symmetric in (α,β) with I_7, we have

$$I_7=\left[\frac{\partial^2 P}{\partial y^2}\int_0^T \left(1-\rho_{\alpha t}^2\right)\upsilon_{\alpha 1,t}\left(\int_0^t \rho_{\beta s}^2\upsilon_{\beta 1,s}ds\right)dt\right]. \tag{C.15}$$

Similarily, for I_6, we have

$$I_6 = \mathbb{E}\left[\frac{\partial^2 P}{\partial x\partial y}\int_0^T L_{\beta t}dH_{\alpha t}\right]=\frac{1}{2}\mathbb{E}\left[\frac{\partial^2 P}{\partial x\partial y}\int_0^T L_{\beta t}\rho_{\alpha t}\frac{\upsilon_{\alpha 1,t}}{(\upsilon_{\alpha 0,t})^{1/2}}dB_t^\alpha\right]-\frac{1}{2}\mathbb{E}\left[\frac{\partial^2 P}{\partial x\partial y}\int_0^T L_{\beta t}\rho_{\alpha t}^2\upsilon_{\alpha 1,t}dt\right]$$

Apply Lemma 17 on the first term, and then use Lemma 19, we obtain

$$I_6=\mathbb{E}\left[\frac{\partial^2 P}{\partial y^2}\int_0^T \rho_{\alpha t}^2\upsilon_{\alpha 1,t}\left(\int_0^t \left(1-\rho_{\beta s}^2\right)\upsilon_{\beta 1,s}ds\right)dt\right], \tag{C.16}$$

and by symmetry we readily have

$$I_8=\mathbb{E}\left[\frac{\partial^2 P}{\partial y^2}\int_0^T \rho_{\beta t}^2\upsilon_{\beta 1,t}\left(\int_0^t \left(1-\rho_{\alpha s}^2\right)\upsilon_{\alpha 1,s}ds\right)dt\right]. \tag{C.17}$$

Finally, by summing up all the eight terms in (C.10)-(C.17), we have

$$\Gamma_T^{\alpha,\beta}=\mathbb{E}\left[\frac{\partial^2 P}{\partial y^2}\int_0^T \left[\int_0^t \upsilon_{\alpha 1,s}ds\right]\upsilon_{\beta 1,t}dt\right]+\mathbb{E}\left[\frac{\partial^2 P}{\partial y^2}\int_0^T \left[\int_0^t \upsilon_{\beta 1,s}ds\right]\upsilon_{\alpha 1,t}dt\right]. \tag{C.18}$$

C.2 Proof of equation (27) in Theorem 3

We observe that the two terms in (C.18) are symmetric in (α,β). Hence, (C.18) is equivalent to

$$\Gamma_T^{\alpha,\beta} = \gamma(\alpha,\beta) + \gamma(\beta,\alpha), \tag{C.19}$$

where

$$\gamma(\alpha,\beta) = \mathbb{E}\left[\frac{\partial^2 P}{\partial y^2}\int_0^T \left[\int_0^t \upsilon_{\alpha 1,s}ds\right]\upsilon_{\beta 1,t}dt\right] = \mathbb{E}\left[\frac{\partial^2 P}{\partial y^2}\int_0^T e^{-\kappa_\beta t}\left[\int_0^t \upsilon_{\alpha 1,s}ds\right]e^{\kappa_\beta t}\upsilon_{\beta 1,t}dt\right].$$

By applying Lemma 18 with $f(t) = e^{-\kappa_\beta t}$ and $Z(t) = \left(\int_0^t \upsilon_{\alpha 1,s}ds\right)e^{\kappa_\beta t}\upsilon_{\beta 1,t}$ which satisfies

$$dZ(t) = e^{\kappa_\beta t}\upsilon_{\alpha 1,t}\upsilon_{\beta 1,t}dt + \left(\int_0^t \upsilon_{\alpha 1,s}ds\right)e^{\kappa_\beta t}\xi_{\beta t}\sqrt{\upsilon_{\beta 0,t}}dB_t^\beta,$$

we have

$$\gamma(\alpha,\beta) \quad = \quad \mathbb{E}\left[\frac{\partial^2 P}{\partial y^2}\int_0^T \left(\int_t^T e^{-\kappa_\beta s}ds\right)e^{\kappa_\beta t}\upsilon_{\alpha 1,t}\upsilon_{\beta 1,t}dt\right] + \mathbb{E}\left[\frac{\partial^2 P}{\partial y^2}\int_0^T \left(\int_t^T e^{-\kappa_\beta s}ds\right)\left(\int_0^t \upsilon_{\alpha 1,u}du\right)e^{\kappa_\beta t}\xi_{\beta t}\sqrt{\upsilon_{\beta 0,t}}dB_t^\beta\right]. \tag{C.20}$$

Consequently, with Lemma 20 we are ready to prove Theorem 3. Denote the first term in (C.20) to be

$$\mathcal{I}_1 = \mathbb{E}\left[\frac{\partial^2 P}{\partial y^2}\int_0^T \left(\int_t^T e^{-\kappa_\beta s}ds\right)e^{\kappa_\beta t}\upsilon_{\alpha 1,t}\upsilon_{\beta 1,t}dt\right],$$

we can directly apply the second equality in Lemma 20 by taking $h(t) = \left(\int_t^T e^{-\kappa_\beta s}ds\right)e^{\kappa_\beta t} = e^{\kappa_\beta t}\omega_{t,T}^{(-\kappa_\beta,1)}$, and readily obtain

$$\mathcal{I}_1 = \left(\omega_{0,T}^{(\kappa_\alpha,\phi_{\alpha 1}),(\kappa_\beta,\phi_{\beta 1}),(-\kappa_\alpha,1),(-\kappa_\beta,1)} + \omega_{0,T}^{(\kappa_\beta,\phi_{\beta 1}),(\kappa_\alpha,\phi_{\alpha 1}),(-\kappa_\alpha,1),(-\kappa_\beta,1)}\right)\mathbb{E}\left[\frac{\partial^4 P}{\partial x^2\partial y^2}\right]$$

because

$$\omega_{t,T}^{(-(\kappa_\alpha+\kappa_\beta),h)} = \int_t^T e^{-(\kappa_\alpha+\kappa_\beta)u}\left(\int_u^T e^{-\kappa_\beta s}ds\right)e^{\kappa_\beta u}du = \omega_{t,T}^{(-\kappa_\alpha,1),(-\kappa_\beta,1)}.$$

For the second term,

$$\mathcal{I}_2 = \mathbb{E}\left[\frac{\partial^2 P}{\partial y^2}\int_0^T \omega_{t,T}^{(-\kappa_\beta,1)}\left(\int_0^t \upsilon_{\alpha 1,u}du\right)e^{\kappa_\beta t}\xi_{\beta t}\sqrt{\upsilon_{\beta 0,t}}dB_t^\beta\right],$$

we apply Lemma 17 along with the Fubini Theorem, and then by Lemma 18, we have

$$\begin{aligned}
\mathcal{I}_2 &= \mathbb{E}\left[\frac{\partial^3 P}{\partial x\partial y^2}\int_0^T \omega_{t,T}^{(-\kappa_\beta,1)}e^{\kappa_\beta t}\rho_{\beta t}\xi_{\beta t}\upsilon_{\beta 0,t}\left(\int_0^t \upsilon_{\alpha 1,u}du\right)dt\right]\\
&= \mathbb{E}\left[\frac{\partial^3 P}{\partial x\partial y^2}\int_0^T \left(\int_0^t e^{\kappa_\beta t}\phi_{\beta 1}(t)\omega_{t,T}^{(-\kappa_\beta,1)}dt\right)\upsilon_{\alpha 1,u}du\right]\\
&= \mathbb{E}\left[\frac{\partial^3 P}{\partial x\partial y^2}\int_0^T \omega_{t,T}^{(\kappa_\beta,\phi_{\beta 1}),(-\kappa_\beta,1)}\upsilon_{\alpha 1,t}dt\right].
\end{aligned}$$

Then, we make use of the first equality in Lemma 20 by taking $h(t) = \omega_{t,T}^{(\kappa_\beta,\phi_{\beta 1}),(-\kappa_\beta,1)}$. Since it holds that by definition

$$\omega_{t,T}^{(-\kappa_\alpha,h)} = \int_t^T e^{-\kappa_\alpha u}\omega_{u,T}^{(\kappa_\beta,\phi_{\beta 1}),(-\kappa_\beta,1)}du = \omega_{t,T}^{(-\kappa_\alpha,1),(\kappa_\beta,\phi_{\beta 1}),(-\kappa_\beta,1)},$$

we see

$$\mathcal{I}_2 = \omega_{0,T}^{(\kappa_\alpha,\phi_{\alpha 1}),(-\kappa_\alpha,1),(\kappa_\beta,\phi_{\beta 1}),(-\kappa_\beta,1)} \mathbb{E}\left[\frac{\partial^4 P}{\partial x^2 \partial y^2}\right]. \tag{C.21}$$

As a result, we obtain

$$\gamma(\alpha,\beta) = C(\alpha,\beta)\,\mathbb{E}\left[\frac{\partial^4 P}{\partial x^4 \partial y^2}\right], \tag{C.22}$$

where

$$C(\alpha,\beta) = \omega_{0,T}^{(\kappa_\alpha,\phi_{\alpha 1}),(\kappa_\beta,\phi_{\beta 1}),(-\kappa_\alpha,1),(-\kappa_\beta,1)} + \omega_{0,T}^{(\kappa_\beta,\phi_{\beta 1}),(\kappa_\alpha,\phi_{\alpha 1}),(-\kappa_\alpha,1),(-\kappa_\beta,1)} + \omega_{0,T}^{(\kappa_\alpha,\phi_{\alpha 1}),(-\kappa_\alpha,1),(\kappa_\beta,\phi_{\beta 1}),(-\kappa_\beta,1)}. \tag{C.23}$$

Combining the results, we are able to arrive the expression

$$c_T^{\alpha,\beta} = C(\alpha,\beta) + C(\beta,\alpha), \tag{C.24}$$

which gives the result (27) in Theorem 3.

D Estimation of the Error Term

Our objective is to evaluate of the error term $\tilde{\varepsilon}_n$ in Theorem 3. To this end, we consider Black-Scholes formula with the underlying prices parametrized by λ as

$$\bar{P}(\lambda,\epsilon) = P\left(\overline{x}(\lambda,\epsilon), \overline{y}(\lambda,\epsilon)\right)$$

where

$$\begin{aligned}
\overline{x}(\lambda,\epsilon) &= x_0 + \sum_{i=1}^{n} \int_0^T [\rho_{it}(1-\lambda)\sigma_{i0,t} + \lambda\sigma_{it}^{\epsilon_i}]\, dB_t^i - \sum_{i=1}^{n} \int_0^T \frac{\rho_{it}^2}{2}\left[(1-\lambda)\upsilon_{i0,t} + \lambda\upsilon_{i,t}^{\epsilon_i}\right] dt \\
&= x' + \lambda\Delta x(\epsilon), \\
\overline{y}(\lambda,\epsilon) &= \sum_{i=1}^{n} \int_0^T (1-\rho_{it}^2)\left[(1-\lambda)\upsilon_{i0,t} + \lambda\upsilon_{it}^{\epsilon_i}\right] dt \\
&= y' + \lambda\Delta y(\epsilon).
\end{aligned}$$

Then $\bar{P}(1,\epsilon) = P(x' + \Delta x(\epsilon), y' + \Delta y(\epsilon))$ and the objective $g(\epsilon)$ is exactly expanded with respect to a new parameter λ, instead of ϵ, as

$$g(\epsilon) = \mathbb{E}[\bar{P}(1,\epsilon)] = \mathbb{E}\left[\bar{P}(0,\epsilon) + \partial_\lambda \bar{P}(0,\epsilon) + \frac{1}{2}\partial_\lambda^2 \bar{P}(0,\epsilon) + \int_0^1 d\lambda \frac{(1-\lambda)^2}{2} \partial_\lambda^3 \bar{P}(\lambda,\epsilon)\right], \tag{D.1}$$

where

$$\begin{aligned}
\partial_\lambda \bar{P}(0,\epsilon) &= \frac{\partial P(x',y')}{\partial x}\left(\sum_{i=1}^n \Gamma_{iT}^{\epsilon_i}\right) + \frac{\partial P(x',y')}{\partial y}\left(\sum_{i=1}^n \Xi_{iT}^{\epsilon_i}\right), \\
\partial_\lambda^2 \bar{P}(0,\epsilon) &= \frac{\partial^2 P(x',y')}{\partial x^2}\left(\sum_{i=1}^n \Gamma_{iT}^{\epsilon_i}\right)^2 + \frac{\partial^2 P(x',y')}{\partial y^2}\left(\sum_{i=1}^n \Xi_{iT}^{\epsilon_i}\right)^2 + 2\frac{\partial^2 P(x',y')}{\partial x \partial y}\left(\sum_{i=1}^n \Gamma_{iT}^{\epsilon_i}\right)\left(\sum_{i=1}^n \Xi_{iT}^{\epsilon_i}\right), \\
\partial_\lambda^3 \bar{P}(\lambda,\epsilon) &= \sum_{l=0}^{3} \binom{3}{l} \frac{\partial^3 P(\overline{x},\overline{y})}{\partial x^l \partial y^{3-l}} \left(\sum_{i=1}^n \Gamma_{iT}^{\epsilon_i}\right)^l \left(\sum_{i=1}^n \Xi_{iT}^{\epsilon_i}\right)^{3-l}.
\end{aligned}$$

It is important to note that the expression in (D.1) is exact. Given that definition, it is straight-forward to verify that $g(\epsilon) = \mathbb{E}[\bar{P}(1,\epsilon)]$ the expansion in previous section can be obtained by keeping λ fixed at 1 with truncation to the second-order. The advantage of considering this expansion with respect to λ is that we can express the error for the expansion formula (B.3) as

$$
\begin{aligned}
\tilde{\varepsilon}_n &= \mathbb{E}[\bar{P}(1,\epsilon)] \\
&\quad - \Bigg\{ \mathbb{E}\left[P(x',y')\right] + \mathbb{E}\left[\frac{\partial P(x',y')}{\partial x} \sum_{i=1}^{n} \left(\epsilon_i \Gamma_{i1,T} + \frac{\epsilon_i^2}{2} \Gamma_{i2,T} \right)\right] \\
&\quad + \mathbb{E}\left[\frac{\partial P(x',y')}{\partial y} \left(\epsilon_i \Xi_{i1,T} + \frac{\epsilon_i^2}{2} \Xi_{i2,T} \right)\right] + \frac{1}{2}\mathbb{E}\left[\frac{\partial^2 P(x',y')}{\partial x^2} \left(\sum_{i=1}^{n} \epsilon_i \Gamma_{i1,T} \right)^2 \right] + \frac{1}{2}\mathbb{E}\left[\frac{\partial^2 P(x',y')}{\partial y^2} \left(\sum_{i=1}^{n} \epsilon_i \Xi_{i1,T} \right)^2 \right] \\
&\quad + \mathbb{E}\left[\frac{\partial^2 P(x',y')}{\partial x \partial y} \left(\sum_{i=1}^{n} \epsilon_i \Gamma_{i1,T} \right) \left(\sum_{i=1}^{n} \epsilon_i \Xi_{i1,T} \right)\right] \Bigg\},
\end{aligned}
$$

which can be computed by substituting $\mathbb{E}[\bar{P}(1,\epsilon)]$ with (D.1) and noting $\bar{P}(0,\epsilon) = P(x',y')$ as

$$
\begin{aligned}
\tilde{\varepsilon}_n &= \sum_{i=1}^{n} \mathbb{E}\left[\frac{\partial P(x',y')}{\partial x} R_{2,T}^{\Gamma_{iT}^{\epsilon_i}} + \frac{\partial P(x',y')}{\partial y} R_{2,T}^{\Xi_{iT}^{\epsilon_i}}\right] \\
&\quad + \frac{1}{2}\mathbb{E}\left[\frac{\partial^2 P(x',y')}{\partial x^2} \left\{ \left(\sum_{i=1}^{n} \Gamma_{iT}^{\epsilon_i} \right)^2 - \left(\sum_{i=1}^{n} \epsilon_i \Gamma_{i1,T} \right)^2 \right\}\right] \\
&\quad + \frac{1}{2}\mathbb{E}\left[\frac{\partial^2 P(x',y')}{\partial y^2} \left\{ \left(\sum_{i=1}^{n} \Xi_{iT}^{\epsilon_i} \right)^2 - \left(\sum_{i=1}^{n} \epsilon_i \Xi_{i1,T} \right)^2 \right\}\right] \\
&\quad + \mathbb{E}\left[\frac{\partial^2 P(x',y')}{\partial x \partial y} \left\{ \left(\sum_{i=1}^{n} \Gamma_{iT}^{\epsilon_i} \right) \left(\sum_{i=1}^{n} \Xi_{iT}^{\epsilon_i} \right) - \left(\sum_{i=1}^{n} \epsilon_i \Gamma_{i1,T} \right) \left(\sum_{i=1}^{n} \epsilon_i \Xi_{i1,T} \right) \right\}\right] \\
&\quad + \mathbb{E}\left[\int_0^1 d\lambda \frac{(1-\lambda)^2}{2} \partial_\lambda^3 \bar{P}(\lambda,\epsilon)\right].
\end{aligned}
$$

To simplify the expression, we consider $\overline{\Gamma}^2(\epsilon) \triangleq \left(\sum_{i=1}^n \Gamma_{iT}^{\epsilon_i}\right)^2$ such that

$$
\begin{aligned}
\frac{\partial \overline{\Gamma}^2(\epsilon)}{\partial \epsilon_i} &= 2\left(\sum_{i=1}^{n} \Gamma_{iT}^{\epsilon_i} \right) \frac{\partial \Gamma_{iT}^{\epsilon_i}}{\partial \epsilon_i}, \\
\frac{\partial^2 \overline{\Gamma}^2(\epsilon)}{\partial \epsilon_i^2} &= 2\left(\frac{\partial \Gamma_{iT}^{\epsilon_i}}{\partial \epsilon_i} \right)^2 + 2\left(\sum_{i=1}^{n} \Gamma_{iT}^{\epsilon_i} \right) \frac{\partial \Gamma_{iT}^{\epsilon_i}}{\partial \epsilon_i}, \\
\frac{\partial^2 \overline{\Gamma}^2(\epsilon)}{\partial \epsilon_i \partial \epsilon_j} &= 2\left(\frac{\partial \Gamma_{iT}^{\epsilon_i}}{\partial \epsilon_i} \right)\left(\frac{\partial \Gamma_{iT}^{\epsilon_j}}{\partial \epsilon_i} \right) + 2\left(\sum_{i=1}^{n} \Gamma_{iT}^{\epsilon_i} \right) \frac{\partial^2 \Gamma_{iT}^{\epsilon_i}}{\partial \epsilon_i \partial \epsilon_j},
\end{aligned}
$$

and

$$
\begin{aligned}
\overline{\Gamma}^2(\epsilon) &= \overline{\Gamma}^2(0) + \sum_i \frac{\partial \overline{\Gamma}^2(0)}{\partial \epsilon_i} \epsilon_i + \frac{1}{2} \sum_{i,j} \frac{\partial^2 \overline{\Gamma}^2(\epsilon)}{\partial \epsilon_i \partial \epsilon_j} \epsilon_i \epsilon_j + R_{2,T}^{\overline{\Gamma}^2(\epsilon)} \\
&= \sum_{i,j} \Gamma_{i1,T} \Gamma_{j1,T} \epsilon_i \epsilon_j + R_{2,T}^{\overline{\Gamma}^2(\epsilon)} = \left(\sum_{i=1}^{n} \epsilon_i \Gamma_{i1,T} \right)^2 + R_{2,T}^{\overline{\Gamma}^2(\epsilon)},
\end{aligned}
$$

since $\Gamma_{iT}^0 = 0$. Similarly, we have

$$
\begin{aligned}
\overline{\Xi}^2(\epsilon) &\triangleq \left(\sum_{i=1}^{n} \Xi_{iT}^{\epsilon_i} \right)^2 = \left(\sum_{i=1}^{n} \epsilon_i \Xi_{i1,T} \right)^2 + R_{2,T}^{\overline{\Xi}^2(\epsilon)}, \\
\overline{\Gamma\Xi}(\epsilon) &\triangleq \left(\sum_{i=1}^{n} \Gamma_{iT}^{\epsilon_i} \right)\left(\sum_{i=1}^{n} \Xi_{iT}^{\epsilon_i} \right) = \left(\sum_{i=1}^{n} \epsilon_i \Gamma_{i1,T} \right)\left(\sum_{i=1}^{n} \epsilon_i \Xi_{i1,T} \right) + R_{2,T}^{\overline{\Gamma\Xi}(\epsilon)}.
\end{aligned}
$$

Hence, by the linearity $R_{2,T}^{\bar{\Gamma}(\epsilon)} = \sum_{i=1}^{n} R_{2,T}^{\Gamma_{iT}^{\epsilon_i}}$, we can express the error term as

$$\tilde{\varepsilon}_n = E_1 + E_2 + E_3,$$

where

$$\begin{aligned}
E_1 &= \mathbb{E}\left[\frac{\partial P(x',y')}{\partial x} R_{2,T}^{\bar{\Gamma}(\epsilon)} + \frac{\partial P(x',y')}{\partial y} R_{2,T}^{\bar{\Xi}(\epsilon)}\right], \\
E_2 &= \frac{1}{2}\mathbb{E}\left[\frac{\partial^2 P(x',y')}{\partial x^2} R_{2,T}^{\bar{\Gamma}^2(\epsilon)}\right] + \frac{1}{2}\mathbb{E}\left[\frac{\partial^2 P(x',y')}{\partial y^2} R_{2,T}^{\bar{\Xi}^2(\epsilon)}\right] + \mathbb{E}\left[\frac{\partial^2 P(x',y')}{\partial x \partial y} R_{2,T}^{\bar{\Gamma}\bar{\Xi}(\epsilon)}\right], \\
E_3 &= \mathbb{E}\left[\int_0^1 d\lambda \frac{(1-\lambda)^2}{2} \partial_\lambda^3 \bar{P}(\lambda,\epsilon)\right].
\end{aligned}$$

Therefore, the evaluation of the error term can be obtained by considering the expectations E_1, E_2 and E_3. This will be calculated explicitly in the next section with the help of some Lemmas and Propositions.

D.1 Evaluation of the Error Term

To estimate the bounds of the error term $\tilde{\varepsilon}$, we need the following Lemmas and Propositions. In what follows, a positive constant C is understood to be the maximum of finitely many positive constants satisfying a condition.

Lemma 21 *For all $(l,m) \in \mathbb{N}^2$, there exists a polynomial $\widetilde{P}$ with positive coefficients such that*

$$\sup_{x\in\mathbb{R}}\left[\frac{\partial^{\ell+m}}{\partial x^\ell \partial y^m} P(x,y)\right] \le \frac{\widetilde{P}(\sqrt{y})}{y^{\frac{(2m+\ell-1)_+}{2}}}.$$

where $P(x,y)$ is the Black-Scholes formula.

Lemma 22 *For $i = 1,2,...,n$, we have for every $p > 0$,*

$$\sup_{0\le\epsilon_i\le 1} \mathbb{E}\left[\left(\int_0^T \upsilon_{it}^{\epsilon_i} dt\right)^{-p}\right] \le \frac{C}{T^p}.$$

For a process $Y = \{Y_t\}$, we denote $Y_t^* = \sup_{0\le s\le t} Y_s$.

Lemma 23 *The residuals for the squared volatility satisfy the following bounds*

$$\begin{aligned}
\|(R_{0,\cdot}[\sigma^{\epsilon_i}])_t^*\|_p &\le C\epsilon_i \xi_{iSup}\sqrt{t}, \\
\|(R_{1,\cdot}[\sigma^{\epsilon_i}])_t^*\|_p &\le C(\epsilon_i \xi_{iSup}\sqrt{t})^2, \\
\|(R_{2,\cdot}[\sigma^{\epsilon_i}])_t^*\|_p &\le C(\epsilon_i \xi_{iSup}\sqrt{t})^3,
\end{aligned}$$

and the lower and upper bounds of the volatility process

$$\begin{aligned}
0 < \min(\sigma_{i0}, \sqrt{\theta_{iInf}}) \le \sigma_{i0,t} &\le \max(\sigma_{i0}, \sqrt{\theta_{iSup}}), \\
\|(\sigma_{i1,\cdot})_t^*\|_p &\le C\xi_{iSup}\sqrt{t}, \\
\|(\sigma_{i2,\cdot})_t^*\|_p &\le C(\xi_{iSup}\sqrt{t})^2,
\end{aligned}$$

in which $\|Z\|_p = \mathbb{E}\left[|Z|^p\right]^{1/p}$ denotes the L_p-norm of a random variable Z.

Proposition 24 *For $i = 1,2,...,n$, we have the following bounds*

$$\begin{aligned}
&\|\Gamma_{iT}^1\|_p \le C(\xi_{iSup}\sqrt{T})\sqrt{T}, && \|R_{2,T}^{(\Gamma_i^1)^2}\|_p \le C(\xi_{iSup}\sqrt{T})^3 T, \\
&\|\Xi_{iT}^1\|_p \le C(\xi_{iSup}\sqrt{T})T, && \|R_{2,T}^{(\Xi_i^1)^2}\|_p \le C(\xi_{iSup}\sqrt{T})^3 T^2, \\
&\|R_{2,T}^{\Gamma_i^1}\|_p \le C(\xi_{iSup}\sqrt{T})^3\sqrt{T}, && \|R_{2,T}^{\Gamma_i^1\Xi_i^1}\|_p \le C(\xi_{iSup}\sqrt{T})^3 T^{\frac{3}{2}}. \\
&\|R_{2,T}^{\Xi_i^1}\|_p \le C(\xi_{iSup}\sqrt{T})^3 T,
\end{aligned}$$

Proof. *The proof for the Lemma (21), (22), (23) and Proposition (24) can be found in Benhamou et al. (2010).* ■

Proposition 25 *For $i, j = 1, 2, ..., n$, $i \neq j$, we have the bounds for the cross terms*

$$\|R_{2,T}^{\Gamma_i^1\Gamma_j^1}\|_p \leq C[(\xi_{jSup}\sqrt{T})^3 + (\xi_{iSup}\sqrt{T})^3]T, \tag{D.2}$$

$$\|R_{2,T}^{\Xi_i^1\Xi_j^1}\|_p \leq C[(\xi_{jSup}\sqrt{T})^3 + (\xi_{iSup}\sqrt{T})^3]T^2, \tag{D.3}$$

$$\|R_{2,T}^{\Gamma_i^1\Xi_j^1}\|_p \leq C[(\xi_{jSup}\sqrt{T})^3 + (\xi_{iSup}\sqrt{T})^3]T^{\frac{3}{2}}. \tag{D.4}$$

Proof. *From Proposition (24), we have the following expansion up to second order as*

$$\Gamma_{iT}^{\epsilon_i}\Gamma_{jT}^{\epsilon_j} = \left(\Gamma_{i0,T} + \epsilon_i\Gamma_{i1,T} + \frac{\epsilon_i^2}{2}\Gamma_{i2,T} + R_{2,T}^{\Gamma_i^{\epsilon_i}}\right)\left(\Gamma_{j0,T} + \epsilon_j\Gamma_{j1,T} + \frac{\epsilon_j^2}{2}\Gamma_{j2,T} + R_{2,T}^{\Gamma_j^{\epsilon_j}}\right),$$

$$\Xi_{iT}^{\epsilon_i}\Xi_{jT}^{\epsilon_j} = \left(\Xi_{i0,T} + \epsilon_i\Xi_{i1,T} + \frac{\epsilon_i^2}{2}\Xi_{i2,T} + R_{2,T}^{\Xi_i^{\epsilon_i}}\right)\left(\Xi_{j0,T} + \epsilon_j\Xi_{j1,T} + \frac{\epsilon_j^2}{2}\Xi_{j2,T} + R_{2,T}^{\Xi_j^{\epsilon_j}}\right),$$

$$\Gamma_{iT}^{\epsilon_i}\Xi_{jT}^{\epsilon_j} = \left(\Gamma_{i0,T} + \epsilon_i\Gamma_{i1,T} + \frac{\epsilon_i^2}{2}\Gamma_{i2,T} + R_{2,T}^{\Gamma_i^{\epsilon_i}}\right)\left(\Xi_{j0,T} + \epsilon_j\Xi_{j1,T} + \frac{\epsilon_j^2}{2}\Xi_{j2,T} + R_{2,T}^{\Xi_j^{\epsilon_j}}\right).$$

Hence, the error can be estimated as

$$R_{2,T}^{\Gamma_i^{\epsilon_i}\Gamma_j^{\epsilon_j}} = \Gamma_{i0,T}R_{2,T}^{\Gamma_j^{\epsilon_j}} + \epsilon_i\Gamma_{i1,T}R_{2,T}^{\Gamma_j^{\epsilon_j}} + \frac{\epsilon_i^2}{2}\Gamma_{i2,T}R_{2,T}^{\Gamma_j^{\epsilon_j}} + R_{2,T}^{\Gamma_i^{\epsilon_i}}\Gamma_{j0,T} + \epsilon_j R_{2,T}^{\Gamma_i^{\epsilon_i}}\Gamma_{j1,T} + \frac{\epsilon_j^2}{2}R_{2,T}^{\Gamma_i^{\epsilon_i}}\Gamma_{j2,T} + R_{2,T}^{\Gamma_i^{\epsilon_i}}R_{2,T}^{\Gamma_j^{\epsilon_j}},$$

$$R_{2,T}^{\Xi_i^{\epsilon_i}\Xi_j^{\epsilon_j}} = \Xi_{i0,T}R_{2,T}^{\Xi_j^{\epsilon_j}} + \epsilon_i\Xi_{i1,T}R_{2,T}^{\Xi_j^{\epsilon_j}} + \frac{\epsilon_i^2}{2}\Xi_{i2,T}R_{2,T}^{\Xi_j^{\epsilon_j}} + R_{2,T}^{\Xi_i^{\epsilon_i}}\Xi_{j0,T} + \epsilon_j R_{2,T}^{\Xi_i^{\epsilon_i}}\Xi_{j1,T} + \frac{\epsilon_j^2}{2}R_{2,T}^{\Xi_i^{\epsilon_i}}\Xi_{j2,T} + R_{2,T}^{\Xi_i^{\epsilon_i}}R_{2,T}^{\Xi_j^{\epsilon_j}},$$

$$R_{2,T}^{\Gamma_i^{\epsilon_i}\Xi_j^{\epsilon_j}} = \Gamma_{i0,T}R_{2,T}^{\Xi_j^{\epsilon_j}} + \epsilon_i\Gamma_{i1,T}R_{2,T}^{\Xi_j^{\epsilon_j}} + \frac{\epsilon_i^2}{2}\Gamma_{i2,T}R_{2,T}^{\Xi_j^{\epsilon_j}} + R_{2,T}^{\Gamma_i^{\epsilon_i}}\Xi_{j0,T} + \epsilon_j R_{2,T}^{\Gamma_i^{\epsilon_i}}\Xi_{j1,T} + \frac{\epsilon_j^2}{2}R_{2,T}^{\Gamma_i^{\epsilon_j}}\Xi_{j2,T} + R_{2,T}^{\Gamma_i^{\epsilon_i}}R_{2,T}^{\Xi_j^{\epsilon_j}}.$$

Applying the bounds based on Proposition (24) gives the result. ∎

Consequently, we are ready to impose the bounds on the error terms E_1, E_2 and E_3 when $\epsilon = 1_n$.

1. The error term E_1 : Noting that

$$\|R_{2,T}^{\Gamma_i^1}\|_2 \leq C(\xi_{iSup}\sqrt{T})^3\sqrt{T},$$

$$\|R_{2,T}^{\Xi_i^1}\|_2 \leq C(\xi_{iSup}\sqrt{T})^3 T,$$

we have

$$\begin{aligned} |E_1| &= \left|\mathbb{E}\left[\frac{\partial P(x', y')}{\partial x}R_{2,T}^{\bar{\Gamma}(\mathbf{1}_n)} + \frac{\partial P(x', y')}{\partial y}R_{2,T}^{\bar{\Xi}(\mathbf{1}_n)}\right]\right| \\ &\leq \sum_{i=1}^{n}\left\{\left\|\frac{\partial \bar{P}}{\partial x}\right\|_2\left\|R_{2,T}^{\Gamma_i^1}\right\|_2 + \left\|\frac{\partial \bar{P}}{\partial y}\right\|_2\left\|R_{2,T}^{\Xi_i^1}\right\|_2\right\} \\ &= 2C\sum_{i=1}^{n}(\xi_{iSup})^3 T^2, \end{aligned} \tag{D.5}$$

where we make use of the inequalities $\|\sum_{i=1}^n X_i\|_2 \leq \sum_{i=1}^n \|X_i\|_2$ and $|\mathbb{E}[XY]| \leq \|X\|_2\|Y\|_2$.

2. The error term E_2 : Noting that

$$\|R_{2,T}^{\Gamma_i^1\Gamma_j^1}\|_2 \leq C[(\xi_{iSup}\sqrt{T})^3 + (\xi_{jSup}\sqrt{T})^3]T,$$

$$\|R_{2,T}^{\Xi_i^1\Xi_j^1}\|_2 \leq C[(\xi_{iSup}\sqrt{T})^3 + (\xi_{jSup}\sqrt{T})^3]T^2,$$

$$\|R_{2,T}^{\Gamma_i^1\Xi_j^1}\|_2 \leq C[(\xi_{iSup}\sqrt{T})^3 + (\xi_{jSup}\sqrt{T})^3]T^{\frac{3}{2}},$$

we have

$$\begin{aligned} |E_2| &= \frac{1}{2}\mathbb{E}\left[\frac{\partial^2 P(x', y')}{\partial x^2}(x(0), y(0))R_{2,T}^{\bar{\Gamma}^2(\mathbf{1}_n)}\right] + \frac{1}{2}\mathbb{E}\left[\frac{\partial^2 P_{BS}}{\partial y^2}(x(0), y(0))R_{2,T}^{\bar{\Xi}^2(\mathbf{1}_n)}\right] + \mathbb{E}\left[\frac{\partial^2 P_{BS}}{\partial x\partial y}(x(0), y(0)R_{2,T}^{\overline{\Gamma\Xi}(\mathbf{1}_n)}\right] \\ &\leq 10C\sum_{i=1}^{n}(\xi_{iSup})^3 T^2. \end{aligned} \tag{D.6}$$

3. The error term E_3 :
Firstly, by Lemma 1 and Lemma 2, we see that for any λ,

$$\begin{aligned}
\left\|\frac{\partial^3 P_{BS}}{\partial x^l \partial y^{3-l}}\left(\overline{x}\left(\lambda,\mathbf{1}_n\right),\overline{y}\left(\lambda,\mathbf{1}_n\right)\right)\right\|_2 &\leq C'\left\|\overline{y}\left(\lambda,\mathbf{1}_n\right)^{-\frac{5-l}{2}}\right\|_4 \\
&\leq C''\left\|\left(\sum_{i=1}^n\int_0^T\left[(1-\lambda)\upsilon_{i0,t}+\lambda\upsilon_{it}^1\right]dt\right)^{-\frac{5-l}{2}}\right\|_4 \\
&\leq C''\sum_{i=1}^n\left[(1-\lambda)\left\|\left(\int_0^T\upsilon_{i0,t}dt\right)^{-\frac{5-2l}{2}}\right\|_4+\lambda\left\|\left(\int_0^T\upsilon_{it}^1dt\right)^{-\frac{5-l}{2}}\right\|_4\right] \\
&= \frac{C''}{\left(\sqrt{T}\right)^{5-l}}. \qquad \text{(D.7)}
\end{aligned}$$

Then, noting that $\|\Gamma_{iT}^1\|_2 \leq C(\xi_{iSup}\sqrt{T})\sqrt{T}$ and $\|\Xi_{iT}^1\|_2 \leq C(\xi_{iSup}\sqrt{T})T$, and consider

$$E_3 = \mathbb{E}\left[\int_0^1 d\lambda\frac{(1-\lambda)^2}{2}\partial_\lambda^3\bar{P}(\lambda,\mathbf{1}_n)\right] = \mathbb{E}\left[\int_0^1 d\lambda\frac{(1-\lambda)^2}{2}\sum_{i=1}^n\sum_{l=0}^3\binom{3}{l}\frac{\partial^3 P_{BS}}{\partial x^l\partial y^{3-l}}\left(\Gamma_{iT}^1\right)^l\left(\Xi_{iT}^1\right)^{3-l}\right]$$

we have

$$\left|\sum_{i=1}^n\sum_{l=0}^3\binom{3}{l}\mathbb{E}\left[\frac{\partial^3 P_{BS}}{\partial x^l\partial y^{3-l}}\left(\Gamma_{iT}^1\right)^l\left(\Xi_{iT}^1\right)^{3-l}\right]\right| \leq \sum_{i=1}^n\sum_{l=0}^3\binom{3}{l}\left\|\frac{\partial^3 P_{BS}}{\partial x^l\partial y^{3-l}}\right\|_2\left\|\Gamma_{iT}^1\right\|_2^l\left\|\Xi_{iT}^1\right\|_2^{3-l} = 8C\sum_{i=1}^n(\xi_{iSup})^3T^2,$$

by applying similar argument to the remaining terms, we have

$$|E_3| \leq \frac{4}{3}C\sum_{i=1}^n(\xi_{iSup})^3T^2. \qquad \text{(D.8)}$$

Therefore, combining all the error terms, we are able to estimate the bound of the expansion errors as

$$|E| \leq |E_1| + |E_2| + |E_3| \leq C\sum_{i=1}^n(\xi_{iSup})^3T^2. \qquad \text{(D.9)}$$